Structural Investigations on N'-Substituted N-Acylguanidines - Intermolecular Interactions with Solvents, Anions and Receptors

Dissertation

zur Erlangung des Doktorgrades der Naturwissenschaften

(Dr. rer. nat.)

an der Fakultät für Chemie und Pharmazie

der Universität Regensburg

vorgelegt von

Roland Kleinmaier

aus Bad Reichenhall.

2010

This PhD-thesis was carried out under supervision of Prof. Dr. Ruth M. Gschwind between March 2007 and May 2010 at the Institute of Organic Chemistry at the University of Regensburg.

The PhD – thesis was submitted on: 06.05.2010

Date of Colloquium: 28.05.2010

Board of Examiners: Prof. Dr. A. Pfitzner   Chairman

Prof. Dr. R. M. Gschwind   1st Referee

Prof. Dr. B. König   2nd Referee

Prof. Dr. A. Buschauer   Examiner

In memoriam iuventutis.

zg

efp

apk

abs

Table of Contents

1 Introduction and Overview

I

1.1 Acylguanidines

Acylguanidines are an abundant class of compounds with various applications in organic and pharmaceutical chemistry. Within the subgroup of N'-substituted and especially monoalkylated N-acylguanidines (Figure 1), highly potent and selective ligands for G protein coupled receptors have been identified in recent years. In the field of molecular recognition, acylguanidines are valued for their ability to form strong fork-like hydrogen bond (H-bond) interactions with carboxylate anions. Although their basicity is decreased in comparison to non-acylated guanidine, they are still charged at physiological pH. Therefore, these strong H-bonds are charge-assisted and thus very similar to salt bridges occurring in natural proteins between arginine side chains and aspartate/glutamate residues as one of the most important interactions for the structure of proteins. However, the actual binding mode of the acylguanidine moiety to a biological target, i.e. the conformation in which it binds, often remains a matter of speculation. This lack of information is in contrast to the fact that an intimate knowledge of general and/or individual conformational preferences of this compound class is highly desirable in order to support the rational design of biologically active compounds.
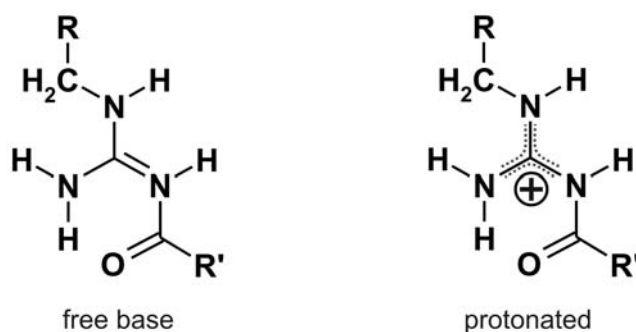
Figure 1: Throughout this work, the term 'monoalkylated acylguanidines' refers to the depicted class of compounds having one N-acyl residue, one N'-substituent with a CH_2 group adjacent to N' and an unsubstituted NH_2 group.

For this reason, in this work a pool of structurally diverse monoalkylated acylguanidines was synthesized, including the labelling synthesis of an N^G-acylated arginine derivative.

The conformations and conformational preferences of acylguanidines are investigated in detail. In order to elucidate the impact of its environment on the structure of an acylguanidine compound, interactions of monoalkylated acylguanidines with a high-affinity model receptor are studied and related to conformational equilibria under the influence of protonation and of interactions with anions and the solvent. A new straightforward approach of conformational assignment of monoalkylated acylguanidines was developed and successfully utilized. Based on experimental results, a rationale was devised for the possible driving forces behind the observed conformational preferences.

1.2   Outline of the chapters

Principally, broadly referenced specific introductory sections leading to the individual topics are found as first part of each publication.

Chapter 2 is a communication in the Journal of the American Chemical Society presenting the first NMR detection of $^{2h}J_{H,P}$ and $^{3h}J_{N,P}$ scalar couplings between two small molecules. This was achieved using the molecular recognition of a side-chain acylated arginine derivative by bisphosphonate tweezers. These investigations ultimately resulted in evidence of the spatial arrangement of the two molecules upon their mutual recognition.

Chapter 3 presents further in-depth studies by NMR on the conformational preferences of N'-monoalkylated N-acylguanidines in order to identify the possible driving forces for the acylarginine guest (discussed in chapter 2) to adopt such a distinct conformation as detected in the bisphosponate complex. With a widened scope, these investigations were conducted in the absence of any receptor molecules in different solvents on a pool of structurally diverse monoalkylated acylguanidines, but of course including the acylarginine guest from the study in chapter 2. However, N^G-acylated arginines are but a mere subgroup to the vast class of compounds that acylguanidines constitute.

The impacts of the formation of complex intermolecular H-bond networks to anions and solvent molecules were elucidated as well as the effect of charge and protonation. Expanding the range of the study even further, two biologically active G-protein coupled receptor ligands were included and in addition, one of these substances was investigated also in a complex with the tweezers. Finally, two new crystal structures of N'monoalkylated N-acylguanidines corroborated the principal results of the NMR study. This article has been submitted to the Journal of the American Chemical Society.

Chapter 4 demonstrates the unambiguous conformational analysis of monoalkylated acylguanidines, which was a central technical point to the study in chapter 3. Since no straightforward approach to achieve a robust and unequivocal chemical shift and conformational assignment for this compound class had been available so far, chapter 4 contains a survey of possible NMR methods for this objective.

A successful approach delivering a thorough assignment of both chemical shifts and conformations of monoalkylated acylguanidines was designed and examined for its powers and limits. This work has been submitted to Magnetic Resonance in Chemistry.

Chapter 5 is an extended study of the rotation of the NH_2 group that is present in monoalkylated acylguanidines by dynamic NMR to obtain the thermodynamic activation parameters $\Delta H^{\ddagger}$ and $\Delta S^{\ddagger}$ for this rotational process. During the investigations described in chapter 3, experimental evidence indicating rotation of this NH_2 group at low temperature led to the suggestion that entropic contributions from this process might be at least in part responsible for the observed preference of one conformation. Therefore, an N-acyl benzamidine was identified by combined NMR and crystal structure analyses as an equivalent model compound to circumvent the overlap of conformational exchange and rotational exchange during the experimental determination of $\Delta H^{\ddagger}$ and $\Delta S^{\ddagger}$ of the NH_2 rotation. The most important implication of this part of the work is that the intramolecular H-bond is weaker in the protonated state of the acylguanidines. In addition, both $\Delta H^{\ddagger}$ and $\Delta S^{\ddagger}$ were found to depend strongly on the formation of H-bond networks to the solvent. This article is close to submission.

In **Chapter 6**, the synthetic strategy to accomplish selective side chain ^{15}N labeling of the acylarginine used in the study discussed in chapter 1 is laid out in detail. Therefore, this chapter may be understood in terms of an extended preparative experimental section adding to the report given in chapter 1. A protected ornithine derivative was guanidinylated with a ^{15}N labeled reagent produced from S-methylisothiourea, which is traced back to commercially available $[^{15}N_2]$ thiourea. This article was published in the Journal of Labelled Compounds and Radiopharmaceuticals.

1.3 Structure of the present work

Aspiring to present a clearly structured and well readable body of text, consecutive numerals for figures, tables and schemes have been introduced corresponding to the leading chapter numbers, replacing the original numerals which adhered to the closed internal logic of each single publication. As a part of this process, the "Supporting Information" (SI) sections of each publication were integrated into the hierarchy of the former main paper. In order to enhance orientation within the text, the numerals of figures, tables and schemes in these sections have been added a leading capital "S" before the chapter number to clarify their

belonging to the SI section. However, both the main publication and SI parts continue each to have separate "references" sections.

2 The H-Bonding Network of Acylguanidine Complexes: Combined Intermolecular $^{2h}J_{H,P}$ and $^{3h}J_{N,P}$ Scalar Couplings Provide an Insight into the Geometric Arrangement*

Guido Federwisch, Roland Kleinmaier, Diana Drettwan, Ruth M. Gschwind

For this study, the synthesis of the bisphosphonate tweezers **T1** was achieved by Dr. Guido Federwisch, the synthesis Bz-Arg(N^{η}-propionyl)-OEt*TFA was done by the author of this thesis and the NMR investigations were performed in close collaboration of all authors.

The above link replaces pages 6 – 18 of the printed version.

3 Conformations, Conformational Preferences and Conformational Exchange of N'-Substituted N-Acylguanidines – Intermolecular Interactions Hold the Key*

Roland Kleinmaier, Max Keller, Patrick Igel, Armin Buschauer, Ruth M. Gschwind

III

Reproduced with permission from the Journal of the American Chemical Society, Copyright 2010, American Chemical Society.

3.1 Abstract

Guanidine and acylguanidine groups are crucial structural features of numerous biologically active compounds. Depending on the biological target, acylguanidines may be considered as considerably less basic bioisosteres of guanidines with improved pharmacokinetics and pharmacodynamics as recently reported for N'-monoalkylated N-acylguanidines as ligands of G-protein coupled receptors (GPCRs). The molecular basis for enhanced ligand-receptor interactions of acylguanidines is far from being understood. So far only few and contradictory results about their conformational preferences have been reported. Therefore, in this study for the first time the conformations, the conformational preferences and the conformational exchange of four unprotonated and seven protonated monoalkylated acylguanidines with up to six anions and with bisphosphonate tweezers are investigated by NMR. Furthermore, the effect of the acceptor properties in acylguanidine salts, of microsolvation by DMSO and of varying acyl- and alkylsubstituents are studied. Throughout the whole study, exclusively two out of eight possible acylguanidine conformations were detected independent of the compound, the anion or the solvent used. For the first time it is shown that the strength and number of intermolecular interactions with anions, solvent molecules or biomimetic receptors are decisive for conformational preferences and exchange rates. Even one recently presented and two new crystal structures resemble the conformational preferences observed in solution. Thus, consistent conformational trends are found throughout the structurally diverse compound pool including two potent GPCR ligands, different anions and receptors. The presented results may contribute to a better understanding of the mechanism of action at the molecular level, the prediction and rational design of these biologically active compounds.

3.2 Introduction

Guanidine compounds are highly valued compounds in various biological, biochemical and medical applications[1-3] such as e.g. inhibition of enzymes[4] and the NHE ion exchanger,[5,6] substances with positive inotropic effects,[7] anticoagulants[8] and highly active ligands of transmembrane receptors from various families, e.g. aminergic and peptidergic G-protein coupled receptors (GPCRs) such as histamine and neuropeptide Y receptors.[9-11] Especially in the field of medicinal chemistry, acylguanidines are greatly appreciated due to their improved pharmacokinetic properties compared to the corresponding guanidines, while retaining or even improving the biological activity.[9-11] The acylation of the guanidine reduces its basicity by 4-5 orders of magnitude, which improves the pharmacokinetic properties, but still retains its general ability to interact with acidic functions of the biological target.[9] Indeed, the increased acidity of the acylguanidinium NH protons leads to stronger binding to carboxylates compared to simple guanidinium cations[12] e.g. in supramolecular assemblies.[13]

Regarding structural and conformational investigations of acylguanidines, extensive theoretical studies about the potassium sparing monoacylguanidine diuretic amiloride and its derivatives have been published in the solid state and in solution.[14-17] In addition, the crystal structure of a protein-amiloride complex proved the formation of charge-assisted H-bonds between the planar acylguanidine moiety and an aspartate sidechain,[18,19] which are much stronger than H-bonds between neutral species.[20,21] These charge-assisted H-bonds are similar to the famous arginine-carboxylate salt bridges, which are crucial to the tertiary structure of many proteins[22] and have been subject of numerous theoretical studies, too.[13,22-24] For monoalkylated acylguanidines, a conformational study of rotationally restricted, i.e. mostly cyclized acylguanidine compounds is available.[25,26] However, to our knowledge for the class of N'-substituted N-acylguanidines (see Figure 3.1, further on referred to as monoalkylated acylguanidines) conformational studies are still missing.

In principle, the acylguanidine moiety of both protonated and uncharged monoalkylated acylguanidines can adopt eight planar conformations. Five of these conformations are energetically unfavourable due to severe sterical hindrance and/or the lack of an intramolecular H-bond (see SI for details). Each of the remaining three conformations (see Figure 3.1) shows an intramolecular H-bond and similar contributions to sterical hindrance suggesting small energetical differences between the conformations I, II and III or I[+], II[+] and III[+].
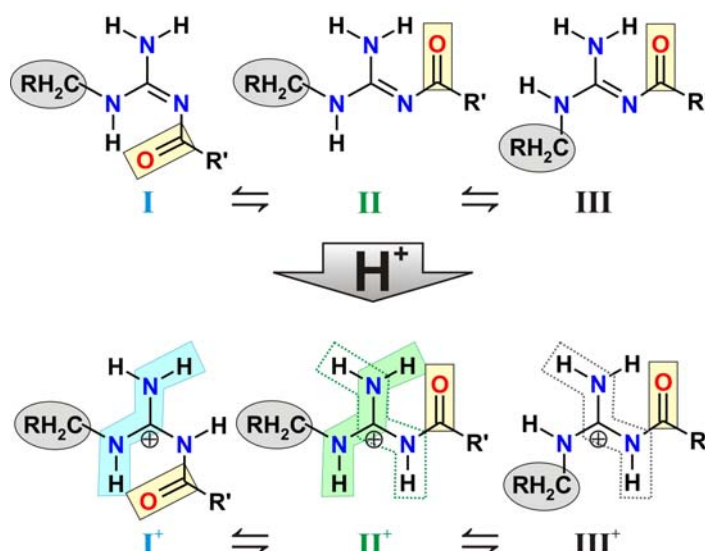
Figure 3.1: Possible conformations of monoalkylated acylguanidines with intramolecular H-bonds in the unprotonated (I-III) and in the protonated state (I[+]-III[+]). Zig-zag pathways leading to $^4J_{H,H}$ scalar couplings between H-atoms are indicated for the protonated forms.

The main difference between conformation I/I[+] compared to II/II[+] and III/III[+] is the formation of the intramolecular H-bond either to the RNH or to the NH_2 group, respectively. In complexes of non-acylated arginines with bisphosphonate tweezers energetic preferences were calculated for intermolecular H-bonds to the RNH group in quantum chemical

calculations[27] and molecular dynamics simulations.[28] Thus, also in acylguanidines a preferred formation of H-bonds to the NH group might be expected (conformation I and I[+]). Indeed, the only crystal structure of a monoalkylated acylguanidine published so far to our knowledge, which is the precursor of a histamine H_2 receptor ligand, crystallized as free base, shows conformation I with an intramolecular H-bond to the NH group (see Figure 3.2a).[9,29]

In contrast, the only existing NMR study about the H-bond pattern of an acylguanidine moiety, which was performed on a complex of an arginine derivative with bisphosphonate tweezers, reports the existence of conformation II[+] in this bioorganic model complex in solution (see Figure 3.2b).[30] Also a docking study of an acylguanidine-type agonist in the binding pocket of the guinea pig H_2 receptor suggests conformation II[+] (see Figure 3.2c).[9] Interestingly, the structure used in this docking study is a detritylated and protonated form of a close analog of the ligand, the precursor of which adopts conformation I in the solid state as mentioned above (Figure 3.2a).
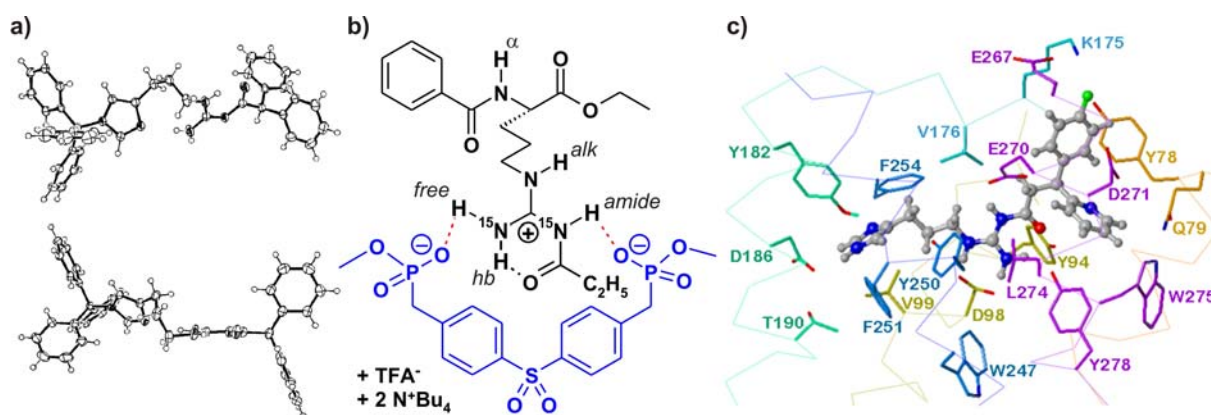
Figure 3.2: a) Crystal structure representation[9,29] (ORTEP diagram) of the free base of trityl-protected acylguanidine in conformation I; b) bioorganic model complex of [$^{15}N_2^n$]-Bz-Arg(N$^\eta$-propionyl)-OEt (conformation II[+]) with bisphosphonate tweezers,[30] and c) computational docking model[9] of the gpH$_2$R binding site for protonated N-acyl-N'-imidazolylpropyl guanidine with H-bond indicating conformation II[+].

These deviating results from theoretical calculations, NMR-, X-ray-, and docking studies show that monoalkylated acylguanidines may not have one generally preferred conformation but suggest that the substituents and the protonation state of the acylguanidine and/or the geometry and the H-bond acceptor qualities of the receptor may substantially influence the conformational preferences. Considering the general importance of pre-organization effects for the binding constants of complexes,[31] e.g. via H-bonding,[32] and the recent theoretical results about facilitated self-assembly of rigidified guanidines,[33] the elucidation and prediction of conformational preferences of monoalkylated acylguanidines may considerably support the rational development of this pharmacologically important class of ligands.

Therefore, in this study, the conformations, the conformational preferences and the conformational exchange of four unprotonated and seven protonated monoalkylated acylguanidines with up to six anions and with bisphosphonate tweezers are investigated by NMR. The effect of the acceptor properties in acylguanidine salts, the influence of microsolvation by DMSO and the contribution of varying acyl and alkyl substituents on the conformational equilibria and their exchange rates is presented. Consistent conformational trends are derived depending on the strengths of intermolecular interactions, which are additionally corroborated by two new crystal structures.

3.3 Results and Discussion

3.3.1 Compound pool and synthesis

For this conformational study of acylguanidines seven model compounds were selected (Figure 3.3). First, $[^{15}N^\eta_2]$-Bz-Arg(N^η-propionyl)-OEt (**1**), the acylguanidine used in the previous NMR complexation study, was chosen to enable a comparison between the acylguanidine conformation in the free state and bound to an artificial receptor molecule.[30] Second, two highly potent acylguanidine-type GPCR ligands were investigated, the histamine H_4 receptor agonist UR-PI294[34] (**2**) and the arginine-derived neuropeptide Y (NPY) Y_1 receptor selective antagonist UR-MK50 (**3**), which is an acylated derivative of the first potent and selective Y_1 receptor antagonist BIBP 3226.[35] Third, N-propionyl-N'-butylguanidine (**4a**) and N-cinnamoyl-N'-butylguanidine (**4b**) were chosen as acylguanidines with very simple alkyl substituents and strongly differing acyl substituents to eliminate any interferences from additional functional groups in the alkyl moiety. Finally, to further investigate the influence of structural and electronic variations in the acyl substituents, the para-substituted benzoic acid derivatives N-p-dimethylaminobenzoyl-N'-butylguanidine (**4c**) and N-p-methoxybenzoyl-N'-butylguanidine (**4d**) were used.
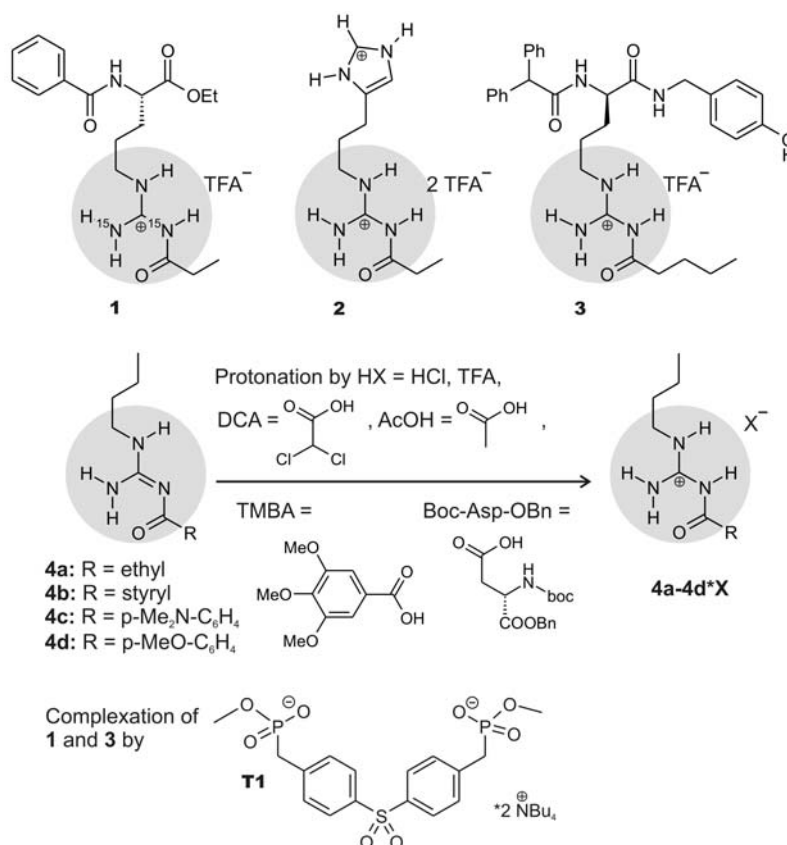
Figure 3.3: Compounds investigated in this work: [^{15}N$^{\eta}_2$]-Bz-Arg(N$^{\eta}$-propionyl)-OEt (**1**), N-propionyl-N'-(3-imidazol-4-ylpropyl)guanidine (**2**), UR-MK50 (**3**) and the simple n-butyl chain analogs N-**p**ropionyl-N'-**b**utylguanidine (**4a**) and N-**c**innamoyl-N'-**b**utylguanidine (**4b**), and benzoic acid derivatives **4c** and **4d**. The free bases **4a-4d** were protonated with one or several of the acids shown to give the 1:1 salts **4a-4d*X**.

The syntheses of [^{15}N$^{\eta}_2$]-Bz-Arg(N$^{\eta}$-propionyl)-OEt (**1**)[30] and N-propionyl-N'-imidazolylpropylguanidine (**2**) [34] have already been reported.

UR-MK50 (**3**) was synthesized (Scheme 3.1a) through acylation of N^G-Boc, O-*tert*-butyl protected BIBP 3226[36] with pentanoic acid anhydride (Scheme 3.1a). Subsequent deprotection and purification with preparative HPLC yielded **3**.

Compound **4a** was prepared (Scheme 3.1b) by nucleophilic attack of excess butylamine at the amidine carbon of N-propionyl-N'-boc-S-methylisothiourea[30] and subsequent boc-deprotection by 50% TFA. S-Methylisothiourea derivatives are standard guanidinylation reagents[37-42] and while often HgCl$_2$ has to be added stoichiometrically to force nucleophilic attack, in this case a five-fold excess of the nucleophile was sufficient to drive the reaction.

4b as well as the structurally very similar compounds **4c** and **4d** were prepared (Scheme 3.1c) by an approach[43,44] omitting the common boc-protection of the 1H-pyrazol-1-carboxamidine-derived guanidinylation reagent that was produced by the acylation of the well-known precursor 1H-pyrazol-1-carboxamidine.[36,45,46] With an excess of butylamine as nucleophile, the reaction was finished smoothly after 2h at r.t. in the case of **4b** and at reflux

for compounds **4c** and **4d**, respectively, and the product was separated from the well-soluble by-product, pyrazole, by a precipitation/recrystallization procedure.

Salts of **4a, 4b** and compounds **4c** and **4d**: See experimental part.
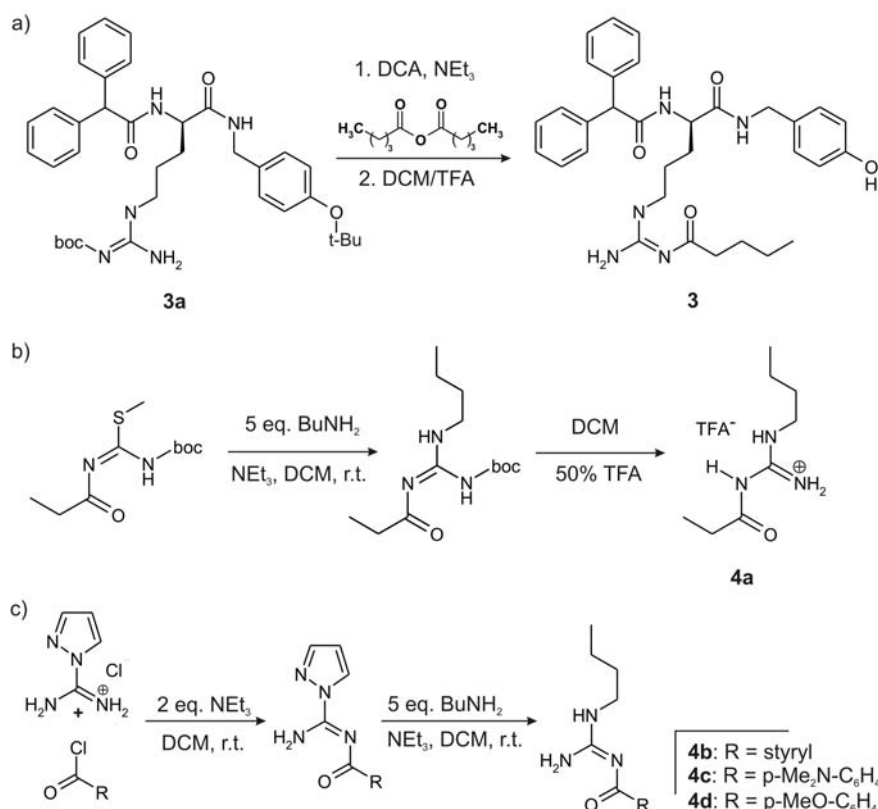
Scheme 3.1: Syntheses of a) UR-MK50 (**3**) via acylation of N^G-Boc, O-*tert*-butyl protected BIBP 3226 (**3a**), b) N-propionyl-N'-butylguanidine (**4a**) from S-methylisothiourea, and c) N-cinnamoyl-N'-butylguanidine (**4b**) and acylguanidines **4c** and **4d** from acylated 1H-pyrazol-1-carboxamidine.

3.3.2 NMR-studies of protonated acylguanidines in solution
Conformational equilibria and conformational assignment

For all NMR investigations of acylguanidines organic solvents were chosen, because recently Limbach et al. showed that the environment of the active site in an enzyme is modelled better by an aprotic solvent than by water.[47] In addition, these solvents strengthen the H-bonds and allow for low temperature measurements to detect conformational equilibria.

To optimize the NMR investigations of protonated monoalkylated acylguanidines and to identify dynamic equilibria between the different possible conformations, first a screening of the spectroscopic properties of **1-3*TFA**, **4b*X** (X = HCl, TFA, DCA, AcOH, Boc-Asp-OBn, TMBA), **4a*X**, (X = HCl, TFA, DCA, AcOH), **4c*X** (X = TFA, Boc-Asp-OBn) and

4d*X (X = HCl, TFA, DCA, Boc-Asp-OBn) was performed in a temperature range between 300 K and 200 K in CD$_2$Cl$_2$/DMSO-d_6 (9:1). This survey revealed for all protonated monoalkylated acylguanidines in this solvent mixture one general ^{1}H signal pattern with a similar temperature dependent behaviour, which is shown on the example of **4d*DCA** in Figure 3.4. At elevated temperatures, four NH signals are detected, which fit perfectly to the four NH protons expected for the acylguanidine moiety (Figure 3.4a). However, upon cooling these NH signals broaden, show coalescence effects and split into eight NH resonances indicating two conformations at low temperature (Figure 3.4b). These two conformations, separable at low temperature, are denoted as I$^+$ and II$^+$ in Figure 3.4b and exchange fast on the NMR time scale at elevated temperature (Figure 3.4a). This general ^{1}H pattern and this trend in the temperature dependence were found for all protonated acylguanidines investigated in this study in this solvent mixture. The individual coalescence temperatures, conformational ratios and absolute chemical shift values of each complex, however, show slight variations and depend on the anion, microsolvation and substitution pattern applied (see discussion below).
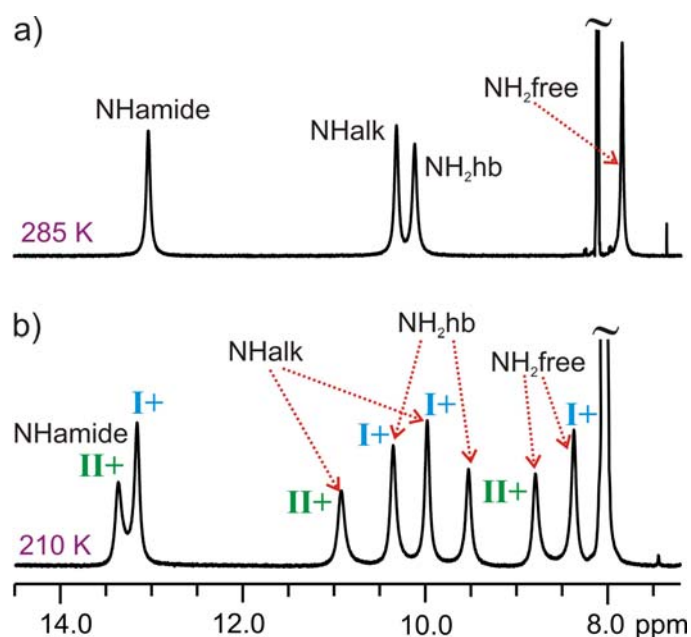
Figure 3.4: Generally observed dynamic behaviour of protonated acylguanidines on the example of **4d*DCA** in CD$_2$Cl$_2$/DMSO-d_6 (9:1); a) at 285 K four NH signals are observed, which split upon cooling to 210 K (b) into eight NH signals indicating the two conformations I$^+$ and II$^+$, which exchange fast on the NMR time scale at elevated temperatures (for labelling see Figure 3.5).

In the case of several protonated acylguanidines, which show not only well separated NH signals but also small line widths at low temperatures, the two conformations I$^+$ and II$^+$ could be unambiguously assigned as elsewhere described and justified in detail.[48] In this assignment, generally ^{1}H, ^{1}H COSY and ^{1}H, ^{13}C HMBC spectra allow the identification of

NHalk and NHamide (for labelling see Figure 3.5). In addition, the differentiation between conformations I^+, II^+, and III^+ (see Figure 3.1) is possible using the spatial information of so called w-couplings within the acylguanidine moiety. These long range $^4J_{H,H}$ scalar couplings are only detectable in a zig-zag arrangement of two NH protons (see marking in Figure 3.1 and Figure 3.5) and therefore allow the identification of the spatial arrangement of pairs of NH protons and result in the assignment of the two conformations I^+ and II^+. This is exemplarily shown on the NH section of a ^{1}H, ^{1}H COSY spectrum of **4b*TMBA** at 200 K in Figure 3.5. For the major conformation, two w-couplings are detected, one to the NHamide (W3) and one to the NHalk (W2). This combination of w-couplings allows identifying the major conformation to II^+. For the minor conformation only one w-coupling to NHalk (W1) is detected, which allows assignment of this conformation to I^+. These assignments are also in accordance with the relative chemical shifts of the NH resonances, which are influenced by the formation of strong H-bonds to the anion (see below).

These relative chemical shift patterns of I^+ and II^+ and the chemical exchange between these two conformations at elevated temperatures were detected for all protonated acylguanidines investigated in this study. However, the NMR survey of the different substances showed that the individual coalescence temperatures, the exchanges rates, and the conformational preferences are strongly dependent on the properties of the anion present. Therefore, next the influence of the anions on the dynamic behaviour of the two conformations I^+ and II^+ was investigated.
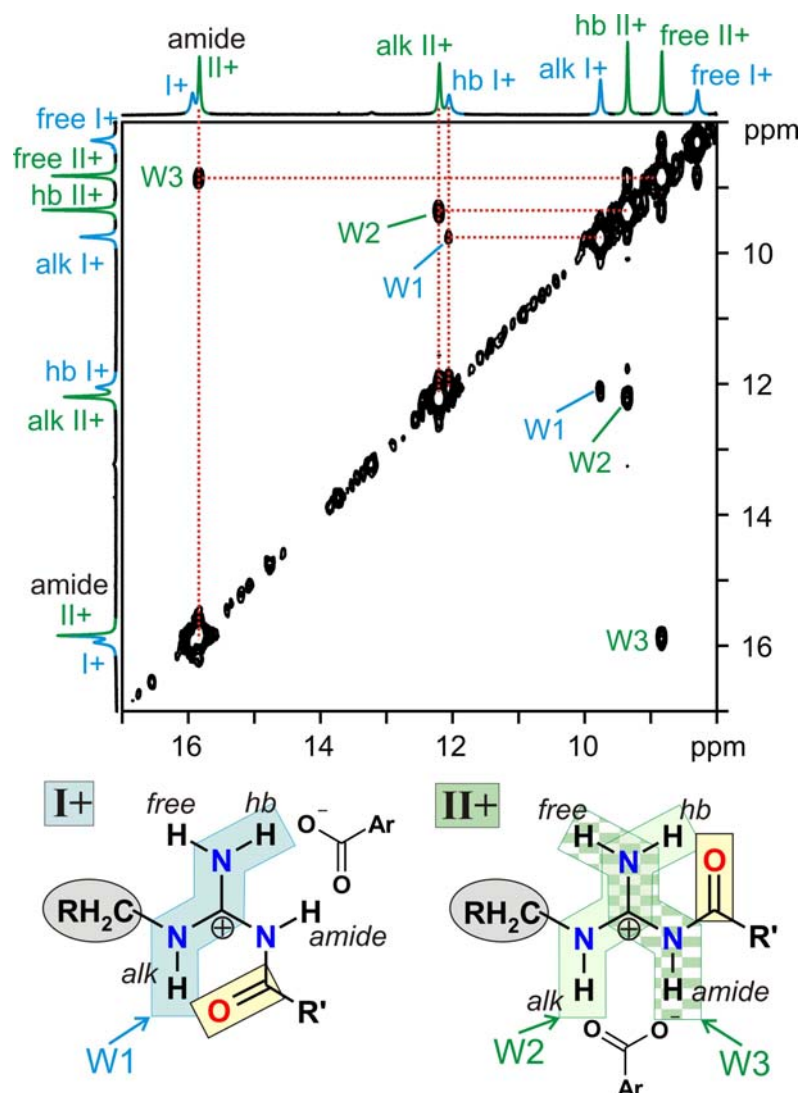
Figure 3.5: NH section of a ^{1}H, ^{1}H COSY spectrum of **4b*TMBA** in CD$_2$Cl$_2$ and DMSO-d_6 (9:1) at 200 K. For the major conformation, the detection of the two $^4J_{H,H}$ long range couplings W2 and W3 allow the assignment to II$^+$; for the minor conformation, W1 allows the identification of I$^+$.

Interaction with anions - a conformational exchange brake

To investigate the influence of the anions on the exchange dynamics between the two conformations of protonated acylguanidines, **4b** in CD$_2$Cl$_2$ and DMSO-d_6 (9:1) was selected, because the NMR survey showed for this combination the best resolved spectra within a wide range of anions. With strong acids, four sharp guanidinium NH signals are detected for **4b** at elevated temperature indicating fast exchange between the two conformations on the NMR time scale. This is shown in Figure 3.6a on the ^{1}H spectrum of **4b*TFA** at 300 K. In addition, the conformational exchange of **4b*TFA** is so fast that the coalescence point is even lower than 210 K (see Figure 3.6b). In contrast, for **4b*AcOH**, the ^{1}H spectra of the acylguanidine moieties change drastically. At 300 K only broad signals are detected, which are close to the

coalescence point (Figure 3.6c), whereas at 210 K the signals sharpen and the typical chemical shift pattern of the conformations I[+] and II[+] is observed (Figure 3.6d).
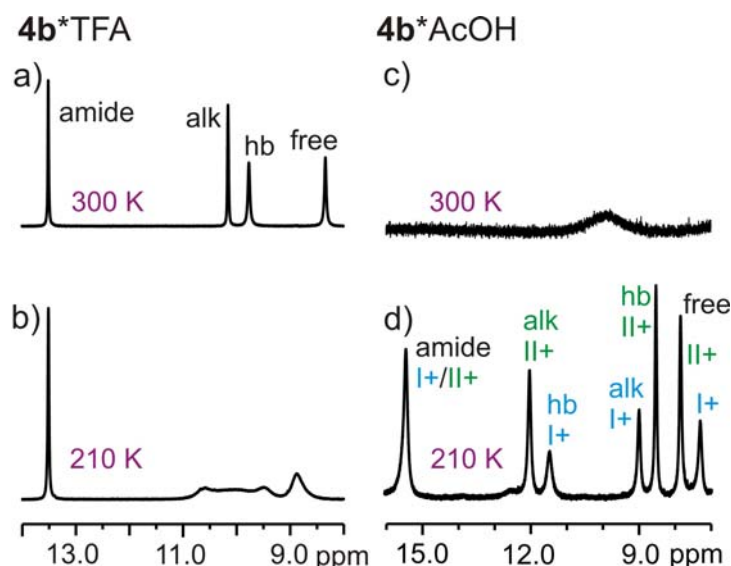
Figure 3.6: NH-Sections of the ^{1}H NMR (600 MHz) spectra of **4b*TFA** (a,b) and **4b*AcOH** (c,d) in CD_2Cl_2 and DMSO-d_6 (9:1) at 300 K (a and c) and at 210 K (b and d), respectively. The conformational exchange is significantly faster with TFA than with AcOH.

These spectra suggest that the exchange rate between the two conformations can be gradually adjusted by the strength of the interaction with the anion. Therefore, the **4b** salts derived from six different acids (HCl, TFA, DCA, AcOH, Boc-Asp-OBn and TMBA) were investigated at 210 K and their ^{1}H spectra are shown in Figure 3.7 ordered by decreasing acidity. With Cl^{-} as anion, only one broad and unresolved ^{1}H signal is detected for all six amine protons of both conformations indicating medium exchange above the coalescence point. With decreasing acidity, i.e. increasing H-bond acceptor strength, the NH signal dispersion becomes better while the resonances are still broad until six separate and rather sharp signals are detected. This indicates reduced conformational exchange with increasing interaction strength between the cationic acylguanidine and its anion.[49] In addition, the signals with the highest chemical shift, the NHamides of II[+] and I[+] and NHalk(II[+]) and NHhb(I[+]), experience a strong further increase in chemical shift with decreasing acidity of the acid, whereas the chemical shifts of the remaining NH signals are nearly unaffected by the change of the anion. These selective low-field shifts in the chemical shift pattern can be attributed to the formation of strong H-bonds to the anion[50] and thus from this chemical shift change the main positions of the anions in conformation I[+] and II[+] are derived as depicted in Figure 3.5.[51]
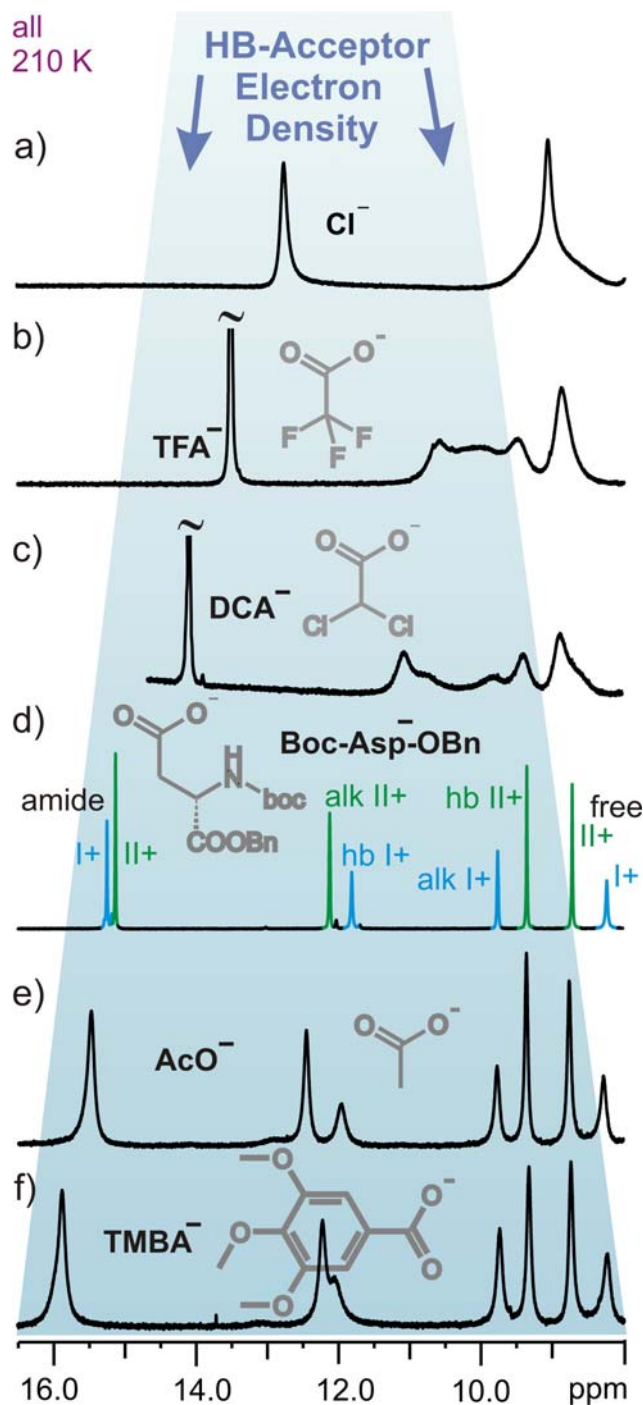
Figure 3.7: Modulation of the conformational exchange rate and the NH signal dispersion by the hydrogen bond acceptor properties of the anion. Shown are the stacked NH sections of ^{1}H spectra of **4b** in CD_2Cl_2 and DMSO-d_6 (9:1) at 210 K, protonated with six different acids whose anions possess increasing electron densities in the carboxylate going from top a) to bottom f). The exchange rate is reduced and the signal separation is enhanced with reduced acid strength.

Both trends, the reduced chemical exchange and the higher chemical shift dispersion of specific NH protons, indicate that in both conformations of protonated acylguanidines specific

R. Kleinmaier, M. Keller, P. Igel, A. Buschauer, R. M. Gschwind, *J. Am. Chem. Soc*, **2010**, submitted.

intermolecular H-bonds exist to the anion. In addition, the conformational exchange rate is modulated by the H-bond strength.[52,53] It can be seen in Figure 3.7 that the higher the H-bond acceptor strength, the stronger are the H-bonds between anion and cation and the lower is the conformational exchange rate. Thus, a strong interaction with the anion acts like a brake for the conformational exchange.

Microsolvation by DMSO

Because of severe solubility problems of protonated monoalkylated acylguanidines in apolar solvents, so far exclusively solvent mixtures (CD_2Cl_2 and DMSO-d_6, 9:1) had been used. In terms of H-bond networks, microsolvation by DMSO means a considerable H-bond acceptor competition between the DMSO solvent molecules and the anion. Additionally, also the electrostatic attraction between the anion and the acylguanidinium cation is weakened by the high susceptibility of DMSO. Therefore, the interaction between anion and acylguanidinium cation should be considerably stronger in solvents with reduced susceptibility and without H-bond acceptor properties such as pure CD_2Cl_2. To enable the investigation of the preferred conformations in pure CD_2Cl_2 and of the effects of microsolvation by DMSO, the compound pool was screened for solubility in pure CD_2Cl_2. **4d***Boc-Asp-OBn, **4d***HCl and **4c***Boc-Asp-OBn were found to be sufficiently soluble in pure CD_2Cl_2 and DMSO-d_6 titration experiments of **4d***Boc-Asp-OBn, **4d***HCl and **4c***Boc-Asp-OBn were conducted at 225 K and 195 K, i.e. temperatures at which the conformational exchange is slow on the NMR time scale. Starting from pure CD_2Cl_2, increasing amounts of DMSO were added and the spectral changes monitored as shown for **4d***Boc-Asp-OBn and **4d***HCl in Figure 3.8. The spectra of **4d***Boc-Asp-OBn (Figure 3.8a, b) show impressively that the microsolvation with DMSO not only affects the conformational exchange rate as expected from the results about the interaction with the anions (see above) but also shifts drastically the ratio of the two conformations. In pure CD_2Cl_2 conformation I$^+$ is strongly predominant over conformation II$^+$ with a ratio of 95:5 (Figure 3.8a). However, upon addition of about 10% DMSO-d_6, the portion of the conformation II$^+$ grows to 50% (Figure 3.8b). Further addition of DMSO changes the conformational distribution only marginally but leads to significant line broadening indicating increased conformational exchange (data not shown). Interestingly, the conformational preference for I$^+$ over II$^+$ (70:30) is significantly smaller for **4d***HCl (see Figure 3.8c), and already addition of less than 5% DMSO (see Figure 3.8d) leads to one set of four NH signals, i.e. fast exchange between the two conformations on the NMR time scale.
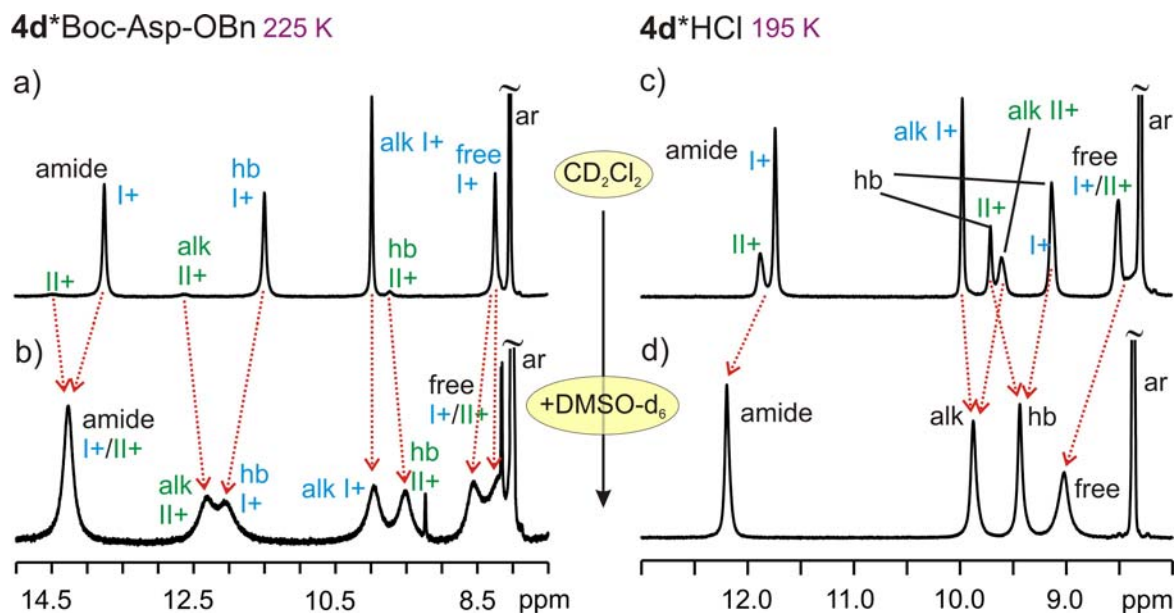
Figure 3.8: Effect of microsolvation by DMSO on the conformational distribution and exchange rate of protonated acylguanidines. The conformational shift from I^+ to II^+ upon microsolvation by DMSO is shown on the ^{1}H sections of 4d*Boc-Asp-OBn at 225 K a) 95/5% I^+/II^+ in pure CD_2Cl_2 and b) 50/50% I^+/II^+ after addition of 10% DMSO-d_6. The acceleration of conformational exchange upon microsolvation by DMSO is demonstrated on the ^{1}H sections of 4d*HCl at 195 K c) in pure CD_2Cl_2 both conformations are detected (70/30% I^+/II^+), whereas d) after addition of 3% DMSO-d_6 one conformationally averaged set of signals is observed.

The described trend in the conformational preferences depending on the amount of microsolvation with DMSO and the anion properties now fit perfectly to the interactions with the anions discussed above. For the combination with the strongest H-bond interaction between acylguanidinium moiety and anion, i.e. with the strong H-bond acceptor (Boc-Asp-OBn) and without competing DMSO molecules, the highest preference for conformation I^+ is observed. Weakening this interaction either through microsolvation by DMSO or through changing the anion properties, i.e. by replacing Boc-Asp-OBn with Cl^-, the conformational preference for I^+ is significantly reduced. By a further weakening of the interaction with the anion e.g. by raising the percentage of DMSO, the conformational exchange between the two conformations becomes too fast to be observed by NMR.

As a result, all data hint at a conformational preference of I^+ induced by a strong interaction with the anion. However, for both conformations forklike H-bonds to two guanidinium protons are proposed and confirmed by the chemical shift pattern of I^+ and II^+ (see Figure 3.5 and discussion above) and in both conformations three NH protons are involved in H-bonds. Thus, at the first glance the interaction patterns look quite similar. However, in I^+ the NH_2 group is involved in the intermolecular H-bond, whereas in II^+ the NH_2 group is involved in the intramolecular H-bond. Therefore, we suggest an entropic contribution from the rotation of the NH_2 group inside the H-bond network as reason for the preference of conformation I^+ in pure CD_2Cl_2. In a partially flexible salt bridge to the anion

R. Kleinmaier, M. Keller, P. Igel, A. Buschauer, R. M. Gschwind, *J. Am. Chem. Soc*, **2010**, submitted.

the rotational barrier of the NH_2 group is expected to be lower than in an intramolecular H-bond to the carbonyl within a rather rigid six-membered ring. In pure CD_2Cl_2, these H-bonds are strong enough to produce a sufficient difference in total energy, which makes I^+ the preferred conformation (for a further reasoning and spectral evidence for a NH_2 rotation, see SI). Additional H-bond acceptors such as DMSO, reduced electrostatic attraction because of higher susceptibility of the solvent, or anions with reduced interaction strength are expected to lead to lower rotational barriers for the NH_2 group in conformation I^+ and thus to a reduced preference of I^+ as observed experimentally.

Impact of alkyl and acyl substituents

The next step was to investigate whether varying substituents of the acylguanidine moiety affect the conformational preferences or exchange rates. First, the influence of different alkyl substituents was investigated. As evident from the compound pool shown in Figure 3.3, with **1**, **2** and **4a,** three different alkyl residues are available with identical acyl moieties. In addition, **3** exhibits only a n-butyl instead of an ethyl group in the acyl rest, which is expected to induce only marginal changes. Therefore, also **3** was included in the comparison. All of these four compounds have an alkyl chain directly attached to the guanidine moiety. In addition, two amino acid scaffolds are present in **1** and **3**, as well as an imidazolium moiety with a second positive charge in **2**. Comparisons of the ^{1}H spectra of the TFA salts of **1**, **2**, **3**, and **4a** shows astonishingly similar signal patterns of the guanidine NH signals and only a slightly reduced exchange for **4a** (see SI for spectra). This shows that for protonated acylguanidines remote changes in the structure, i.e. the presence of additional functional groups potentially capable of forming additional but weaker H-bonds, do not affect the structural properties of the acylguanidine moiety significantly.

Second, the influence of structural changes in the acyl moiety was investigated on **4a-d**, which have the identical alkyl group but deviating acyl substituents. The ^{1}H spectra of the NH region of the TFA salts of **4a**, **4b** and **4d** at 215 K are shown in Figure 3.9. Interestingly, the spectra of **4a** with an ethyl rest and of **4b** with a styryl rest are very similar (see Figure 3.9a and b), beside small low field shifts for **4b**. This indicates the formation of slightly stronger H-bonds in **4b**, supported by the additional π-system, which do not significantly affect the exchange rates. In contrast, for **4c** and **4d**, much higher exchange rates are observed. The TFA salts of **4c** and **4d** (see Figure 3.9c and d) show only four separate peaks with quite narrow line widths, indicating conformational exchange being already fast on the NMR time scale. As discussed above, this faster conformational exchange can be slowed down by using lower amounts of DMSO (see SI for spectra). A possible reason for the increased exchange rate is the reduced strength of the intramolecular H-bond caused by the para-substituted phenyl rings acting as electron-donor. Additionally, the delocalization of the positive charge of the guanidinium carbon over the π-system may weaken the electrostatic interactions with the anions and thus reduce the salt-bridge character of the intermolecular H-bonds. This trend is

also evident from the increased chemical shift when comparing **4c** and **4d**: The p-dimethylamino-substituted aromatic ring in **4c** is a better mesomeric electron donator than the p-methoxy-substituted one in **4d**. Therefore, in **4c** the positive charge of the guanidine unit may be attenuated more than in **4d**. This makes the acylguanidine unit of **4c** a weaker H-bond donor, which manifests in lower chemical shifts of the NH protons affected by H-bonds.[47] Consequently, the most acidic proton, i.e. NHamide, shows the greatest chemical shift change.

These comparisons show that structural changes in remote parts of the alkylsubstituent, i.e. additional functional groups, being capable of forming weak H-bonds, do not affect the structural properties of the acylguanidine moiety significantly. In contrast, acyl substituents which change the electronic or mesomeric properties of the acylguanidine moiety can change the strength of the H-bond network.
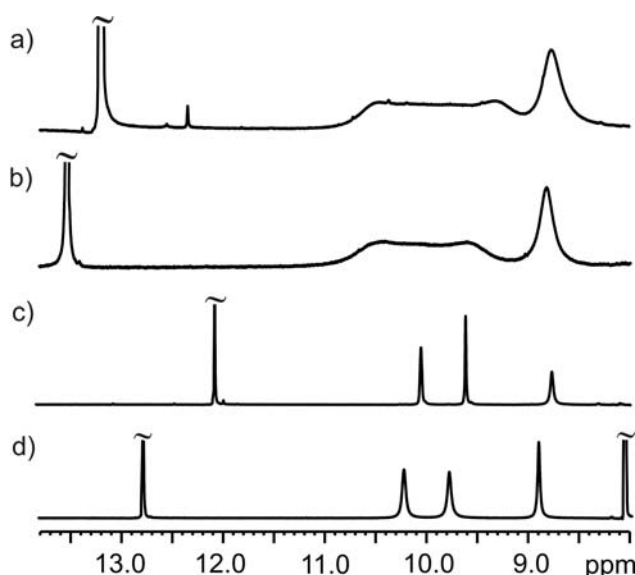
Figure 3.9: Influence of the electronic properties of the acyl substituent on the strengths of the H-bond network shown on the ^{1}H sections of a) **4a***TFA, b) **4b***TFA c) **4c***TFA and d) **4d***TFA at 215 K in CD_2Cl_2 and DMSO-d_6 (9:1). Exchange is much faster leading to four sharp lines in c) and d) because the H-bond network is weakened due to delocalization of the charge.

Conformations of the free base

In addition to the protonated acylguanidines also the spectral and conformational properties of the free acylguanidine bases were investigated to elucidate the effect of protonation on preferred conformations and conformational exchange. For this purpose the free bases of **4a-d** were synthesized and investigated NMR spectroscopically. In accordance with previous reports about the acylimino tautomer as preferred conformation of unprotonated acylguanidines,[17,54,55] in our spectra of **4a-d** no hint of protonation of the amide nitrogen was

found. Therefore, in Figure 3.1 and in the following, only conformations of the acylimino tautomer are discussed.

The NMR investigations of **4a-c** revealed again the existence of two conformations at low temperatures, which show conformational exchange at elevated temperatures and a shift in the conformational preferences upon microsolvation by DMSO. Both effects are exemplarily shown on the ^{1}H spectra of **4d** in Figure 3.10. Again, the assignment of the NHalk resonances of both conformations was unambiguously performed by ^{1}H, ^{1}H COSY cross peaks to the alkyl substituents. Regarding the NH_2 protons, in the spectra of conformation II of **4d** even a $^2J_{NH2}$ splitting of 4.5 Hz was observed confirming the assignment. However, in contrast to the protonated acylguanidines, in unprotonated acylguanidines for none of the compounds w $^4J_{H,H}$ scalar couplings were detected, which was attributed to the reduced delocalisation of the double bond. Therefore, the further conformational assignment was based on the interpretation of chemical shift differences and dimerization trends measured by ^{1}H, ^{1}H DOSY spectra. Interestingly, for the two sets of NH signals very similar diffusion coefficients were measured indicating dimers for both conformations in pure CD_2Cl_2 (for details see SI). As evident from Figure 3.1, conformation I and II exhibit both structurally typical and very similar dimerization sites with the unprotonated amide nitrogen and one NH proton on the same side. In contrast, conformation III does not possesses such an H-bond donor/ acceptor pair and intermolecular interactions to the amide nitrogen are hampered by severe sterical hindrance. These structural features of III should lead to a significantly reduced aggregation tendency compared to I and II. Therefore, based on the nearly equal diffusion coefficients of the two observed conformations, conformation III was excluded.

The remaining assignment of the two sets of signals (see Figure 3.10b-d) to I and II can be easily performed by the relative chemical shifts of the two unambiguously assigned NHalk signals. In I, the NHalk proton is in the intramolecular H-bond and will exert the highest chemical shift. This is found for the conformation with the broad line widths (see Figure 3.10b-d). In contrast, in the second set of signals, NHalk has the lowest chemical shift value in accordance with conformation II. For further interpretations of the line widths and chemical shift patterns of I and II see SI.
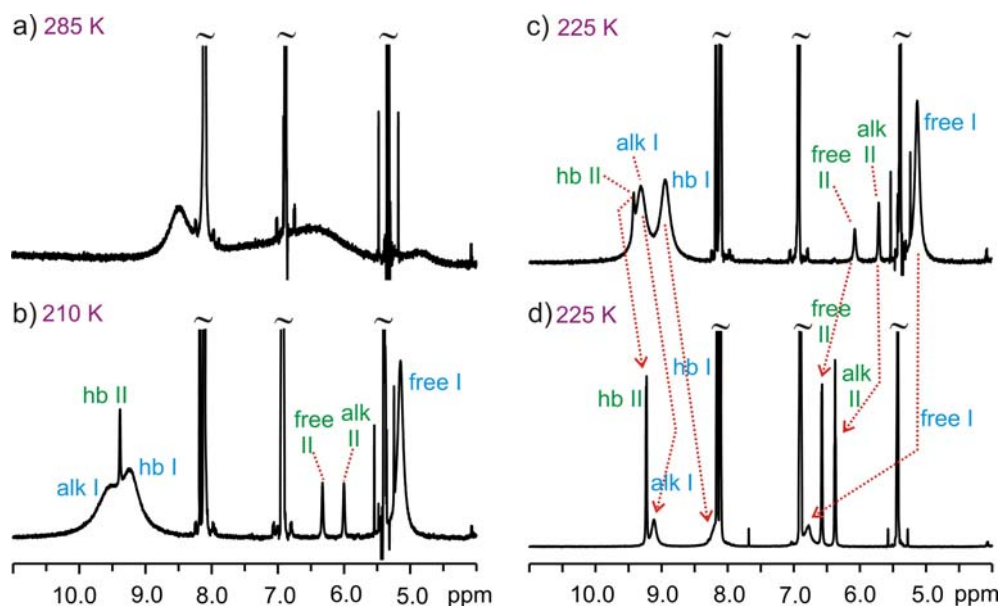
Figure 3.10: Unprotonated acylguanidines: Again increased temperature leads to conformational exchange as shown on the NH sections of the ^{1}H-spectra of **4d** in pure CD_2Cl_2 at a) 210 K, b) 285 K, and again a conformational shift from I to II upon microsolvation by DMSO is observed as shown on the ^{1}H-spectra of **4d** at 225 K in c) pure CD_2Cl_2 and d) CD_2Cl_2 and DMSO-d_6 (9:1).

The ^{1}H-spectra of **4d** in pure CD_2Cl_2 (Figure 3.10c) and after addition of 10% DMSO (Figure 3.10d) now reveal that also in the unprotonated acylguanidines conformation I is highly preferred (about 93/7% I/II) and that microsolvation with 10% DMSO shifts the preferred conformation to II (about 42/58% I/II). Similar to the protonated acylguanidines, the conformational preference for I in pure CD_2Cl_2 might be driven by intermolecular interactions, which are weakened upon microsolvation by DMSO, allowing the portion of conformation II to grow. In contrast to the protonated acylguanidines, in which the interaction with the anion determines the conformational preference, one can speculate that in unprotonated acylguanidines the dimerization properties of the conformations may be crucial for the conformational preference. Besides stronger H-bonds in the dimer of I, which are suggested by the chemical shift pattern and geometry optimized structure of the dimer (see SI for details), again the entropic properties seem to promote conformation I in the dimer. This is strongly suggested by the broad line widths of the NH signals in I indicating conformational flexibility within the dimer even in pure CD_2Cl_2 (see Figure 3.10b and c).

3.3.3 Conformational preferences in more complex receptors

With regard to the relevance of acylguanidines as ligands for pharmacologically important receptor proteins, as next step information about the conformational preferences in more complex receptor systems was collected. One example, recently published by our group,[30] is

R. Kleinmaier, M. Keller, P. Igel, A. Buschauer, R. M. Gschwind, *J. Am. Chem. Soc*, **2010**, submitted.

the additional complexation of **1***TFA by a bisphosphonate tweezers molecule, which resembles an artificial arginine fork (see Figure 3.2a). In agreement with our actual studies this complex was also measured under DMSO microsolvation conditions in a solvent mixture of CD_2Cl_2/DMSO-d_6 (9:1). Interestingly, the acylguanidine was found to adopt exclusively conformation II^+ at 220 K. The NMR detection of scalar couplings across two H-bonds in combination with the significantly reduced line widths of the NH signals allow to exclude significant contributions of any chemical exchange or rotational movements within the H-bond network.

In addition, the complex of the NPY Y_1 receptor antagonist **3** with **T1** (see Figure 3.11) was investigated. This highly biologically active ligand contains various additional functional groups that are expected to form additional H-bonds. The ^1H spectra of this complex show one major conformation (ca. 60%) with sharp line widths and one minor conformation with mainly extremely broad NH signals (for spectra and details see SI). The major conformation could be assigned to II^+ by long range $^4J_{H,H}$ couplings as described above and four $^{2h}J_{H,P}$ scalar couplings could be detected indicating intermolecular H-bonds (see Figure 3.11a and SI for spectra). For the minor conformation no structural information could be detected due to the broad line widths. Therefore, it can not be distinguished whether this minor conformation shows deviations in the acylguanidine conformation or different modes of interaction or conformations in the part of **3** remote from the acylguanidine.
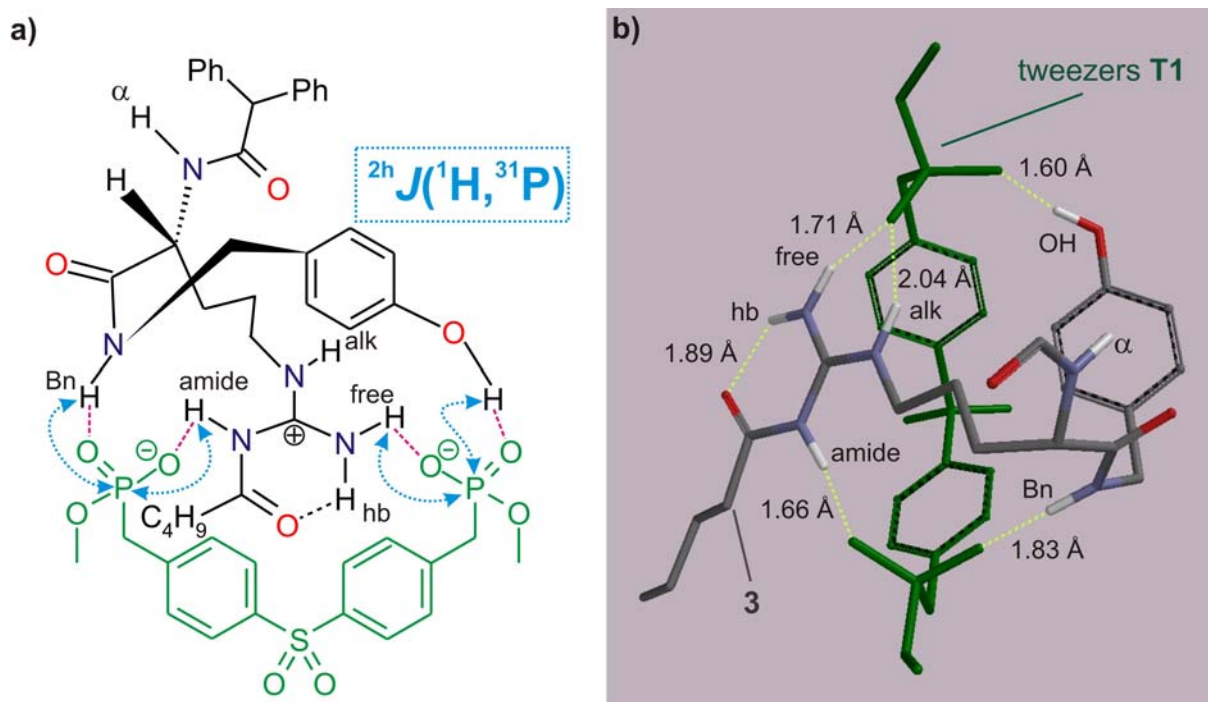
Figure 3.11: Complex between **3** and bisphosphonate tweezers **T1** (green); a) schematic representation adapted to the H-bond pattern observed. $^{2h}J_{H,P}$ scalar couplings (dotted arrows) indicate the experimentally determined intermolecular H-bonds shown by dashed lines (magenta); b) geometry optimized 3D representation showing the four experimentally detected plus one additional intermolecular H-bonds (dashed lines, yellow) with H⋯O distances as calculated by Spartan[56] (for details see SI).

R. Kleinmaier, M. Keller, P. Igel, A. Buschauer, R. M. Gschwind, *J. Am. Chem. Soc*, **2010**, submitted.

These results seem to suggest that additional strong H-bond acceptors do not reverse the conformational trends described above for the free acylguanidine salts but rather support the preference and stability of conformation II^+ in complex H-bond networks. This trend is also in agreement with a docking study of the histamine H_2 GPCR ligand in the binding pocket of the guinea pig H_2 receptor (see Figure 3.2c), which results in conformation II^+ for the complex receptor surrounding in the active site of the trans membrane protein.[9]

3.3.4   Conformational preferences in crystal structures

In addition to the NMR studies, further conformational information about monoalkyl-substituted acylguanidines was collected from X-ray structures. Besides the one previously published crystal structure of an unprotonated imidazolylpropylguanidine,[9] which adopts conformation I (see Figure 3.2a), two further crystal structures were obtained from our compound pool, **4b** and **4d***HCl (see Figure 3.12). All attempts to crystallize further compounds failed, especially those to obtain crystals of carboxylate salts.

In the crystal structure of the unprotonated **4b**, the intramolecular H-bond is found to be highly probable between the NHalk group and the carbonyl oxygen indicating conformation I (see Figure 3.12a). Thus, in both crystal structures of monoalkylated acylguanidines known so far conformation I is observed, which nicely agrees with the major conformation in pure CD_2Cl_2 found in the NMR studies (see Figure 3.10b and c).

In contrast, the crystal structure of the protonated **4d***HCl shows conformation II^+ with a complex network of H-bonds (see Figure 3.12b). The chloride is in H-bonding distance (<2.5 Å) to three NH protons and interconnects two parallel planes in the crystal, which are formed by antiparallel strands of **4d***HCl. These strands themselves are interconnected via H-bonds between two antiparallel acylguanidinium units. Interestingly, the observed conformation II^+ is again closely related to the NMR observations. First, the NMR-spectra of HCl salts of acylguanidines in pure CD_2Cl_2 contain considerable amounts of conformation II^+ (e.g. 30% II^+ for **4d***HCl see Figure 3.8). Second, the complex H-bond network observed in the crystal structure might resemble the complex H-bonds induced upon DMSO microsolvation in solution and further supports the preference for conformation II^+. Thus, the three crystal structures of monoalkylated acylguanidines known so far adopt not only exclusively the conformations found in our NMR studies, but in addition resemble the principal conformational preferences observed in solution.
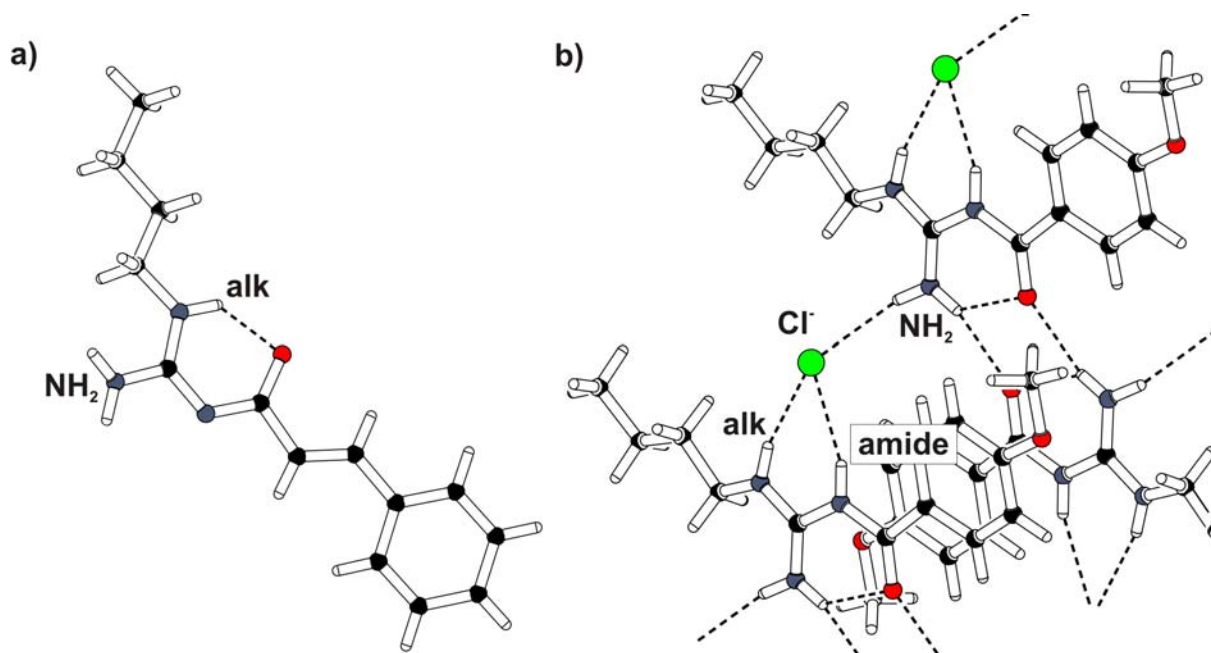
Figure 3.12: Crystal structures of a) unprotonated **4b** showing conformation I and b) **4d***HCl adopting conformation II$^+$ in a complex H-bond network between antiparallel strands of **4d***HCl (see text).

3.4 Conclusion

In this study, the conformations and conformational preferences and the conformational exchange of monoalkylated acylguanidines in solution are for the first time investigated in detail by NMR studies. In addition, the conformational preferences of a pharmacologically active acylguanidine in bisphosphonate tweezers and two new crystal structures of monoalkylated acylguanidines are presented. The compound pool comprises four unprotonated acylguanidines and seven protonated acylguanidines with up to six different anions, among them two biologically active substances. Studies in pure CD$_2$Cl$_2$ as well as in solvent mixtures of CD$_2$Cl$_2$ and DMSO were performed. Throughout the whole study, exclusively two (I/I$^+$ and II/II$^+$) out of eight possible acylguanidine conformations were detected in both the unprotonated and the protonated state independent of the compound, the anion or the solvent used. For the first time it is shown that the intermolecular interactions between the monoalkylated acylguanidines and the anions, solvent molecules or biomimetic receptors are decisive for both the conformational preferences and exchange rates. Under experimental conditions promoting the formation of only few strong and specific intermolecular H-bonds, conformation I/I$^+$ is preferred for both unprotonated and protonated acylguanidines, possibly due to entropic reasons. These strong and specific H-bonds, e.g. in pure CD$_2$Cl$_2$ and/or with anions with good H-bond acceptor properties, occur within dimers formed by the unprotonated acylguanidines and in salt bridges between the anion and protonated acylguanidines. The conformational preference shifts to II/II$^+$ and conformational

R. Kleinmaier, M. Keller, P. Igel, A. Buschauer, R. M. Gschwind, *J. Am. Chem. Soc*, **2010**, submitted.

exchange between I/I$^+$ and II/II$^+$ is accelerated as soon as more complex H-bond networks are established and/or the specific H-bonds are weakened. Typical experimental scenarios for this are microsolvation by DMSO and/or the use of anions with reduced H-bond acceptor properties, e.g. Cl$^-$. In accordance with these conformational trends, also in the presence of receptor molecules forming additional strong H-bonds to protonated acylguanidines, exclusively conformation II$^+$ was found for two different acylguanidines in NMR studies with bisphosphonate tweezers and also in a previous docking study with a membrane protein. Even the crystal structures of acylguanidines known so far resemble the conformational trend identified in this study. The two crystal structures of unprotonated acylguanidines with relatively isolated H-bond networks adopt conformation I, whereas the solid state structure of a protonated acylguanidine has a complex H-bond network and shows conformation II$^+$.

In summary, this study gives for the first time detailed insight into the conformational preferences of monoalkylated acylguanidines. In addition, consistent conformational trends are found throughout the compound pool including structurally diverse acylguanidines, two potent G-protein coupling receptor ligands as well as different anions and receptors. Considering the potential of these acylguanidines in medicinal chemistry and the fact that in the past such known preferences often lead to ligands with greatly increased affinity through the rigidization of the ideal binding conformation,[57-59] the presented work may contribute to the prediction and rational design of biologically active compounds containing monoalkylated acylguanidines.

3.5 Experimental

Routine NMR measurements were conducted on Bruker Avance 300 MHz, 400 MHz and 600 MHz spectrometers equipped with 5 mm BBI or TBI probeheads. The variable temperature experiments were conducted on a Bruker Avance 600 MHz spectrometer equipped with a BVT 3000 variable temperature unit. Deuterated NMR solvents were purchased from Aldrich, Deutero and Merck.

Starting materials were obtained from Sigma-Aldrich and Merck. Solvents were distilled prior to use.

(***R***)-***N***$^\alpha$-(2,2-Diphenylacetyl)-***N***-(4-hydroxybenzyl)-***N***$^\omega$-pentanoylargininamide (3, UR-MK50). Pentanoic anhydride (97.6 mg, 0.52 mmol, 1.1 eq) was added to a solution of N^G-Boc, O-*tert*-butyl protected BIBP 3226 (**3a**, 300 mg, 0.48 mmol, 1 eq) and NEt$_3$ (48 mg, 66 µL, 0.48 mmol, 1 eq) in CH$_2$Cl$_2$ (10 mL). The mixture was stirred at rt for 5 h. TFA (10 mL) was added and stirring was continued at rt for 2 h. MeOH (30 mL) was added followed by evaporation under reduced pressure. Purification with preparative HPLC (column: Eurospher-

100 C18, 250 × 32 mm, 5 μm; Knauer, Berlin, Germany) and lyophilization afforded the product as a white fluffy solid (190 mg, 0.28 mmol, 59 %). Mp > 118 °C (decomp.); ^{1}H-NMR (400 MHz, CD$_3$OD, COSY): δ (ppm) 0.93 (t, 3H, ^3J = 7.35 Hz, CH$_3$), 1.37 (m, 2H, C$\underline{H}_2$-CH$_3$), 1.48-1.76 (bm, 5H, CH-C$\underline{H}_2$-C$\underline{H}_2$, C$\underline{H}_2$-CH$_2$-CH$_3$), 1.83 (m, 1H, CH-C$\underline{H}_2$-CH$_2$), 2.45 (t, 2H, ^3J = 7.44 Hz, CH$_2$-CO), 3.23 (m, 2H, CH$_2$-C$\underline{H}_2$-NH), 4.2 (d, 1H, ^2J = 14.6 Hz, C$\underline{H}_2$-ArOH), 4.26 (d, 1H, ^2J = 14.59 Hz, C$\underline{H}_2$-ArOH), 4.43 (m, 1H, CH$^\alpha$), 5.07 (s, 1H, C$\underline{H}$-(Ph)$_2$), 6.7 (d, 2H, ^3J = 8.6 Hz, AA'BB'), 7.04 (d, 2H, ^3J = 8.62 Hz, AA'BB'), 7.16-7.31 (m, 10H, Ph); RP-HPLC (210 nm): 99 % (t$_R$ = 16.6 min, k = 5.1); HRMS: (FAB$^+$, MeOH/glycerin): *m/z* calcd. for [C$_{32}$H$_{39}$N$_5$O$_4$ + H]$^+$ 558.3080, found: 558.3080; C$_{32}$H$_{39}$N$_5$O$_4$ × C$_2$HF$_3$O$_2$ (671.7)

N-Propionyl-N'-butylguanidine (4a)

The preparation of [^{15}N$_2$]-N(boc)-N'(propionyl)-S-methylisothiourea has been published elsewhere.[30] According to that protocol, the unlabelled compound N(boc)-N'(propionyl)-S-methylisothiourea was prepared and reacted with an excess of butylamine to yield N(boc)-N'(propionyl)-N''-butylguanidine, which was boc-deprotected to obtain **4a**.

N(boc)-N'(propionyl)-N''-butylguanidine

N(boc)-N'(propionyl)-S-methylisothiourea (0.35 g, 1.42 mmol) was dissolved in DCM (5 ml) at r.t. and butylamine (0.69 ml, 7.10 mmol) was added in one batch via syringe. The mixture was stirred for 3h, then washed once with sat. aq. NaHCO$_3$-solution, water and brine, respectively. The organic phase was dried over Na$_2$SO$_4$ and the solvents evaporated under reduced pressure. The colorless oily residue was purified by column chromatography over silica gel to yield pure N(boc)-N'(propionyl)-N''-butylguanidine (0.30 g, 78%). ^{1}H-NMR (300 MHz, CDCl$_3$, 300 K) δ 0.90 (t, 3H), 1.18 (t, 3H), 1.35 (m, 2H), 1.48 (s, 9H), 1.51 (m, 2H), 2.42 (q, 2H), 3.39 (q, 2H), 8.95 (as, 1H), 12.43 (s, 1H).

N-Propionyl-N'-butylguanidine (4a)

TFA and DCA salts:

N(boc)-N'(propionyl)-N''-butylguanidine was dissolved in dry DCM with 50% TFA or DCA, respectively, upon cooling with an ice bath, then allowed to warm up to r.t. After 3h the solvents were evaporated in vacuo and the product purified. The oily residue was subjected to column chromatography over silica gel to yield the pure TFA or DCA salts.

R. Kleinmaier, M. Keller, P. Igel, A. Buschauer, R. M. Gschwind, *J. Am. Chem. Soc*, **2010**, submitted.

TFA salt: 0.30 g (1.11 mmol) of starting compound gave 0.21 g of product (80%). ^{1}H-NMR (300 MHz, CDCl$_3$, 300 K) δ 0.96 (t, 3H, ^3J = 7.31 Hz), 1.16 (t, 3H, ^3J = 7.49 Hz), 1.42 (m, 2H), 1.65 (m, 2H), 2.55 (q, 2H, ^3J = 7.49 Hz), 3.30 (m, 2H), 7.34 (s, 1H), 9.74 (s, 1H), 9.86 (as, 1H), 13.07 (s, 1H);

DCA salt: 0.09 g (0.33 mmol) of starting compound gave 0.05 g of product (50%). ^{1}H-NMR (300 Hz, CDCl$_3$, 300 K) δ 0.96 (t, 3H, ^3J = 7.31 Hz), 1.16 (t, 3H, ^3J = 7.49 Hz), 1.43 (m, 2H), 1.67 (m, 2H), 2.55 (q, 2H), 3.38 (m, 2H), 5.89 (s, 1H, DCA), 7.30 (s, 1H), 9.82 (s, 1H), 10.06 (s, 1H), 13.40 (s, 1H);

*Liberation of free base of **4a**:*

N(boc)-N'(propionyl)-N''-butylguanidine (0.10 mg, 0.37 mmol) was deprotected with 50% TFA in dry DCM. The crude product (oily residue) was subjected to column chromatography over silica gel in the presence of 5% TEA to yield the pure free base after evaporation of solvents (0.05 g, 78%). ^{1}H-NMR (300 MHz, CDCl$_3$, 300 K): δ 0.89 (t, 3H, ^3J = 7.31 Hz), 1.06 (t, 3H, ^3J = 7.49 Hz), 1.37 (m, 2H), 1.55 (m, 2H), 2.23 (q, 2H, ^3J = 7.49 Hz), 3.10 (m, 2H); ^{13}C-NMR δ 10.0, 13.6, 20.0, 30.8, 33.4, 40.8, 161.1, 186.9. HR-Mass (EI) calc. 171.1372, found 171.1369.

HCl salt: The free base was treated with a mixture of 10% conc. HCl aq. and 90% MeCN at r.t., stirred for 5 min and the solvents evaporated to yield the colorless solid product quantitatively. ^{1}H-NMR (600 MHz, CD$_2$Cl$_2$/10% (CD$_3$)$_2$SO, 285 K, ref. TMS internal) δ 0.95 (t, 3H, ^3J = 7.31 Hz), 1.16 (t, 3H, ^3J = 7.49 Hz), 1.42 (m, 2H), 1.62 (m, 2H), 2.53 (q, 2H, ^3J = 7.49 Hz), 3.29 (m, 2H), 8.66 (s, 1H), 8.80 (s, 1H), 9.27 (as, 1H), 12.58 (s, 1H); for complete ^{13}C data (assignment via HSQC, HMBC) see Supporting Information.

AcOH salt: Prepared in situ by titration of the free base with AcOH, both dissolved in the required NMR solvent, until integration proved a 1:1 ratio. For spectral data see Supporting Information.

N-Cinnamoyl-N'-butylguanidine (4b)

1H-Pyrazol-1-carboxamidine-hydrochloride

Aminoguanidinium-hydrogencarbonate (13.60 g, 100 mmol) was dissolved in water (25 ml) upon addition of conc. HCl (17 ml). To the resulting clear solution 1,1,3,3-tetramethoxy-propane (17.29 ml, 105 mmol) was added over 15 min using a dropping funnel. The mixture was warmed to 45 °C and stirred for 3h at that temperature. Evaporation of the solvent to the beginning of crystallization and completion upon resting in the fridge yielded large colorless crystals of 1H-Pyrazol-1-carboxamidine-hydrochloride, which were sucked off to obtain the

clean product. Yield: 10.3 g, 70.3 mmol, 70.3%. ^{1}H-NMR (300 MHz, CD$_3$OD, 300 K): δ 6.75 (dd, 1H, ^3J = 1.45 Hz, ^3J = 3.05 Hz, pyrazol-4-H), 7.98 (d, 1H, ^3J = 1.45 Hz, pyrazol-H), 8.48 (d, 1H, ^3J = 3.05 Hz, pyrazol-H).

N-Cinnamoyl-1H-pyrazol-1-carboxamidine

1H-Pyrazol-1-carboxamidine-hydrochloride (1.00 g, 6.84 mmol) was dissolved in DCM (15 ml) and TEA (1.94 ml, 13.68 mmol) was added. Cinnamoylchloride (1.14 g, 6.84 mmol) dissolved in DCM (10 ml) was added upon cooling in an ice bath through a dropping funnel. After 3h of stirring, the mixture was washed once with sat. aq. NaHCO$_3$-solution, water and brine, respectively. The organic phase was dried over Na$_2$SO$_4$ and the solvent evaporated under reduced pressure. Column chromatography in DCM over silica gel (Rf = 0.5) was necessary to isolate the pure product (0.90 g, 55%). ^{1}H-NMR (400 MHz, CDCl$_3$, 300 K) δ 6.46 (dd, 1H, ^3J = 1.59 Hz, ^3J = 2.76 Hz), 6.75 (d, 1H, ^3J = 15.91 Hz), 7.32-7.43 (m, 3H, Ph), 7.55-7.63 (m, 2H, Ph), 7.72 (1H pyrazol + 1H NH), 7.85 (d, 1H, ^3J = 15.91 Hz), 8.57 (d, 1H, ^3J = 2.76 Hz), 10.00 (bs, 1H, NH).

N-Cinnamoyl-N'-butylguanidine (4b)

N-Cinnamoyl-1H-Pyrazol-1-carboxamidine (0.50 g, 2.08 mmol) was dissolved in DCM (5 ml) and TEA (0.29 ml, 2.08 mmol) was added. Butylamine (1.05 ml, 10.4 mmol)) was added via syringe and the mixture stirred at r.t. for one hour. The solvents were evaporated, the oily residue was taken up in ethyl acetate and petrol ether was added. Upon resting in the fridge the clean product precipitated (0.31 g, 61 %). Recrystallization following the same procedure yielded crystals of **4B** suitable for x-ray crystallography. ^{1}H-NMR (600 MHz, CDCl$_3$, 300 K) δ 0.96 (t, 3H, ^3J = 7.42 Hz), 1.44 (m, 2H), 1.64 (m, 2H), 3.18 (m, 2H), 6.60 (d, 1H, ^3J = 15.91 Hz), 7.28-7.38 (m, 3H, Ph), 7.62 (d, 1H, ^3J = 15.91 Hz); HR-Mass (EI) calc. 245.1528, found 245.1534.

Preparation of salts:

HCl salt: Prepared by treating the free base with a mixture of 10% conc. HCl aq. and 90% MeCN at r.t., stirring for 5 min. The solvents were evaporated to yield the colourless solid product quantitatively. For complete ^{1}H and ^{13}C (assignment via HSQC, HMBC) data see Supporting Information.

TFA salt: Prepared by treating the free base with 5 % TFA in MeCN at r.t.and stirring for 5 min. The solvents were evaporated to yield the colourless solid product quantitatively.

R. Kleinmaier, M. Keller, P. Igel, A. Buschauer, R. M. Gschwind, *J. Am. Chem. Soc*, **2010**, submitted.

Salts with DCA and AcOH: Prepared in situ by titration of the free base with a carboxylic acid, both dissolved in the required NMR solvent, until integration proved a 1:1 ratio. For spectral data see Supporting Information.

Salts with Boc-L-Asp-OBn and 3,4,5-trimethoxybenzoic acid: Free base and the respective acid were weighed in at 1:1 stoichiometry and dissolved in the required NMR solvent. For spectral data see Supporting Information.

N-p-Dimethylaminobenzoyl-N'-butylguanidine (4c)

N-p-Dimethylaminobenzoyl-1H-Pyrazol-1-carboxamidine

p-Dimethylaminobenzoylchloride was prepared by refluxing p-dimethylaminobenzoic acid (2 g, 12.1 mmol) in 15 ml CHCl3 with 0.5 ml dimethylformamide and thionylchloride (1.73 g, 14.5 mmol) for one hour. This reaction solution was added in one batch to a solution of 1H-Pyrazol-1-carboxamidine-hydrochloride (2.13 g, 14.5 mmol) in $CHCl_3$ (15 ml) and TEA (8.4 ml, 60.5 mmol) while cooling with an ice bath. The mixture was allowed to warm up to r.t., stirred for 2 h, then washed once with sat. aq. $NaHCO_3$-solution, water and brine, respectively. The organic phase was dried over Na_2SO_4 and the solvent evaporated under reduced pressure. The product crystallized from $CHCl_3$ pure enough for the next step. (2.90 g, 93%). ^{1}H-NMR (300 MHz, $CDCl_3$, 300 K) δ 3.06 (s, 3H, -NMe$_2$), 6.46 (dd, 1H, ^3J = 1.59 Hz, ^3J = 2.76 Hz), 6.69 (m, 2H), 7.5-7.75 (s, 1H pyrazol + bs, 1H NH), 8.20 (m, 2H), 8.63 (d, 1H, 2.76 Hz), 10.04 (bs, 1H, NH).

N-p-Dimethylaminobenzoyl-N'-butylguanidine (4c)

N-p-dimethylaminobenzoyl-1H-Pyrazol-1-carboxamidine (1.0 g, 3.89 mmol) was dissolved in $CHCl_3$ (5 ml) and butylamine (1.90 ml, 19.5 mmol)) was added via syringe and the mixture stirred at r.t. for one hour. Since TLC analysis showed no conversion, the reaction mixture was heated under refluxing conditions for 3h. The solvents were evaporated and a solution of the oily product mixture in diethylether was prepared, from which the pure product was precipitated as sulphate salt by addition of 1M H_2SO_4 aq. The free base was liberated by addition of 1M NaOH aq. to the crystalline salt covered by ethylacetate. After phase separation the pure free base was obtained by evaporation of the solvent. ^{1}H-NMR (600 MHz, CD_2Cl_2, 300 K) δ 0.95 (t, 3H, ^3J = 7.35 Hz), 1.42 (m, 2H), 1.61 (m, 2H), 2.99 (s, 3H, -NMe$_2$), 3.20 (bas, 2H), 6.65 (m, 2H, ar), 8.01 (m, 2H, ar); HR-Mass (EI) calc. 262.1794, found 262.1789.

R. Kleinmaier, M. Keller, P. Igel, A. Buschauer, R. M. Gschwind, *J. Am. Chem. Soc*, **2010**, submitted.

N-p-Methoxybenzoyl-N'-butylguanidine (4d)

N-p-Methoxybenzoyl-1H-Pyrazol-1-carboxamidine

1H-Pyrazol-1-carboxamidine-hydrochloride (1.00 g, 6.84 mmol) was dissolved in $CHCl_3$ (15 ml) and TEA (1.94 ml, 13.68 mmol) was added. P-methoxybenzoylchloride (1.14 g, 7.52 mmol) dissolved in $CHCl_3$ (5 ml) was added upon cooling in an ice bath through a dropping funnel. The mixture was allowed to warm up to r.t., stirred for 2 h, then washed once with sat. aq. $NaHCO_3$-solution, water and brine, respectively. The organic phase was dried over Na_2SO_4 and the solvent evaporated under reduced pressure. Column chromatography in etylacetate / petrolether (2:5) over silica gel (R_f = 0.5) was necessary to isolate the pure product (1.50 g, 90%). ^{1}H-NMR (300 MHz, $CDCl_3$, 300 K) δ 3.88 (s, 3H, -OMe), 6.49 (dd, 1H, ^3J = 1.59 Hz, ^3J = 2.76 Hz), 6.95 (m, 2H), 7.75 (1H pyrazol + 1H NH), 8.26 (m, 2H), 8.65 (as, 1H), 10.08 (bs, 1H, NH).

N-p-Methoxybenzoyl-N'-butylguanidine (4d)

N-p-Methoxybenzoyl-1H-Pyrazol-1-carboxamidine (0.75 g, 3.07 mmol) was dissolved in $CHCl_3$ (5 ml) and butylamine (1.56 ml, 15.4 mmol)) was added via syringe and the mixture stirred at r.t. for one hour. The solvents were evaporated and crude column chromatography in ethylacetate / petrolether yielded the crude product with pyrazol impurity. The pure HCl-salt crystallized after addition of HCl. aq (1M) to a solution of the oily product mixture in diethylether. This yielded crystals of the HCl salt suitable for x-ray crystallography. The free base was liberated from the crystalline salt by dissolution in $CHCl_3$ and addition of 1M aq. NaOH. *HCl-salt*: ^{1}H-NMR (600 MHz, $CDCl_3$, 300 K) δ 0.97 (t, 3H, ^3J = 7.42 Hz), 1.49 (m, 2H), 1.73 (m, 2H), 3.48 (m, 2H), 3.86 (s, 3H, -OMe), 6.99 (m, 2H, ar), 7.77 (s, 1H, NH), 8.29 (m, 2H, ar), 9.53 (s, 1H, NH), 10.03 (s, 1H, NH), 11.89 (s, 1H, NH); HR-Mass (EI) calc. 249.1477, found 249.1476.

Computational details:

Equilibrium geometry calculations at ground state were carried out by means of the Spartan '06[56] program package using the standard Hartree-Fock 3-21G basis set.

Supporting Information Available: Description of the material included. Complete reference 04. Crystallographic data (.cif) files for **4b** (CCDC 772555) and **4d*HCl** (CCDC 772556). This material is available free of charge via the Internet at http://pubs.acs.org.

R. Kleinmaier, M. Keller, P. Igel, A. Buschauer, R. M. Gschwind, *J. Am. Chem. Soc*, **2010**, submitted.

3.6 Acknowledgement

3.7 References

(1)   Katritzky, A. R.; Rogovoy, B. V.; Cai, X.; Kirichenko, N.; Kovalenko, K. V. *J. Org. Chem.* **2004**, *69*, 309-313.

(2)   Saczewski, F.; Balewski, Ł. *Expert Opin. Ther. Patents* **2009**, *19*, 1417-1448.

(3)   Berlinck, R. G. S.; Burtoloso, A. C. B.; Kossuga, M. H. *Nat. Prod. Rep.* **2008**, *25*, 919–954.

(4)   Cole, D. C., et al. *Bioorg. Med. Chem. Lett.* **2008**, *18*, 1063-1066.

(5)   Lee, S.; Kim, T.; Lee, B. H.; Yoo, S.; Lee, K.; Yi, K. Y. *Bioorg. Med. Chem. Lett.* **2007**, *17*, 1291-1295.

(6)   Baumgarth, M.; Beier, N.; Gericke, R. *J. Med. Chem.* **1997**, *40*, 2017-2034.

(7)   Buschauer, A. *J. Med. Chem.* **1989**, *32*, 1963-1970.

(8)   O'Connor, S. P.; Atwal, K.; Li, C.; Liu, E. C.-K.; Seiler, S. M.; Shi, M.; Shi, Y.; Stein, P. D.; Wang, Y. *Bioorg. Med. Chem. Lett.* **2008** *18*, 4696–4699.

(9)   Ghorai, P.; Kraus, A.; Keller, M.; Goette, C.; Igel, P.; Schneider, E.; Schnell, D.; Bernhardt, G.; Dove, S.; Zabel, M.; Elz, S.; Seifert, R.; Buschauer, A. *J. Med. Chem.* **2008**, *51*, 7193–7204.

(10)   Schneider, E.; Keller, M.; Brennauer, A.; Hoefelschweiger, B. K.; Gross, D.; Wolfbeis, O. S.; Bernhardt, G.; Buschauer, A. *ChemBioChem* **2007**, *8*, 1981 – 1988.

(11)   Brennauer, A.; Dove, S.; Buschauer, A. In *Neuropeptide Y and related peptides, Handbook of Experimental Pharmacology*; Michel, M. C., Ed.; Springer: Berlin, Heidelberg, 2004; Vol. 162, p 505-546.

(12)   Schug, K. A.; Lindner, W. *Chem. Rev.* **2005**, *105*, 67-113.

(13)   Schlund, S.; Schmuck, C.; Engels, B. *J. Am. Chem. Soc.* **2005**, *127* 11115-11124.

(14)   Noel, J.; Germain, D.; Vadnais, J. *Biochemistry* **2003**, *42*, 15361-15368

(15)   Pretscher, A.; Brisander, M.; Bauer-Brandl, A. a.; Hansen, L. K. *Acta Crystallogr.* **2001**, *C57*, 1217-1219.

(16)   Buono, R. A.; Venanzi, T. J.; Zauhar, R. J.; Luzhkov, V. B.; Venanzi, C. A. *J. Am. Chem. Soc.* **1994**, *116*, 1502-1513.

(17)   Smith, R. L.; Cochran, D. W.; Gund, P.; Cragoe Jr., E. J. *J. Am. Chem. Soc.* **1979**, *101*, 191-201.

(18)   Zeslawska, E.; Schweinitz, A.; Karcher, A.; Sondermann, P.; Sperl, S.; Stuerzebecher, J.; Jacob, U. *J. Mol. Biol.* **2000**, *301*, 465-475.

(19)   Zeslawska, E.; Oleksyn, B.; Stadnicka, K. *Struct. Chem.* **2004**, *15*, 567-572.

(20)   Schmuck, C.; Wienand, W. *J. Am. Chem. Soc.* **2003**, *125*, 452-459.

(21)   Steiner, T. *Angew. Chem.* **2002**, *114*, 50-80.

(22)   Melo, A.; Ramosa, M. J.; Floriano, W. B.; Gomes, J. A. N. F.; Leao, J. F. R.; Magalhaes, A. L.; Maigret, B.; Nascimento, M. C.; Reuter, N. *J. Mol. Struc. (Theochem)* **1999**, *463*, 81–90.

(23)   Condic-Jurkic, K.; Perchyonok, V. T.; Zipse, H.; Smith, D. M. *J. Comput. Chem.* **2008**, *29*, 2425-2433.

(24)   Zheng, Y.-J.; Ornstein, R. L. *J. Am. Chem. Soc.* **1996**, *118*, 11237-11243.

(25)   Greenhill, J. V.; lsmail, M. J.; Bedford, G. R.; Edwards, P. N.; Taylor, P. J. *J. Chem. Soc., Perkin Trans. 2* **1985**, 1265-1274.

(26)   Greenhill, J. V.; lsmail, M. J.; Bedford, G. R.; Edwards, P. N.; Taylor, P. J. *J. Chem. Soc., Perkin Trans. 2* **1985**, 1255 - 1264.

(27)   Kirchner, B.; Reiher, M. *J. Am. Chem. Soc.* **2005**, *127*, 8748-8756.

(28)   Gschwind, R. M.; Armbrüster, M.; Zubrzycki, I. Z. *J. Am. Chem. Soc.* **2004**, *126*, 10228-10229.

(29)   CCDC 686506 contains the supplementary crystallographic data for the compound shown in Figure 3.2 (available free of charge at The Cambridge Crystallographic Data Centre via www.ccdc.cam.ac.uk/data_request/cif).

(30)   Federwisch, G.; Kleinmaier, R.; Drettwan, D.; Gschwind, R. M. *J. Am. Chem. Soc.* **2008**, *130*, 16846–16847.

(31)   Hettche, F.; Rei, P.; Hoffmann, R. W. *Chem. Eur. J.* **2002**, *8*, 4946-4956.

(32)   Alvarez, J.; Wang, Y.; Gomez-Kaifer, M.; Kaifer, A. E. *Chem. Commun.* **1998**, 1455 - 1457.

(33)   Schlund, S.; Schmuck, C.; Engels, B. *Chem. Eur. J.* **2007**, *13*, 6644-6653.

(34)   Igel, P.; Schneider, E.; Schnell, D.; Elz, S.; Seifert, R.; Buschauer, A. *J. Med. Chem.* **2009**, *52*, 2623-2627.

(35)   Rudolf, K.; Eberlein, W.; Engel, W.; Wieland, H. A.; Willim, K. D.; Entzeroth, M.; Wienen, W.; Beck-Sickinger, A. G.; Doods, H. N. *Eur. J. Pharmacol.* **1994**, *271*, R11-R13.

(36)   Keller, M.; Pop, N.; Hutzler, C.; Beck-Sickinger, A. G.; Bernhardt, G.; Buschauer, A. *J. Med. Chem.* **2008**, *51*, 8168–8172.

(37)   Feichtinger, K.; Sings, H. L.; Baker, T. J.; Matthews, K.; Goodman, M. *J. Org. Chem.* **1998**, *63*, 8432-8439.

(38)   Bergeron, R. J.; McManis, J. S. *J. Org. Chem.* **1987**, *52*, 1700-1703.

(39)   Kent, D. R.; Cody', W. L.; Doherty, A. M. *Tetrahedron Lett.* **1996**, *37*, 8711-8714.

(40)   Lal, B.; Gangopadhyay, A. K. *Tetrahedron Lett.* **1996**, *37*, 2483-2486.

(41)   Williams, R. M.; Yuan, C.; Lee, V. J.; Chamberland, S. *The Journal of Antibiotics* **1997**, *51*, 189-201.

(42)   Boy, K. M.; Zhu, S.; Macor, J. E.; Shi, S.; Gerritz, S.; Office, U. S. P. a. T., Ed. United States, 2007.

(43)   Fobare, W. F.; Solvibile, W. R.; Robichaud, A. J.; Malamas, M. S.; Manas, E.; Turner, J.; Hu, Y.; Wagner, E.; Chopra, R.; Cowling, R.; Jind, G.; Bard, J. *Bioorg. Med. Chem. Lett.* **2007**, *17*, 5353–5356.

(44)   Jennings, L. D.; Cole, D. C.; Stock, J. R.; Sukhdeo, M. N.; Ellingboe, J. W.; Cowling, R.; Jin, G.; Manas, E. S.; Fan, K. Y.; Malamas, M. S.; Harrison, B. L.; Jacobsen, S.; Chopra, R.; Lohse, P. A.; Moore, W. J.; O'Donnell, M.-M.; Hu, Y.; Robichaud, A. J.; Turner, M. J.; Wagner, E.; Bard, J. *Bioorg. Med. Chem. Lett.* **2008**, *18* 767–771.

(45)   Bernatowicz, M. S.; Wu, Y.; Matsueda, G. R. *J. Org. Chem.* **1992**, *57*, 2497-2502.

(46)   Bernatowicz, M. S.; Wu, Y.; Matsueda, G. R. *Tetrahedron Lett.* **1993**, *34*, 3389-3392.

(47)   Sharif, S.; Fogle, E.; Toney, M. D.; Denisov, G. S.; Shenderovich, I.; Buntkowsky, G.; Tolstoy, P. M.; Huot, M. C.; Limbach, H.-H. *J. Am. Chem. Soc.* **2007**, *129*, 9558-9559.

(48)   Kleinmaier, R.; Gschwind, R. M. *Magn. Reson. Chem.* **2010**, submitted.

(49)   Simulations of the conformational exchange rates between I$^+$ and II$^+$ for **4b***Boc-Asp-OBn and **4b***TFA showed that the broadening of the signals in

R. Kleinmaier, M. Keller, P. Igel, A. Buschauer, R. M. Gschwind, *J. Am. Chem. Soc*, **2010**, submitted.

48

Figure 3.7 is dominated by the exchange rate and that the different chemical shift dispersions affect the exchange rates only marginally. According to these simulations, at 210 K the rate constant for the conformational exchange is increased by a factor of 30 when going from the strong H-bond acceptor Boc-Asp-OBn to the much weaker TFA as anions.).

(50)   Sharif, S.; Denisov, G. S.; Toney, M. D.; Limbach, H.-H. *J. Am. Chem. Soc* **2007**, *129*, 6313-6327.

(51)   DOSY spectra of **4a***DCA at 300 K and **4d***DCA at 270 K showed identical diffusion coefficients for the anion and the cation. Due to the fast exchange of the NH protons in acylguanidines, the positions of the anions could not be verified by NOESY cross peaks..

(52)   We correlate here the H-bond acceptor strength of the anion with the electron density available for H-bonding in the carboxylate moiety, which is typically the higher the more basic the anions are, i.e. the weaker the acids they are derived from. This concept of ordering the anions by their electron densities has been checked and confirmed by an analysis of the ^{13}C chemical shifts of the carboxylic carbons of alkali salts of the acids used here (see SI).

(53)   Gojło, E.; Smiechowski, M.; Panuszko, A.; Stangret, J. *J. Phys. Chem. B* **2009**, *113*, 8128–8136.

(54)   Skawinski, W. J.; Ofsievich, A.; Venanzi, C. A. *Struct. Chem.* **2002**, *13*, 73-80.

(55)   Venanzi, C. A.; Plant, C.; Venanzi, T. J. *J. Comp. Chem.* **1991**, *12*, 850-861.

(56)   Wavefunction, Inc.;: Irvine, CA., 1991-2007.

(57)   Boeckler, F.; Gmeiner, P. *Pharmacol. Therapeut.* **2006**, *112*, 281-333.

(58)   Boeckler, F.; Gmeiner, P. *Biochim. Biophys. Acta* **2007**, *1768*, 871–887.

(59)   Kubinyi, H. *Pharm. Acta Helv.* **1995**, *69*, 259-269.

3.8   Supporting Information

Conformations, Conformational Preferences and Conformational Exchange of N-Substituted N'-Acylguanidines - Intermolecular Interactions Hold the Key

Roland Kleinmaier, Max Keller, Patrick Igel, Armin Buschauer, Ruth M. Gschwind*

3.8.1   Possible conformations of monoalkylated acylguanidines
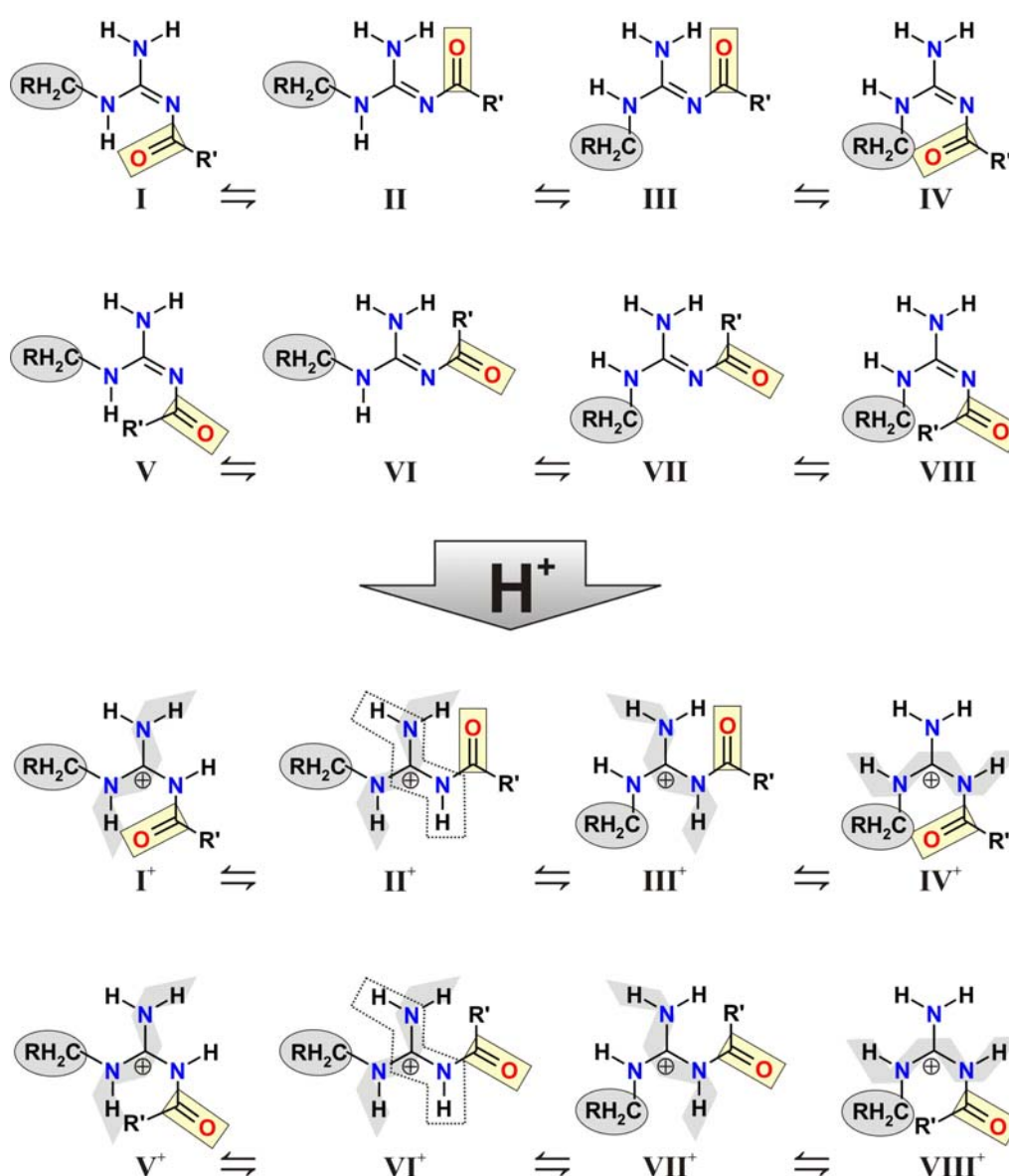
Scheme S3.2: Complete representation of the 8 planar conformations of monoalkylated acylguanidines in both unprotonated and protonated states, respectively.

Conformaitons IV through VIII can be excluded due to the missing intramolecular H-bond or severe sterical hindrance.

3.8.2 Preference of conformation I^+ in strong and specific H-bond networks – considerations to the entropy gain by rotation of the NH_2 group

Depicted below are four drawings of a contact ion pair between an acylguanidinium fragment and acetic acid, which are meant to visualize the rationale behind the postulation that an entropic contribution from the rotational flexibility of the NH_2 group is responsible for the energetic difference between the conformations I^+ and II^+, leading to the preference of conformation I^+ in a strongly coordinated contact ion pair.

In all these considerations, rotation of the NHalk group is neglected because in that case, a full rotation by 360° is required to form an H-bond again while for the NH_2 group, this state is reached after only 180°. Besides, rotation of the NHalk group by 180° to achieve planarity again would result in a different conformation, for which no spectral evidence was found. Thus, the focus is here solely on the differences in energy occurring upon rotational movements of the NH_2 group around the $H_2N\text{-}C^G$ bond in conformation I^+ versus conformation II^+.

The first picture (Figure S3.13) shows the acylguanidinium moiety in conformation I^+ in fully planar alignment with three H-bonds approximately in the C-N plane.

The second picture (Figure S3.14) suggests a transition state from the rotation of the NH_2 group where it has rotated by almost 90° but still the H-bonds to the anion may remain intact because the anion offers enough flexibility itself (i.e. it "follows the path" of the NH_2 group) to keep close enough to linearity in the bond path that the rotational barrier is lower than in the case of the second conformation, which will be discussed next.

The third picture (Figure S3.15) shows the same fragment as before, but now in conformation II^+, again with three H-bonds in an approximately even plane.

In the fourth picture (Figure S3.16), in contrast, it can be seen that upon rotation of the NH_2 group, the intramolecular H-bond to the carbonyl group will break almost immediately as soon as the bonding hydrogen atom moves out of plane because the carbonyl oxygen has very limited flexibility. Its free electron pairs are strictly in the plane and because of the C=O double bond, they cannot rotate freely. The initial geometry of the intramolecular H-bond closing a six membered ring differs from the case of the fork-like salt bridge described above; there seems to be a heavy kink in the donor-H-acceptor line. However, owing to the favoured H-bond acceptor directionality of 120° for a carbonyl type oxygen,[1] this is actually the ideal arrangement in this case and stabilizes the planarity and electron delocalized state of the acylguanidinium moiety, but it hinders in turn the free rotation of the NH_2 group out of the plane, at least when compared to the situation of the NH_2 group in the salt bridge. It is

R. Kleinmaier, M. Keller, P. Igel, A. Buschauer, R. M. Gschwind, *J. Am. Chem. Soc*, **2010**, submitted.

generally known that strong H-bonds prefer a linear arrangement in the donor-H-acceptor geometry[1] and this arrangement is lost very quickly in the case of the NH_2 group forming the intramolecular H-bond in conformation II^+.

There is, however, also spectral evidence for the rotation of the NH_2 group in conformation I^+, as line broadened signals for both NH_2 protons of conformation I^+ are obtained e.g in the spectrum of **4d***Boc-Asp-OBn in pure CD_2Cl_2 at 200 K (Figure S3.17). This is interpreted as effect of rotation close to slow exchange on the NMR time scale.

R. Kleinmaier, M. Keller, P. Igel, A. Buschauer, R. M. Gschwind, *J. Am. Chem. Soc*, **2010**, submitted.
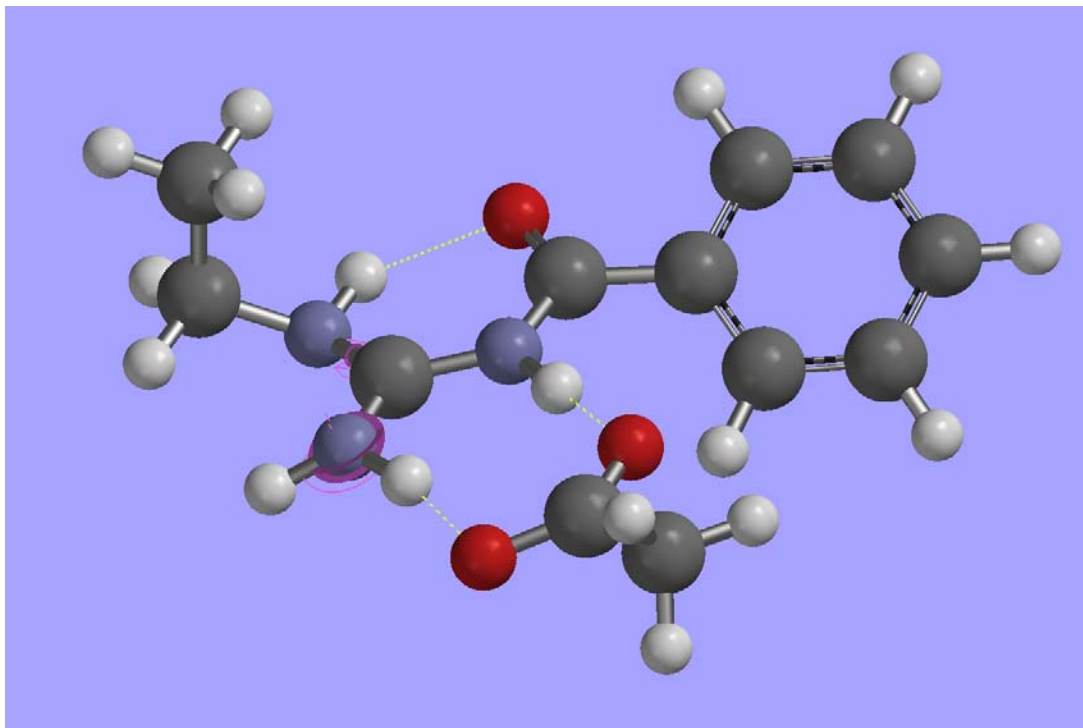
Figure S3.13: Illustration of conformation I+ with three H-bonds in the C-N plane.
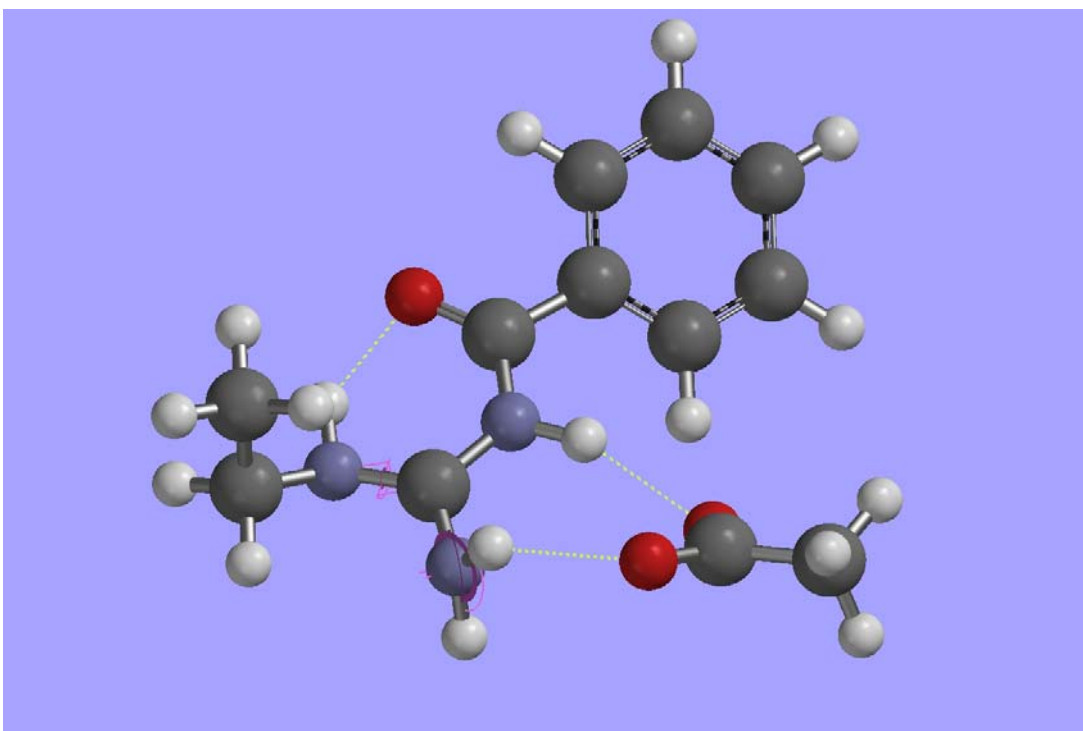
Figure S3.14: Illustration of conformation I$^+$ with NH$_2$ group turned out of plane by almost 90°. The flexibly bonded anion may follow the rotation and thus keep H-bonds intact.

R. Kleinmaier, M. Keller, P. Igel, A. Buschauer, R. M. Gschwind, *J. Am. Chem. Soc*, **2010**, submitted.
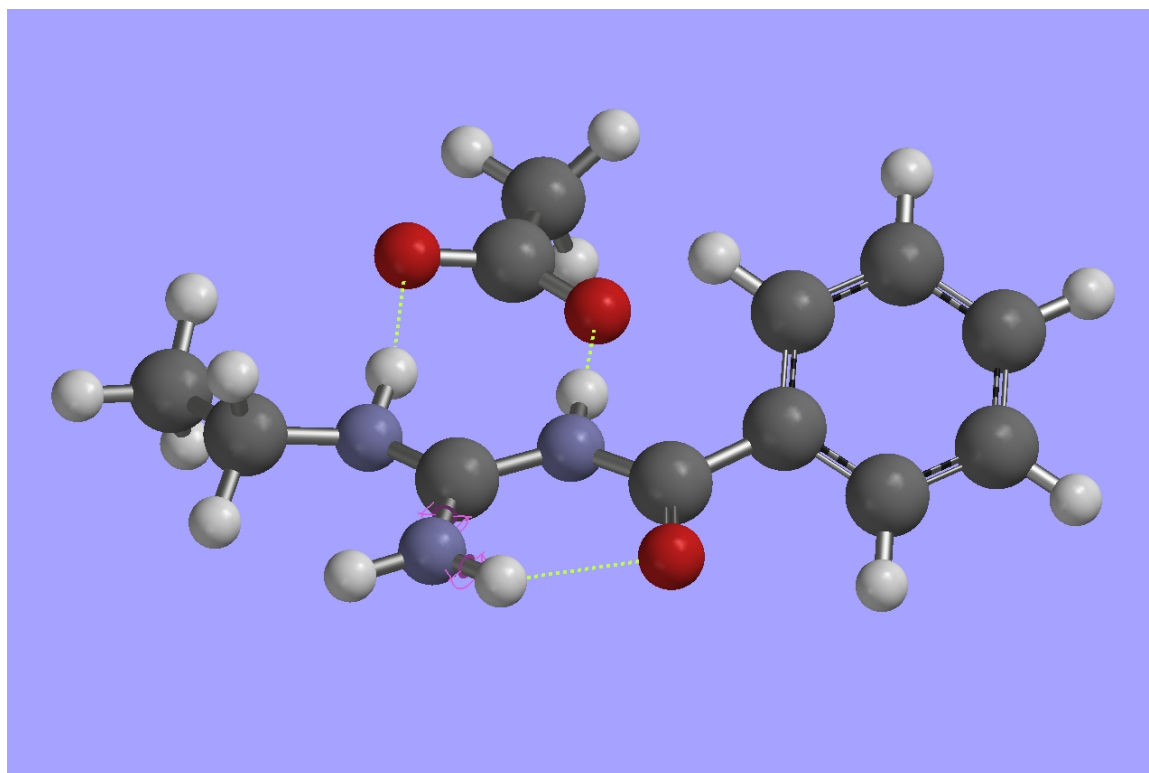
Figure S3.15: Illustration of conformation II^+ with NH_2 group in a planar intramolecular H-bond, again lying in the C-N plane.
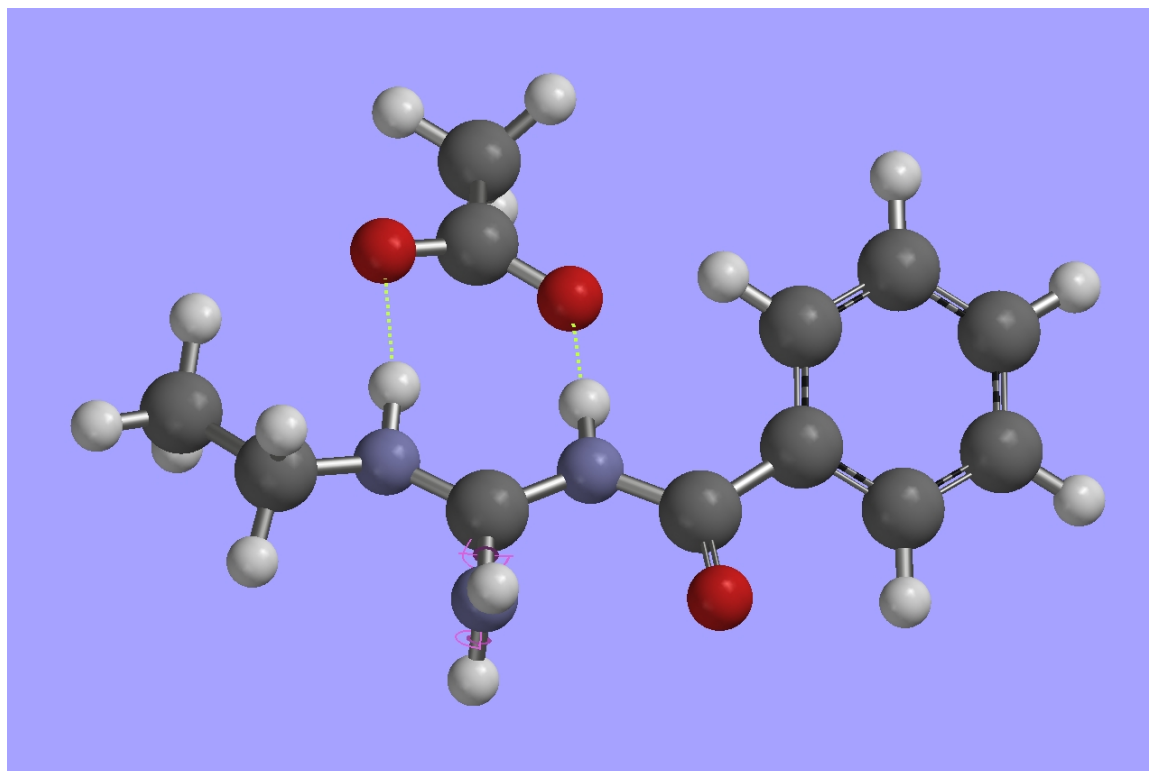
Figure S3.16: Illustration of conformation II^+ with the NH_2 group rotated out of the C-N plane. The carbonyl group cannot compensate for the increased distance (H-O) and the highly unfavourable geometry of this suggested transition state.

Spectral evidence of NH$_2$ rotation
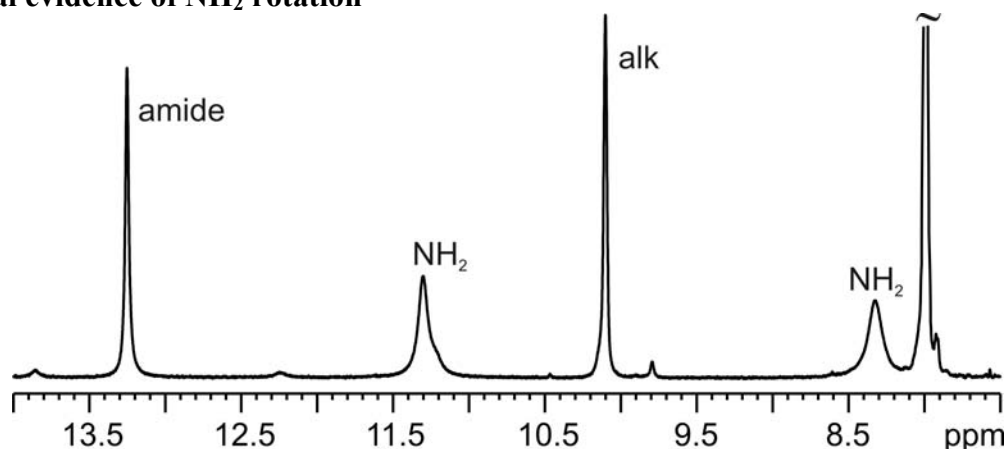
Figure S3.17 ^{1}H spectrum (600 MHz) of **4d***Boc-Asp-OBn in pure CD$_2$Cl$_2$ at 200 K. The NH$_2$ signals show significant line broadening effects (47 Hz and 64 Hz) compared to NHalk (15 Hz) and NHamide (lw 16 Hz).

Concluding, a possible rationale has been presented for the preference of conformation I$^+$ in strongly coordinated ion pairs in pure CD$_2$Cl$_2$. Geometrical considerations of the H-bond arrangements in both conformations have been combined with spectral evidence to support this theory. Accordingly, the higher degree of rotational freedom experienced by the NH$_2$ group in conformation I$^+$ results in an entropy gain that makes this the preferred conformation.

3.8.3 Dimerisation of the unprotonated acylguanidines - NMR-diffusion measurements on 4d

The general assignment of conformations in the free base is described in the main paper. Two sets of signals are observed, each delivering one NHalk cross peak with the CH$_2$ group. The high shifted NHalk must be in the intramolecular H-bond, i.e. this is conformation I, the low-shifted one belongs then to conformation II.

Signal broadening of conformation I in spectra of **4d** in pure CD$_2$Cl$_2$ at 225 K compared to conformation II was observed, which might be due to different aggregation behaviour of the two conformations. However, DOSY measurements[2,3] delivered nearly equal diffusion constants for both conformations.

The degree of aggregation obtained from these measurements points to the formation of dimers. The estimation of the degree of aggregation using van der Waals volumina[4,5] is known to produce values that are too large,[6] while a simple mass estimation[7] cannot regard any shape factors. However, for this relatively small molecule, the formation of dimers is

quite reliably indicated here. Overall, a significant difference in aggregation between the two conformations is not found.

Table S3.1: Degrees of aggregation derived from VdW volumes, via mass estimation and experimental diffusion coefficients D in $*10^{-10}$ m²/s from DOSY measurements of **4d** in CD_2Cl_2 at 225 K. For the dimers, VdW volumina are very close to double those of the monomers. Therefore, the degree of aggregation is half that of the monomer in both cases. Clearly, for the mass estimation, this is mathematical. However, the formation of at least dimers is indicated.

Species	Monomer I	Monomer II	Dimer I-I	Dimer I-II
Degree of agg via method				
VdW-Volume Chen-Sphere	**3.4**	**3.7**	**1.7**	**1.8**
Mass estim.	**2.0**	**2.2**	**1.0**	**1.1**
exp. D (mean) ($*10^{-10}$ m²/s)	**2.33** ±0.07	**2.23** ±0.04	**2.33** ±0.07	**2.23** ±0.04

Methodic aspects

For the estimation of the degree of aggregation using VdW volumina, the mean average was taken of values from calculations according to Zhao(Zhao_2003_JOC), Bondi[4] and obtained from energy minimized Spartan structures[8] and this number was employed as theoretical hydrodynamic volume.

Viscosity correction on TMS was done, a quasi-spheric shape of the solute was assumed and the microfriction factor according to Chen et al.[6] was used for the calculation of the experimental hydrodynamic volumina.

Dimeric structures were computed with Spartan in order to obtain VdW volumina for these species and to compare them to those for the monomers. However, it turned out that the calculated volumina of the dimers are very close to double those of the monomers. For the dimers, the mass is twice that of the monomer and for the VdW volume, the mean value of the calculated hydrodynamic volumina of the three possible dimers (Homo I-I, Homo II-II and Hetero I-II) was used, because these values are within 0.1% deviation. Hence, the degree of aggregation was calculated for the two different mean diffusion constants but with the averaged hydrodynamic volume, because no guess can be made about the type of dimer that would be present. The degree of aggregation obtained for the dimers has to be multiplied by a factor of two to be comparable to those for the monomers.

3D structures of dimers

A comparison of the structures of the two homodimers I-I and II-II as obtained by Hartree-Fock calculations with Spartan is depicted in Figure S3.18. These dimers form a symmetric structure with regard to the donor-acceptor pairs of the two mutual H-bonds. As already mentioned, no differentiation of these dimers is possible by their expected molecular volumes.

We propose only homodimers because there are only two sets of signals present in the spectra and no line broadening is observed for the second set, which must occur if the homodimers were exchanging with the heterodimer. Secondly, the difference in line width between the two signal sets is retained when DMSO is added and the portion of the sharp one increases. If this sharp species would be the heterodimer with exchange being suppressed by the large amount of conformation I present, then line broadening must be observed when increasing the portion of the heterodimer.

R. Kleinmaier, M. Keller, P. Igel, A. Buschauer, R. M. Gschwind, *J. Am. Chem. Soc*, **2010**, submitted.
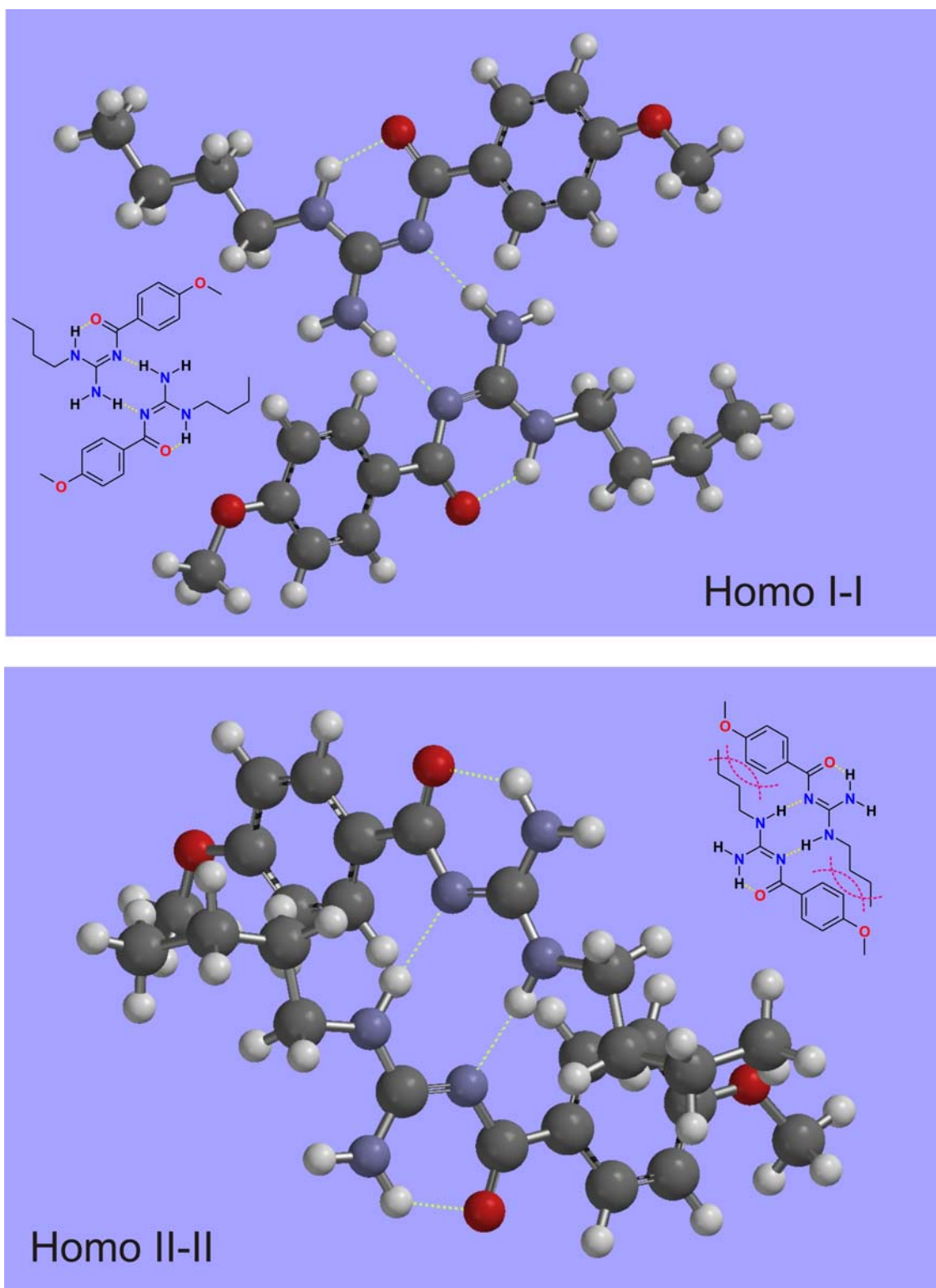
Figure S3.18: Geometry optimized Spartan[8] structures of the homodimers I-I and II-II, showing how steric bulk in II-II might weaken the intermolecular H-bonds and hinder molecular motion.

Steric hindrance in II-II may be the reason for the sharp signals, because the structure of II-II is more rigid than the one of I-I and therefore, less conformational exchange around the sidechains is expected in II-II leading to line broadening effects.

The Spartan structure shows that in Homo I-I, there is only little steric repulsion between the alkyl residue of one part and the respective acyl residue of the second part of the dimer. Thus, the intermolecular H-bonds are expected to be quite undisturbed, i.e. strong, and so the chemical shift of the NH protons forming these two symmetric H-bonds is almost as high as of the ones in the intramolecular H-bonds to the carbonyl oxygen. The signal broadening as compared to the second species is also due to the absence of steric hindrance because it allows for relatively free molecular motions of the single parts of the dimer.

3.8.4 ^{13}C chemical shift analysis of carboxylic carbons

The ^{13}C chemical shift of the carboxylate carbon can be used as indicator of the electron density present in the carboxylate oxygens. A reduction of the ^{13}C shift points towards increased electron density at this carbon, i.e. electron density being removed from the oxygens inductively by the electron withdrawing effect of electronegative substituents such as halogen atoms in the α-position. Regarding TMBA (3,4,5-trimethoxybenzoic acid), a strong mesomeric electron donating effect of the p-methoxy group increases the electron density at the carboxylic oxygens. Therefore, the ^{13}C chemical shift is not as directly indicative of this effect in this case. However, it is still almost as high in the acetate.

The trend observed for the alkali salts is also found for the esters with methanol or ethanol.

Overall, the ordering of the anions by their HBA strength as the inverse of their acid strength is confirmed by the ^{13}C chemical shifts: The higher the chemical shift, the greater the HBA strength of the anion.

Table S3.2: ^{13}C chemical shifts of alkali salts and aliphatic esters of carbonyl carbons of several carboxylic acids. As pendant for Boc-Asp-OBn, Na-hydrogen aspartate was chosen. Both in the alkali salts and the esters, there is an obvious trend towards lower chemical shift with reduced electron density.

compound	alkali salt in D_2O	ester	
acetate	**186.2** (Li-salt)	**171.5** (-OMe)	
sodium hydrogen L-aspartate	**178.4** (beta-CO) **175.1** (alpha-CO)	-	
TMBA	**174.2** (Na-salt)	**166.24** (-OEt)	
dichloroacetate	**171.6** (Na-salt)	**165.3** (-OMe)	
trifluoroacetate	**159.0, 158.7, 158.4 ,158.1** Na-salt in DMSO	**158.9, 158.6, 158.1, 157.7** (-OMe)	

With the exception of sodium 3,4,5-trimethoxybenzoate, the spectral data in this table were obtained from SDBSWeb: http://riodb01.ibase.aist.go.jp/sdbs/ (National Institute of Advanced Industrial Science and Technology, 09.04.2010). SBDS numbers: SDBS No.: 12693 (lithium acetate); SDBS No.: 2778 (methyl acetate); SDBS No.: 3672 (sodium dichloroacetate); SDBS No. 2478 (methyl dichloroacetate); SDBS No.: 11725 (sodium trifluoroacetate); SDBS No. 747 (methyl trifluoroacetate); SDBS No.: 18164 (methyl 3,4,5-trimethoxybenzoate); SDBS No. 2989 (sodium hydrogen L-aspartate); sodium 3,4,5-trimethoxybenzoate was produced by addition of 1eq NaOH to a solution of 3,4,5-trimethoxybenzoic acid in D_2O.

3.8.5 Complexation of 3 (UR-MK50) by Bisphosphonate Tweezers

A 1:1 complex of **3** and the symmetric bisphosphonate tweezers T1 (Figure S3.19) was investigated in CD_2Cl_2/10% DMSO-d_6 solution by low temperature NMR (210 K). Transfer of magnetization over NH···OP hydrogen bonds was achieved in this system and additionally, a hydrogen bond between the phenolic OH of **3** and the tweezers was found strong enough to do the same. Overall, 4 strong hydrogen bonds could be detected in this way. Besides, there is now strong indication for the existence of some other conformation (with a portion of less than 40%) which under the given conditions showed extreme line broadening that did not permit any deeper insight to its identity.

R. Kleinmaier, M. Keller, P. Igel, A. Buschauer, R. M. Gschwind, *J. Am. Chem. Soc*, **2010**, submitted.
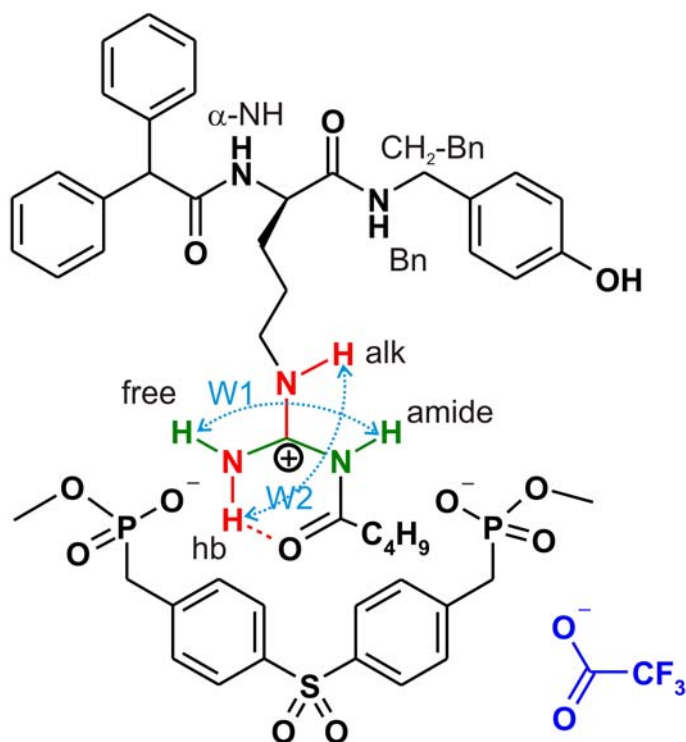
Figure S3.19: Schematic drawing of complex between 3 and T1 including nomenclature convention for NH protons. The dotted arrows (cyan) assign the two w-couplings W1 and W2 that were detected in the 210 K COSY spectrum of the complex in CD$_2$Cl$_2$ and DMSO-d6 (9:1).

The NH region of the proton spectrum of the complex at 210 K shows a lot more than the expected six NH plus one OH resonances (Figure S3.20), which is interpreted as a sign for the existence of more than one conformation. The ^{1}H decoupled ^{31}P spectrum also shows more than two peaks (Figure S3.20).

R. Kleinmaier, M. Keller, P. Igel, A. Buschauer, R. M. Gschwind, *J. Am. Chem. Soc*, **2010**, submitted.
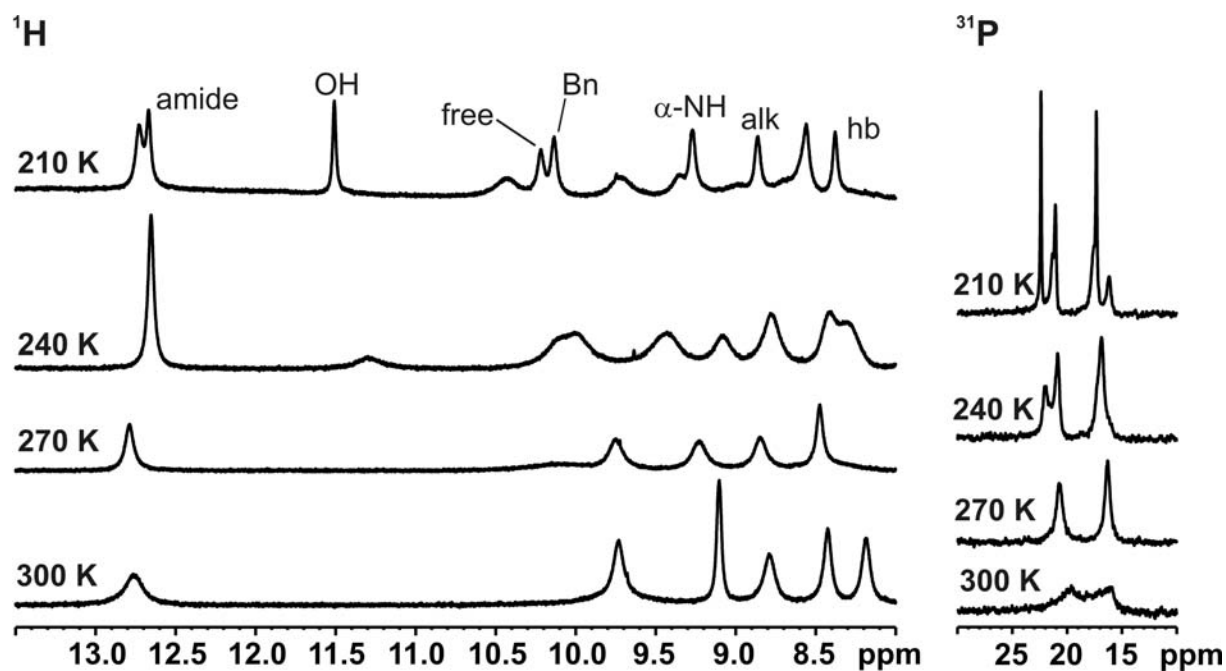
Figure S3.20: [1]H (NH section) and ^{31}P temperature series showing initial line broadening of proton signals and strong reduction of line widths for both ^{1}H and ^{31}P at 210 K; additionally the ^{1}H signals split up heavily.

The assignment of the NH protons naturally starts from those that have cross peaks to aliphatic protons: These are α-NH, NHalk and NHBn in the present molecule. Their assignment was complicated by diastereotopic splitting that is supposed to only become visible because of the rotational restriction imposed by the complexation (Figure S3.21).
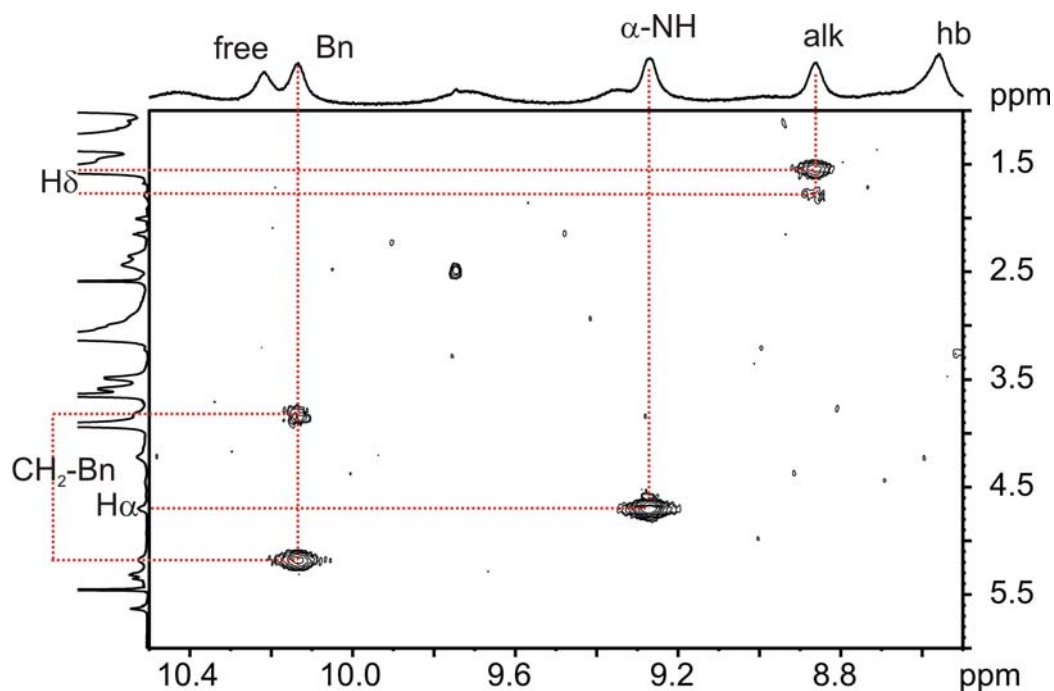
Figure S3.21: Assignment of α-NH, NHBn and NHalk via alipahtic crosspeaks was possible in the 210 K COSY spectrum, although it was slightly complicated by diastereotopic splitting.

Nevertheless, the latter three protons could be assigned and thus the w-coupling pattern could be solved to assign the remaining NH protons (see Figure S3.19 and Figure S3.22).
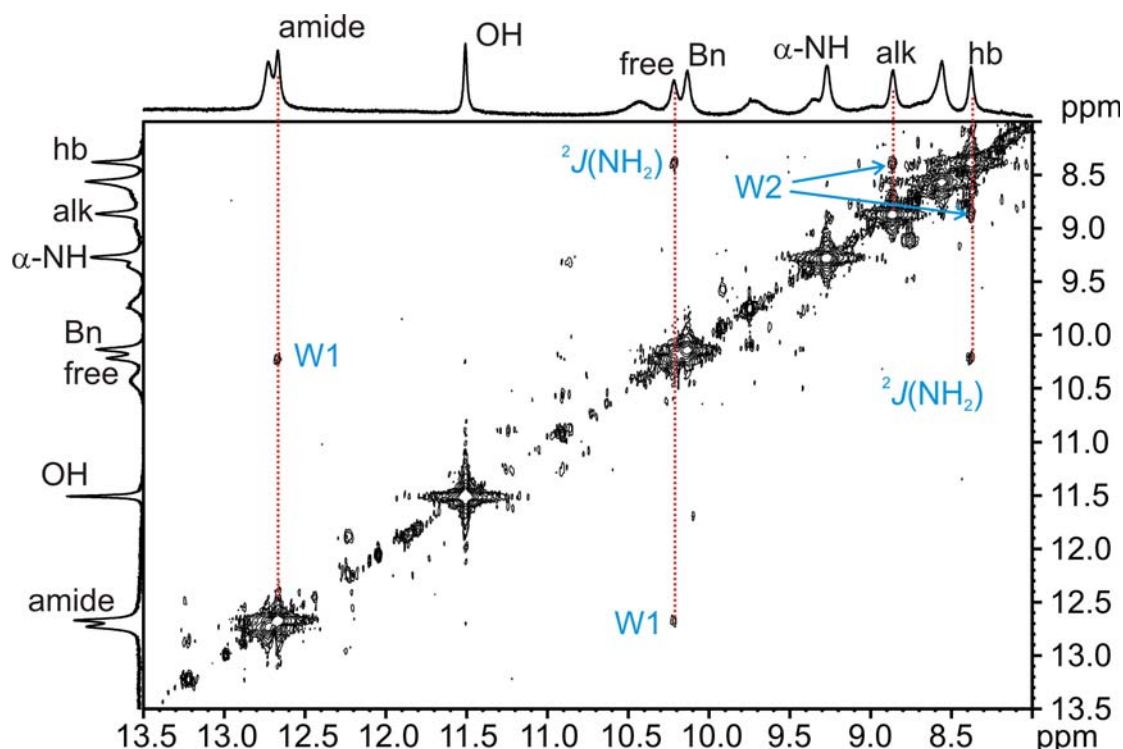
Figure S3.22: NH section of COSY spectrum at 210 K. The w-coupling pattern was solved knowing NHalk from its aliphatic crosspeak. There is one w-coupling between NHamide and NH2free and one between NHalk and NH2hb. In addition there is a crosspeak between the two NH$_2$ protons.

This way one consistent set of sharp resonances has been extracted and comparison to the ^{1}H,^{31}P HMBC spectrum confirms the assignment (Figure S3.23). This spectrum shows four peaks caused by transfer of magnetization over H-bonds via scalar couplings in addition to those caused by scalar couplings inside the tweezers. The strongest resonance is the one from the OH. NH$_2$free couples to the same phosphorous as does OH while NHamide and NHBn show couplings to the other one (Figure S3.23).
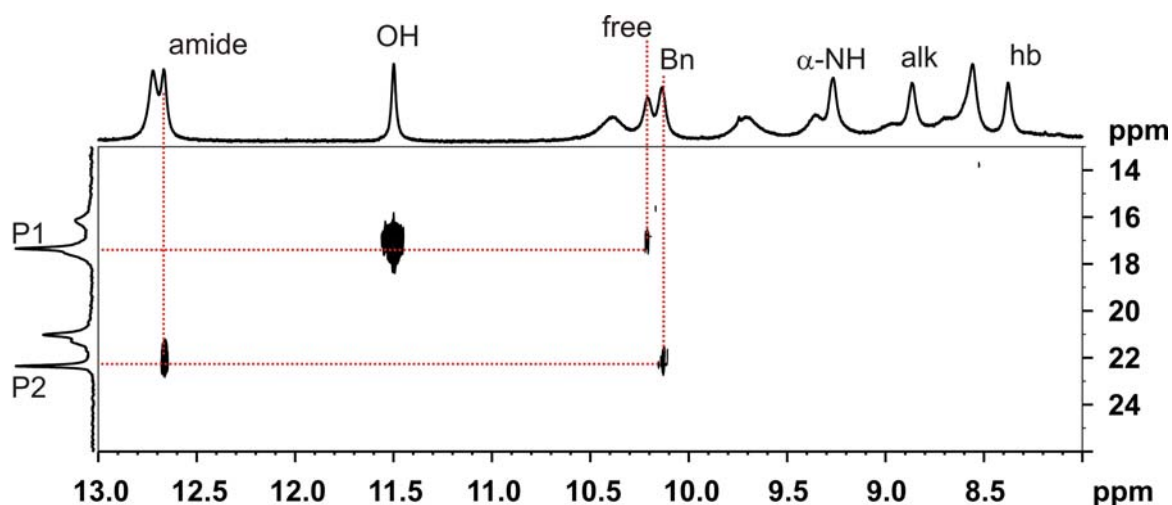
Figure S3.23: ^{1}H, ^{31}P HMBC at 210 K in CD$_2$Cl$_2$ and DMSO-d6 (9:1). The strongest peak is the one from OH to P1. NH$_2$free couples to the same phosphorous while NHamide and NHBn show couplings to the other one.

R. Kleinmaier, M. Keller, P. Igel, A. Buschauer, R. M. Gschwind, *J. Am. Chem. Soc*, **2010**, submitted.

For experimental details on the detection of trans-H-bond scalar couplings between ^{1}H and ^{31}P see Federwisch et al.[9]

A schematic representation of the complex as it is postulated from the findings layed out here in detail is found in Figure 11 in the main text of the paper. In that figure it can be seen that the quite low chemical shift of the protons of the δ–CH2 group may be due to its positioning in the anisotropy cone of the phenol ring that is fixed by the H-bond of its OH group to the tweezers, which is a further hint to the correctness of the representation as postulated from the ^{1}H, ^{31}P HMBC.

Geometry optimization of the complex 3-T1

3 and the **T1** tweezers moietes of the complex were calculated separately by Spartan[8] (Hartree-Fock, 3-21 G basis set). Afterwards the two parts were positioned "by hand" in the mode of binding postulated from the NMR experiments. The four intermolecular H-bonds detected by the ^{1}H, ^{31}P HMBC were inserted as covalent bonds (using hydrogens from the inorganic set with two valences) and the complex was then submitted to geometry optimization (Hartree-Fock, 3-21 G basis set).

The resulting model was then led back to non-covalent H-bonds by removing the "covalent H-bonds" and replacing the divalent H-atoms by the classic ones. However, after additional manual adjustment of the position of the acylguanidinium group, four intermolecular H-bonds were indicated by the program. Subsequent energy minimization and geometry optimization (Hartree-Fock 3-21 G basis set) retained those H-bonds with bond lengths as indicated in the main text and led to the 3D graphic representation used to clarify the possible spatial arrangement.

3.8.6 HPLC analysis of (R)-N$^{\alpha}$-(2,2-Diphenylacetyl)-N-(4-hydroxybenzyl)-N$^{\omega}$-pentanoylargininamide (3, UR-MK50).

Purification of **3** with preparative HPLC was performed on a system from Knauer (Berlin, Germany) consisting of two K-1800 pumps and a K-2001 detector. A Eurospher-100 C18 (250 × 32 mm, 5 μm; Knauer, Berlin, Germany) served as RP-column at a flow rate of 38 mL/min. Mixtures of acetonitrile and 0.1 % aq. TFA were used as mobile phase. Acetonitrile was removed from the eluates under reduced pressure (final pressure: 60 mbar) at 40 °C prior to lyophilization. Reversed-phase analytical HPLC analysis of **3** was performed on a system from Thermo Separation Products consisting of a SN400 controller, a P4000 pump, a

degasser (Degassex DG-4400, phenomenex), an AS3000 autosampler and a Spectra Focus UV-VIS detector. A Eurospher-100 C18 (250 × 4 mm, 5 µ, Knauer, Berlin, Germany) was used as stationary phase at a flow rate of 0.8 mL/min. Acetonitrile (A) and 0.05 % aq. TFA (B) were used as mobile phase components. The oven temperature was set to 30°C. The solution for injection (50 µM, inj. vol.: 100 µL) was prepared in a mixture of A and B corresponding to the composition at the beginning of the gradient. The following gradient was used for analytical HPLC analysis of **3**: 0 to 30 min: A/B 20/80 to 95/5, 30 to 40 min: 95/5.

for data processing:

The retention (capacity) factor k was calculated according to $k = (t_R - t_0)/t_0$.
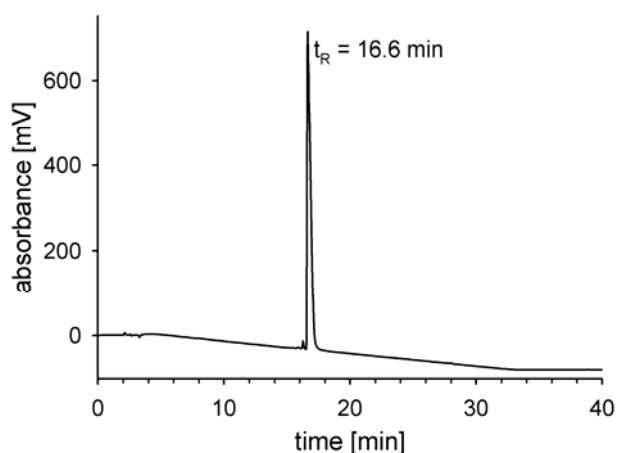
Figure S3.24: HPLC purity control of **UR-MK50** (**3**). Eluent: mixtures of acetonitrile (A) and 0.05 % aq. TFA (B), gradient: 0 to 30 min: A/B 20/80 to 95/5, 30 to 40 min: 95/5, detection: 210 nm, injection: 100 µL of a 50 µM solution of **3** in a mixture of acetonitrile and 0.05 % aq. TFA (20/80) prepared from a 10 mM solution in acetonitrile, t_R = 16.6 min, k = 5.1.

3.8.7 Low temperature spectra of salts of 4a
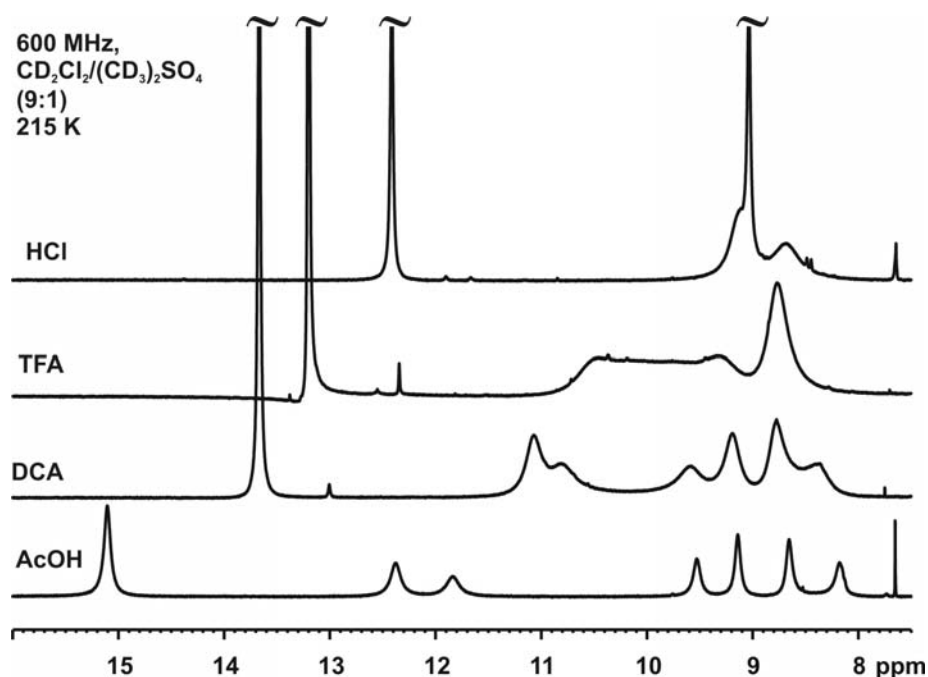
Figure S3.25: [1]H spectra of **4a** with anions of HCl, TFA, DCA and AcOH in CD_2Cl_2 and DMSO-d_6 at 215 K. The gradually increasing signal dispersion is visible as described in the text of the main paper.

3.8.8 Comparison of low temperature spectra of TFA salts of 1, 2, 3 and 4a
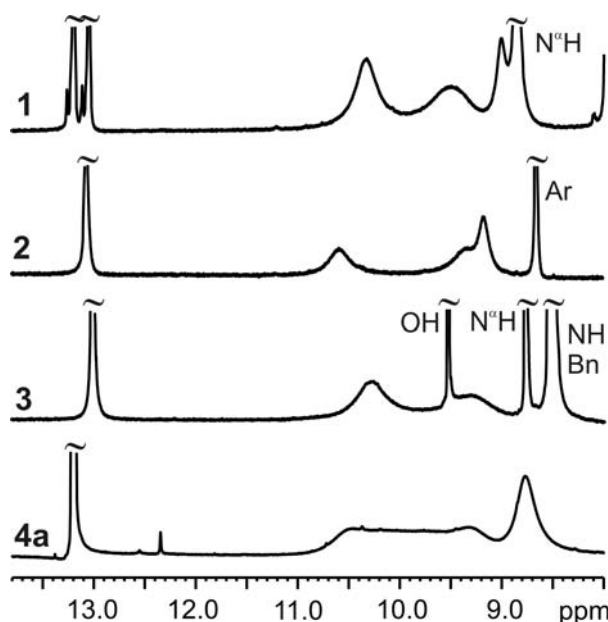
Figure S3.26: NH sections of ^{1}H spectra of the TFA salts of **1**, **2**, **3** and **4a** at 215 K in CD_2Cl_2 and DMSO-d_6 (9:1). The general peak pattern is consistent; all guanidinium NH resonances except those for NHamide are broadened, indicating coalescence of the two conformations.

3.8.9 Conformational exchange in 4d is reduced with lower amounts of DMSO
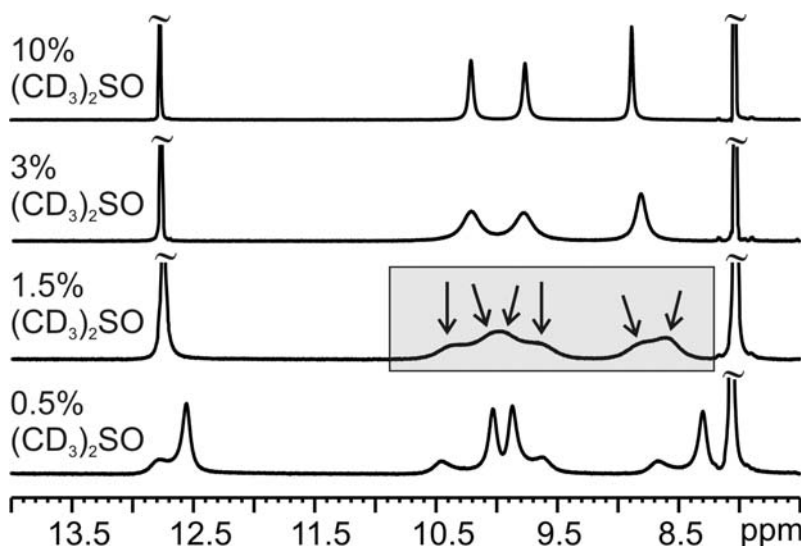
Figure S3.27: NH sections of ^{1}H spectra of the TFA salts of **4d** at 215 K in CD_2Cl_2 and DMSO-d_6. Depending on the amount of DMSO present as microsolvating agent, conformational exchange is fast enough to produce 4 sharp signals (10% DMSO) or slowed down so much as to allow for the detection of 8 resonances (0.5% DMSO).

3.8.10 Sample concentration and DMSO content

Titration of the free acylguanidine bases with acid dissolved in the respective NMR solvent is possible in the case Boc-Asp-OBn, TMBA, DCA and AcOH because they possess non-exchangeable protons visible in a ^{1}H NMR experiment. Thus 1:1 stoichiometry could be ensured by theses titration procedures. Solvents employed were CD_2Cl_2 and CD_2Cl_2 with approximately 10% DMSO-d_6, a value which can only be given exactly in the volume of DMSO added, whereas the percentage is not as exact due to the high volatility of CD_2Cl_2 and the need to replace CD_2Cl_2 evaporating over time from the samples.

However, in the concentration range of the samples used in the current work (20 – 50 mM), already one percent of DMSO-d_6 corresponds to an over 40-fold excess respective to the substrate so that slight deviations in the DMSO-d_6 content cannot be suspected to have any influence on the general picture.

3.8.11 Spectral data

3.8.11.1 ^{1}H NMR of salts

^{1}H NMR of N-propionyl-N'-butylguanidinium acetate (**4a*AcOH**), (600 MHz, CD$_2$Cl$_2$/ 10% (CD$_3$)$_2$SO, 300 K, TMS) δ 0.94 (t, 3H), 1.01 (t, 3H), 1.39 (m, 2H), 1.59 (m, 2H), 1.87 (s, 3H), 2.45 (m, 2H), 3.19 (m, 2H).

^{1}H NMR of N-cinnamoyl-N'-butylguanidinium acetate (**4b*AcOH**), (600 MHz, CD$_2$Cl$_2$/ 10% (CD$_3$)$_2$SO, 270 K, TMS) δ 0.96 (t, 3H), 1.41 (m, 2H), 1.62 (m, 2H), 1.96 (s, 3H), 3.23 (m, 2H), 6.89 (d, 2H), 7.43 (m, 3H), 7.63 (m, 2H) 7.74 (d, 2H).

^{1}H NMR of N-cinnamoyl-N'-butylguanidinium dichloroacetate (**4b*DCA**), (600 MHz, CD$_2$Cl$_2$/ 10% (CD$_3$)$_2$SO, 300 K, TMS) δ 0.97 (t, 3H), 1.43 (m, 2H), 1.65 (m, 2H), 3.29 (m, 2H), 5.96 (s, 1H), 6.91 (d, 2H), 7.43 (m, 3H), 7.62 (m, 2H) 7.79 (d, 2H), 8.29 (s, 1H), 9.96 (s, 1H), 10.37 (s, 1H), 14.11 (s, 1H).

^{1}H NMR of N-cinnamoyl-N'-butylguanidinium trifluoroacetate (**4b*TFA**), (600 MHz, CD$_2$Cl$_2$/ 10% (CD$_3$)$_2$SO, 300 K, TMS) δ 0.97 (t, 3H), 1.43 (m, 2H), 1.65 (m, 2H), 3.30 (m, 2H), 6.86 (d, 2H), 7.43 (m, 3H), 7.61 (m, 2H) 7.81 (d, 2H), 8.34 (s, 1H), 9.77 (s, 1H), 10.15 (s, 1H), 13.51 (s, 1H).

^{1}H NMR of N-cinnamoyl-N'-butylguanidinium*Boc-Asp-OBn (**4b*Boc-Asp-OBn**), (600 MHz, CD$_2$Cl$_2$/ 10% (CD$_3$)$_2$SO, 300 K, TMS) δ 0.96 (t, 3H), 1.39 + 1.43 (s + m, together 12H), 1.62 (m, 2H), 2.61 (d, 1H), 2.94 (d, 1H), 3.23 (m, 2H), 4.47 (m, 1H), 5.08 (d, 1H), 5.18 (d, 1H), 6.09 (d, 1H), 6.83 (d, 2H), 7.21-7.33 (m, 5H), 7.35-7.43 (m, 3H), 7.63-7.69 (m, 2H), 7.72 (d, 2H).

^{1}H NMR of N-cinnamoyl-N'-butylguanidinium*3,4,5-trimethoxybenzoate (**4b*TMBA**), (600 MHz, CD$_2$Cl$_2$/ 10% (CD$_3$)$_2$SO, 300 K, TMS) δ 0.98 (t, 3H), 1.45 (m, 2H), 1.67 (m, 2H), 3.29 (m, 2H), 3.80 (s, 3H), 3.90 (s, 6H), 7.11 (d, 1H), 6.09 (d, 1H), 7.35-7.45 (m, 5H), 7.65 (m, 2H), 7.78 (d, 1H).

3.8.11.2   COSY section with w-couplings in 1 ([$^{15}N^{\eta}_2$]-Bz-Arg(N$^{\eta}$-propionyl)-OEt*TFA)
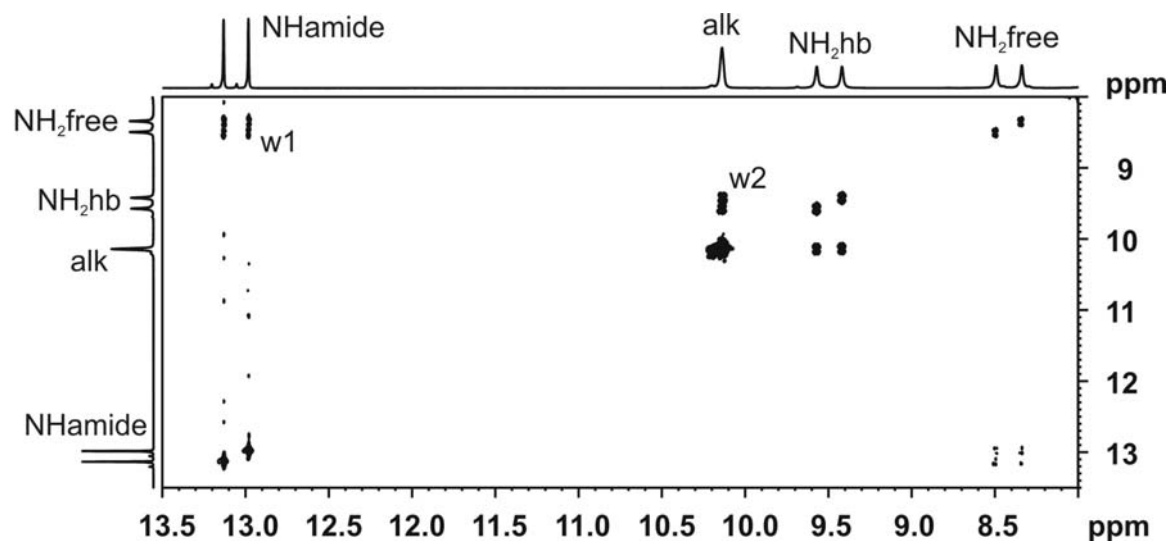
Figure S3.28: Section of COSY spectrum of **1** ([$^{15}N^{\eta}_2$]-Bz-Arg(N$^{\eta}$-propionyl)-OEt*TFA) in CD$_2$Cl$_2$/(CD$_3$)$_2$SO 9:1 at 300 K. W1 and W2 assign the w-couplings. These cross peaks contain multiplet information, which distinguishes them from mere exchange peaks.
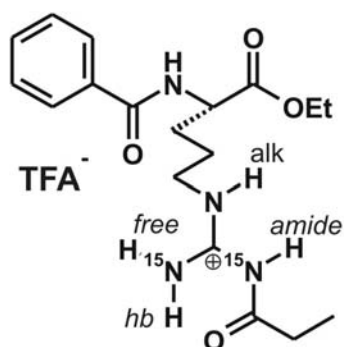
Figure S3.29: Structural formula of **1** ([$^{15}N^{\eta}_2$]-Bz-Arg(N$^{\eta}$-propionyl)-OEt*TFA) with assignment.

3.8.11.3 COSY section with w-couplings in 2
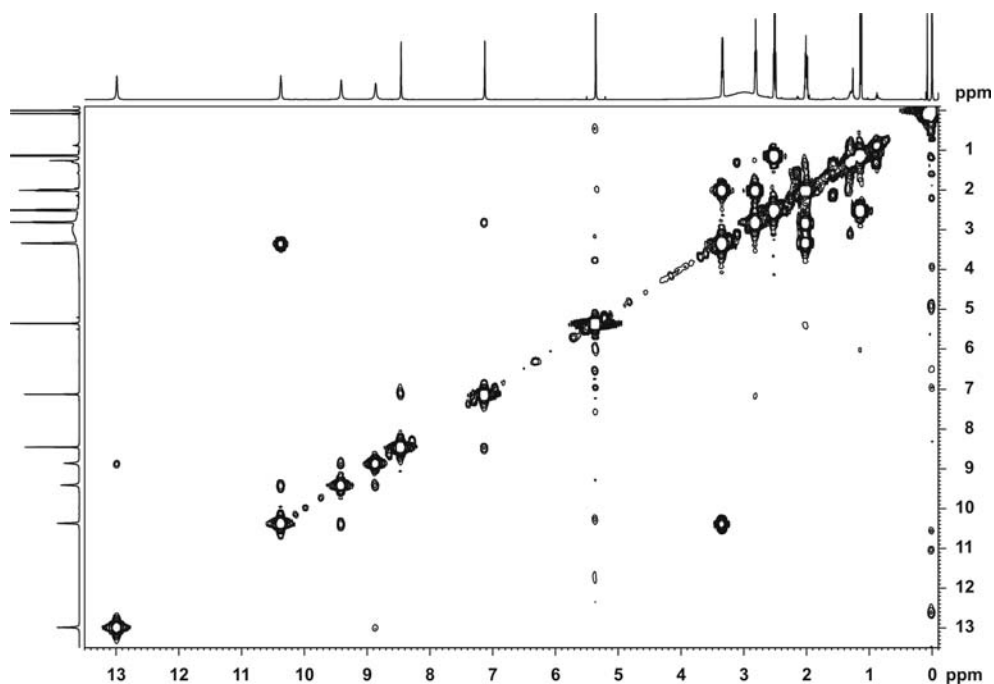
Figure S3.30: COSY spectrum of N-propionyl-N'-imdazolylpropylguanidinium*TFA (**2**) at 300 K in CD$_2$Cl$_2$/(CD$_3$)$_2$SO 9:1. W-couplings between guanidinium NHs are clearly visible.

R. Kleinmaier, M. Keller, P. Igel, A. Buschauer, R. M. Gschwind, *J. Am. Chem. Soc*, **2010**, submitted.

3.8.11.4 Additional spectra for 4b showing splitting to two conformations
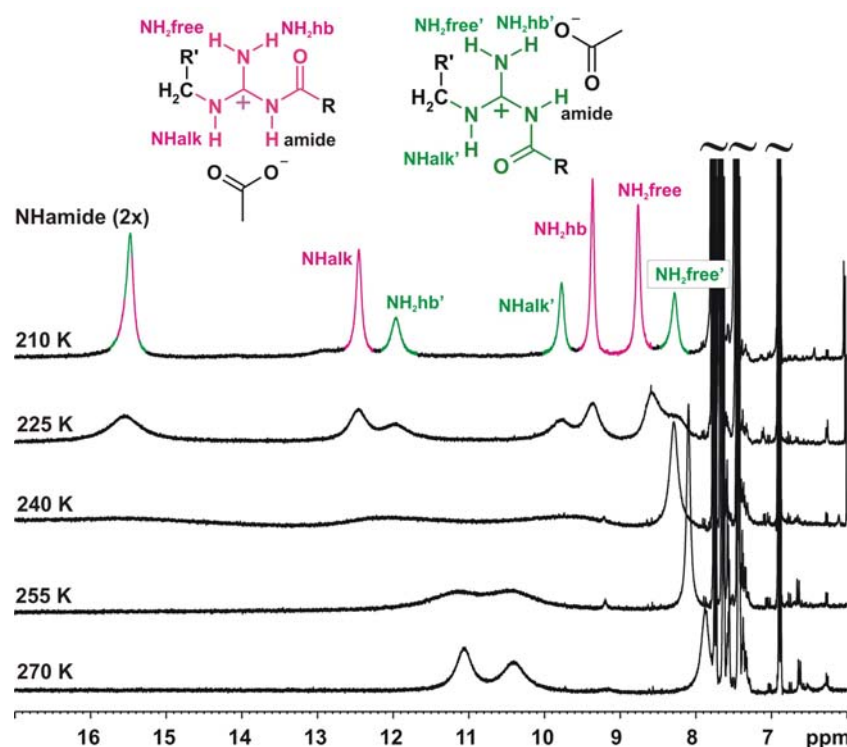
Figure S3.31: Colour coded temperature stack of ^{1}H NMR sections (600 Mhz) of **4b*AcOH** (N-cinnamoyl-N'-butylguanidinium acetate) in CD$_2$Cl$_2$/ DMSO-d_6 9:1 at temperatures from 270 K to 210 K. Red = conformation II$^+$, green is conformation I$^+$.
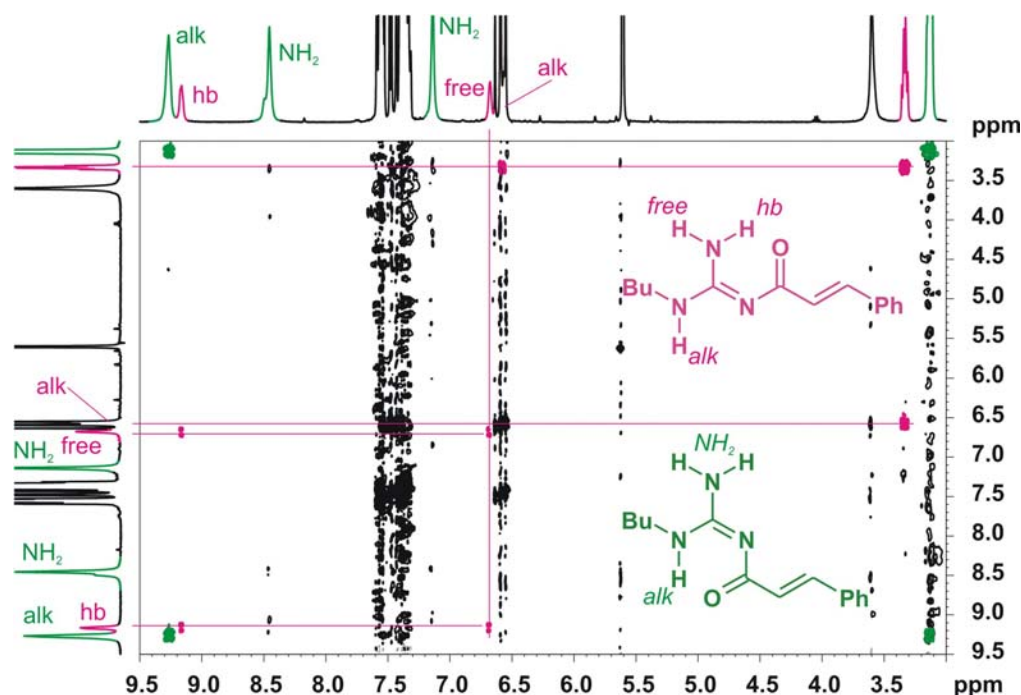
Figure S3.32: Colour-coded assignment of the two conformations detectable for the free base of **4b** (N-cinnamoyl-N'-butylguanidine) in COSY spectrum (600 MHz) in CD$_2$Cl$_2$/DMSO-d_6 1:1 at 238 K. The two signals between 3.0 and 3.5 ppm belong to the CH$_2$-group directly neighbouring NHalk and thus their ^3J crosspeak with NHalk is the starting point of assignment. (Red = conformation II, green is conformation I).

R. Kleinmaier, M. Keller, P. Igel, A. Buschauer, R. M. Gschwind, *J. Am. Chem. Soc*, **2010**, submitted.

3.8.11.5 Assignment tables

4a*HCl

Table S3.3: Assignment of **4a*HCl** (N-propionyl-N'-butylguanidine*HCl) in DCMd2 + 10% DMSOd6, 285 K, referenced to TMS internal.

Assignment	δ ^{1}H	m	δ ^{13}C	^{3}J H-H (Hz)	^{1}J ^{1}H-^{13}C (Hz)
nBu-CH$_3$	0.95	t	13.8	7.37	125.2
propionyl-CH$_3$	1.16	t	8.6	7.44	128.7
nBu-CH$_2$-b	1.42	m	20.2	-	133.0
nBu-CH$_2$-c	1.61	m	30.6	-	126.6
propionyl-CH$_2$	2.53	q	31.0	7.44	128.7
nBu-CH$_2$-d	3.30	b-q	41.6	n.a.	139.6
NH$_2$-free	8.66	s	-	-	
NH$_2$-hb	8.80	s	-	-	
NH-CH$_2$	9.27	a-s	-	-	
NH-amide	12.58	s	-	-	
Carbons:					
C-guanidinium	-	-	154.8	-	-
CONH	-	-	177.4	-	-

4b*HCl

Table S3.4: Assignment of **4b*HCl** (N-cinnamoyl-N'-butylguanidine*HCl) in CD$_2$Cl$_2$ with 7% DMSOd6 at 285 K; NH$_2$ differenciated via analogy to COSY at 300 K. Referenced to TMS internal.

Assignment	δ ^{1}H	m	δ ^{13}C	^{3}J H-H (Hz)	^{1}J ^{1}H-^{13}C (Hz)
nBu-CH$_3$	0.96	t	13.8	-	125.9
nBu-CH$_2$-b	1.44	m	20.3	-	126.8
nBu-CH$_2$-c	1.65	m	30.6	-	129.3
nBu-CH$_2$-d	3.34	m	41.7	-	139.5
cinnamoyl-CH-α	6.73	d	119.0	15.84	163.5
cinnamoyl-CH-β	7.91	d	146.4	15.84	155.0
NH$_2$-free	8.64	s	-	-	-
NH$_2$-hb	8.94	s	-	-	-
NH-CH$_2$	9.42	a-s	-	-	-
NH-amide	12.90	s	-	-	-
Ar-ortho	7.63	m	129.2		
Ar-meta Ar-para	7.40-7.45	m	129.4 + 131.5		
Carbons:					
C-guanidinium	-		155.3		-
CONH	-		168.2		-

R. Kleinmaier, M. Keller, P. Igel, A. Buschauer, R. M. Gschwind, *J. Am. Chem. Soc*, **2010**, submitted.

C-ar-quaternary	-		134.1	-	-
	-	-		-	
	-	-		-	

Assignment of 4c free base
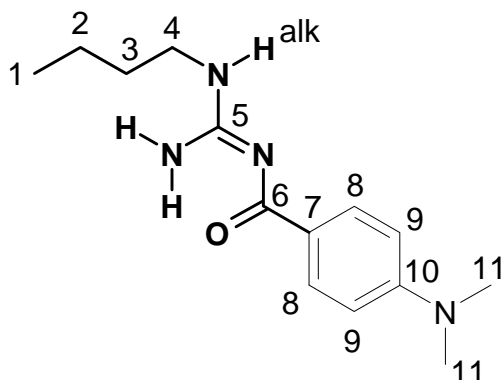
Figure 3.33: Structural formula of 4c with atom numbering used in the assignment table.

Table S3.5: Assignment of **4c** at 225 K in CD$_2$Cl$_2$, referenced to TMS internal. Two sets of signals for the two conformations that can be distinguished at 225 K are denoted A and B both for protons and carbons.

Group	δ ^{1}H (A)	δ ^{13}C (A)	δ ^{1}H (B)	δ ^{13}C (B)
1-CH3	0.879	14.08	0.910	14.31
2-CH2	1.327	20.49	1.327	20.49
3-CH2	1.496	30.70	1.496	32.30
4-NCH2	3.1 (overlap)	40.4-41.1	3.442	40.4-41.1
5-C^G	-	161.74	-	161.74
6- CO	-	177.36	-	177.36
7-Cquart	-	125.55	-	125.55
8-CHar	8.020	130.51	8.083	130.82 (HSQC)
9-CHar	6.669	110.73	6.669	110.73
10-Cquart-N	-	152.34	-	152.34
11-NCH3	3.029	40.4-41.1	3.029	40.4-41.1
NHalk	9.413	-	5.725	-

R. Kleinmaier, M. Keller, P. Igel, A. Buschauer, R. M. Gschwind, *J. Am. Chem. Soc*, **2010**, submitted.

4d free base
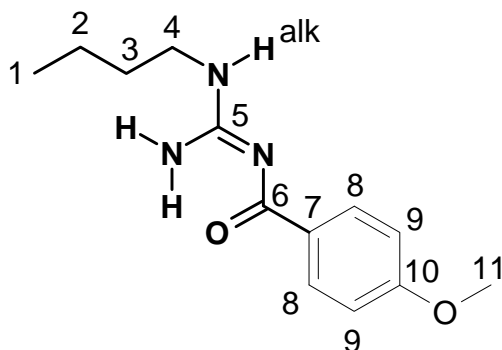
Figure S3.34: Structural formula of **4d** with atom numbering used in the assignment table.

Table S3.6: Assignment of **4d** at 225 K in CD$_2$Cl$_2$, referenced to TMS internal. Two sets of signals for the two conformations that can be distinguished at 225 K are denoted A and B both for protons and carbons.

Group	δ ^{1}H (A)	δ ^{13}C (A)	δ ^{1}H (B)	δ ^{13}C (B)
1-CH3	0.862	14.05	0.905	14.27
2-CH2	1.307	20.47	1.307	20.47
3-CH2	1.459	30.55	1.459	30.55
4-NCH2	3.027	41.07	3.458	41.07
5-C^G	-	161.78	-	161.78
6- CO	-	176.67	-	176.67
7-Cquart	-	overlapped(131)	-	overlapped(131)
8-CHar	8.107	130.82	8.180	131.10 (HSQC)
9-CHar	6.925	113.24	6.925	113.24
10-Cquart-O	-	161.98	-	161.98
11-OCH3	3.85	55.80	3.86	55.80
NHalk	9.367	-	5.766	-

R. Kleinmaier, M. Keller, P. Igel, A. Buschauer, R. M. Gschwind, *J. Am. Chem. Soc*, **2010**, submitted.

3.8.12 Thermal ellipsoid plots of the crystal structures

4b CCDC 772555 (ur-rk81fb)
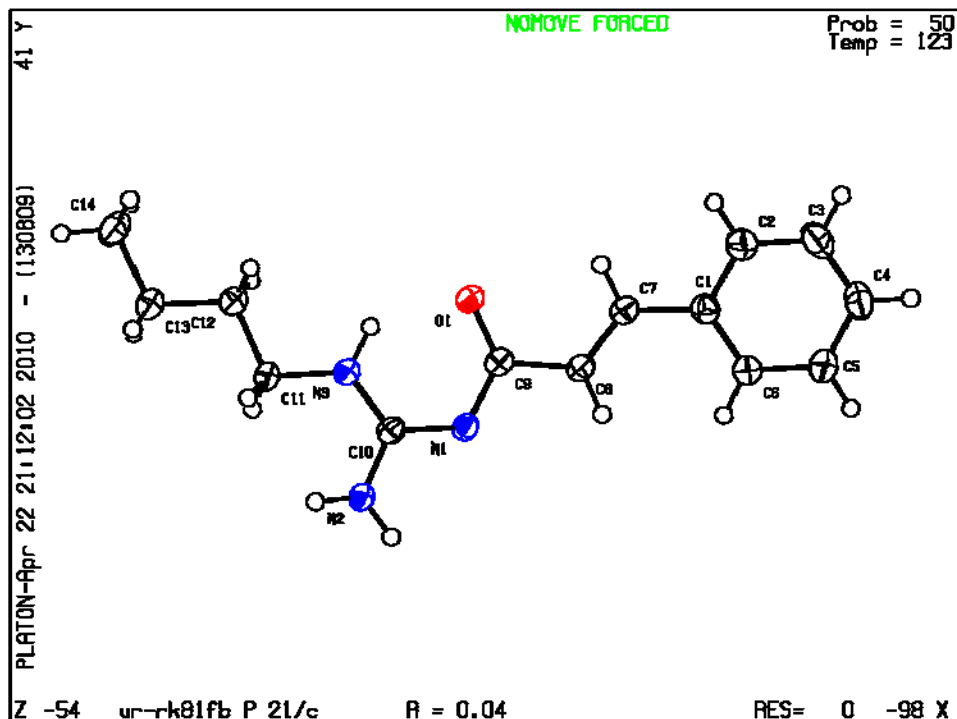
4d*HCl CCDC 772556 (ur-rk117hcl)

R. Kleinmaier, M. Keller, P. Igel, A. Buschauer, R. M. Gschwind, *J. Am. Chem. Soc*, **2010**, submitted.
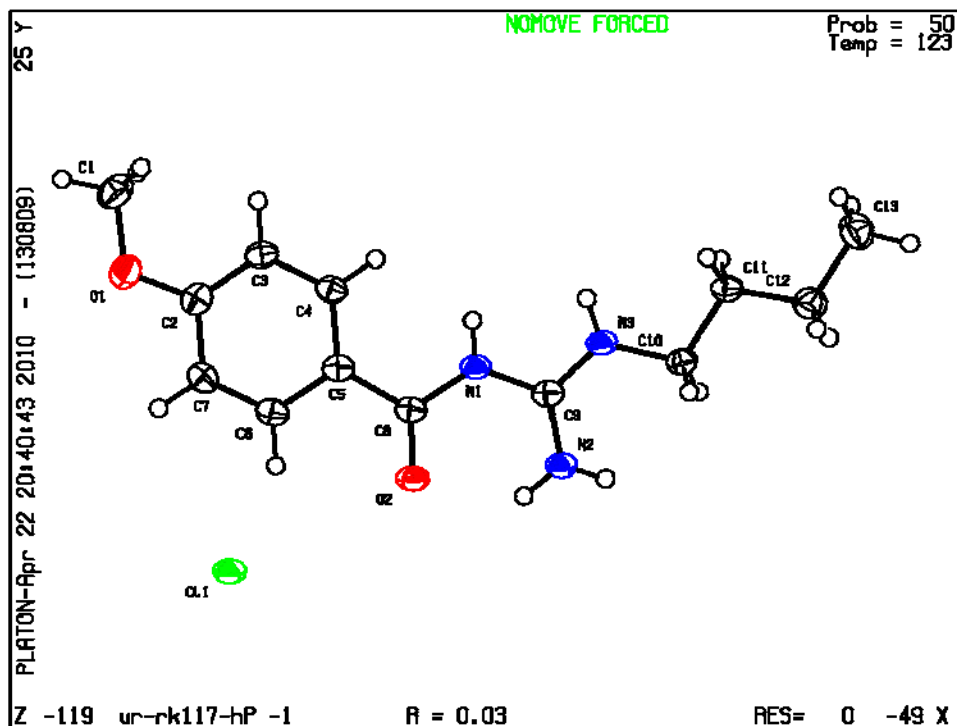
3.8.13   Full citation for reference Nr. 4 (Cole et al.)

Cole, D. C.; Stock, J. R.; Chopra, R.; Cowling, R.; Ellingboe, J. W.; Fan, K. Y.; Harrison, B. L.; Hu, Y.; Jacobsen, S.; Jennings, L. D.; Jin, G.; Lohse, P. A.; Malamas, M. S.; Manas, E. S.; Moore, W. J.; O'Donnell, M.-M.; Olland, A. M.; Robichaud, A. J.; Svenson, K.; Wu, J.; Wagner, E.; Bard, J. *Bioorg. Med. Chem. Lett.* **2008**, *18*, 1063-1066.

3.8.14   References

(1)   Steiner, T. *Angew. Chem.* **2002**, *114*, 50-80.

(2)   Johnson Jr., C. S. *Prog. NMR Spectr.* **1999**, *34*, 203-256.

(3)   Jerschow, A.; Müller, N. *J. Magn. Reson.* **1997**, *125*, 372-375.

(4)   Bondi, A. *J. Phys. Chem.* **1964**, *68*, 441 - 451.

(5)   Zhao, Y. H.; Abraham, M. H.; Zissimos, A. M. *J. Org. Chem.* **2003**, *68*, 7368-7373.

(6)   Chen, H. C.; Chen, S. H. *J. Phys. Chem.* **1984**, *88*, 5118-5121.

(7)   Crutchfield, C. A.; Harris, D. J. *J. Magn. Res.* **2007**, *185* 179–182.

(8)   Wavefunction, Inc.;: Irvine, CA., 1991-2007.

(9)   Federwisch, G.; Kleinmaier, R.; Drettwan, D.; Gschwind, R. M. *J. Am. Chem. Soc.* **2008**, *130*, 16846–16847.

R. Kleinmaier, M. Keller, P. Igel, A. Buschauer, R. M. Gschwind, *J. Am. Chem. Soc*, **2010**, submitted.

77

4 Chemical Shift Assignment and Conformational Analysis of Monoalkylated Acylguanidines*

Roland Kleinmaier, Ruth M. Gschwind

IV

4.1 Abstract

Monoalkylated acylguanidines are important functional groups in many biologically active compounds and additionally applied in coordination chemistry. Yet a straightforward assignment of the individual NH chemical shifts and the acylguanidine conformations is still missing. Therefore, in this study, NMR spectroscopic approaches for the chemical and especially the conformational assignment of protonated monoalkylated acylguanidines are presented. While NOESY and $^3J_{H,H}$ scalar couplings cannot be applied successfully for the assignment of acylguanidines, $^4J_{H,H}$ scalar couplings in ^{1}H,^{1}H COSY spectra allow for an unambiguous chemical shift and conformational assignment. It is shown that these $^4J_{H,H}$ long-range couplings between individual acylguanidinium NH resonances are observed solely across all-trans (w) pathways. Already one cis orientation in the magnetisation transfer pathway leads to signal intensities below the actual detection limit and significantly lower than cross peaks from $^2J_{NH,NH}$ couplings or chemical exchange. However, it should be noted that also in the case of conformational exchange being fast on the NMR time scale, averaged cross peaks from all trans $^4J_{H,H}$ scalar couplings are detected, which may lead at first glance to an incomplete or even wrong conformational analysis.

4.2 Introduction

Acylguanidines are highly important in many fields of chemistry,[1, 2] e.g. in biologically active substances[3-8] and in coordination chemistry.[9, 10] Specifically, monoalkylated acylguanidines recently gained attention because they provided highly potent and often selective ligands of G-protein coupling receptors.[6, 11, 12] In view of this huge pharmacological relevance,[2] it would be highly valuable if their conformational preferences were understood in order to enhance the rational design of new active compounds and ligands. Therefore, a reliable method for the conformational assignment of this class of compounds is needed.

In the simple unsubstituted guanidine base as well as in its guanidinium cation (see Figure 4.1a), the two (three) NH$_2$ groups are almost equivalent because of rapid exchange by inversion[13] as well as rotational and chemical exchange and no distinction in their NMR resonances has been achieved so far.
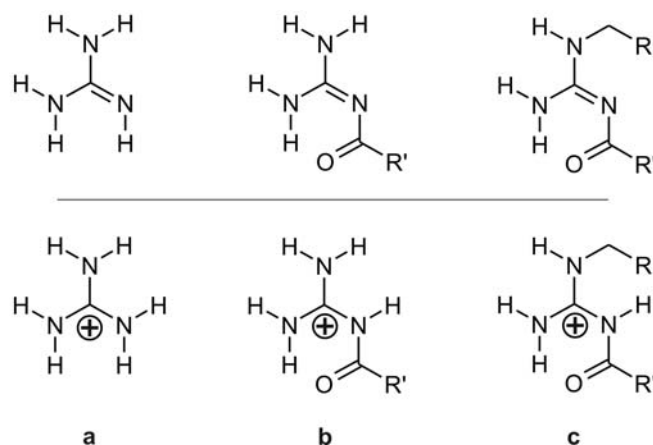
Figure 4.1: Structural formulas of a) guanidine/ guanidinium; b) acylguanidine/ acylguanidinium with two unsubstituted NH_2 groups and c) monoalkylated acylguanidine/ acylguanidinium with three differently substituted nitrogens.

In contrast, substitution of one or more protons by carbon substituents often may allow the differentiation of the two amino groups. For example, complexation of an arginine side chain by a biomimetic receptor allowed the detection of individual resonances for all five guanidinium protons.[14] In the case of unsubstituted acylguanidines (see Figure 4.1b), the presence of a carbonyl group as intramolecular H-bond acceptor often enables the assignment of the two amino groups without need for any additional receptor in order to reduce exchange. This has been shown e.g. in the conformational investigation of amiloride,[15] one of the most prominent acylguanidines in literature.[16-20] The application of cryo-solvents allowed to freeze the rotation around the bond between the central guanidine carbon (C^G) to the acylated nitrogen. Thus, it was possible to differentiate the two amino groups into one that is H-bonded to the carbonyl and a second one that is not. Nevertheless, a differentiation of the individual NH protons of the NH_2 groups was not achieved in this case.

The situation becomes even more advantageous for the differentiation of the individual NH protons by NMR spectroscopy in monoalkylated acylguanidines (see Figure 4.1c), because now three differently substituted nitrogens are present in the guanidine. In recent NMR studies of protonated monoalkylated acylguanidinium moieties, four distinct NH resonances have been observed in ^{1}H NMR spectra in aprotic solvents.[9, 21] This indicates a differentiation of the two protons of the NH_2 group by intra- and/or intermolecular H-bonds in these systems.

However, the protonated monoalkylated acylguanidine moiety can adopt three distinct planar conformations stabilized by an intramolecular H-bond (see Figure 4.2). Therefore, the unambiguous assignment of these four NH protons in monoalkylated acylguanidines is not trivial, directly connected to the identification of the conformation and has not been described so far.
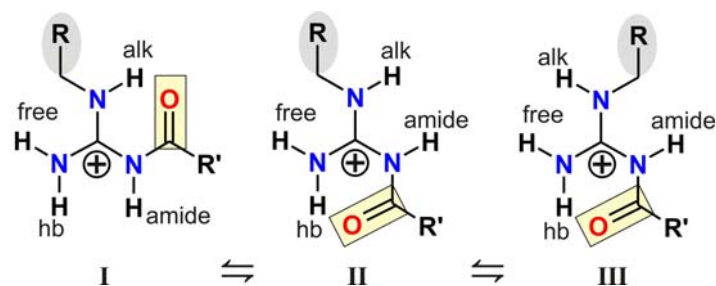
Figure 4.2: Representation of the monoalkylated acylguanidinium moiety in the three conformations that are stabilized by an intramolecular H-bond and the NH nomenclature used in the assignment.

Therefore, in this study several NMR spectroscopic approaches for the chemical shift and conformational assignment of protonated monoalkylated acylguanidinium moieties are discussed. It is shown that zig-zag $^4J_{NH,NH}$ long range couplings (further on "w-couplings") over the electron delocalized acylguanidinium moiety allow the conformational assignment. Further on, the effect of conformational exchange on these w-couplings is discussed.

4.3   Results and Discussion

In this study, four monoalkylated acylguanidines were employed in order to prove the generality of the observations. The first of these compounds, **1** (Figure 4.3), is based on the natural amino acid arginine but carries an acyl residue on its guanidine function and contains atom-specific ^{15}N labelling in the two terminal nitrogens of the side chain.[21, 22] This compound was chosen because the isotopic label allows for an unambiguous assignment of the guanidinium NH protons and can be used to confirm the general assignment approach for the unlabelled acylguanidines. The other three compounds **2-4** have a simple butyl chain as alkyl residue but structurally more diverse acyl residues (see Figure 4.3). To study the conformations of acylguanidines, samples of **1*TFA** and of **2-4** with a variety of anions (chloride, acetate, trifluoroacetate, dichloroacetate, 3,4,5-trimethoxybenzoate, Boc-Asp-OBn) were measured in pure CD$_2$Cl$_2$ and in mixtures of CD$_2$Cl$_2$ and DMSO-d_6 at temperatures between 300 K and 195 K.
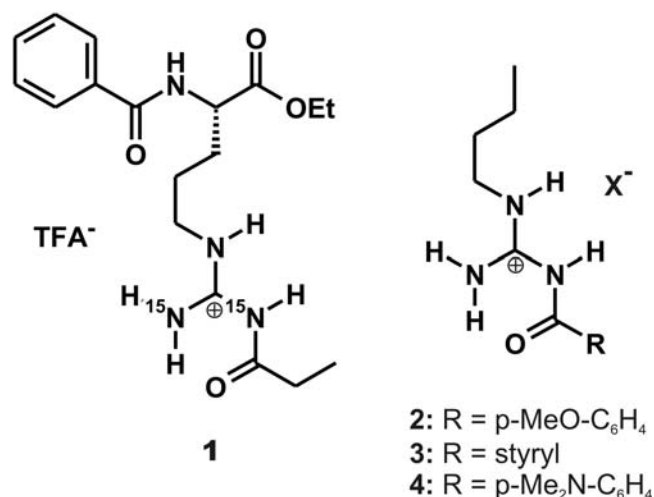
Figure 4.3: Compound pool investigated in this study. **1** is derived from the natural amino acid arginine

In all these samples, one general pattern of four NH resonances was detected at elevated temperatures around 300 K. At reduced temperatures, the slowdown of conformational exchange becomes visible in broadening of the lines. At low temperatures around 200 K, two sets of four signals indicating two conformations are observed. The respective temperatures of fast vs. slow conformational exchange on the NMR tome scale depend strongly on stabilizing interactions between the anion and the compound which are modulated by the solvent, type of anion and the compound itself.[23] In Figure 4.4, a representative stack of the NH sections from the ^{1}H spectra of **2*DCA** at temperatures from 210 K to 285 K is depicted. In ^{1}H spectra of **2*DCA** in CD_2Cl_2 and 1.5% DMSO-d_6 at 285 K, four rather sharp signals are detected for the four NH protons of the protonated acylguanidine moiety. However, strong broadening of the guanidinium NH resonances is observed upon cooling, indicating a decrease in the rate of conformational averaging. Finally, eight sharp resonances are observed. This shows clearly that at 285 K two conformations are rapidly equilibrating, while at 210 K they are resolved, i.e. exchange is slow on the NMR timescale.

Interestingly, out of 25 samples investigated in this study, **2*DCA** is the single example where four sharp and separate NH signals at elevated temperature and eight sharp and separate NH signals at low temperature are detected on one and the same sample regarding the type of anion and content of DMSO, because the exchange of the conformations is modulated in its rate by the anion and by DMSO.[23] In all other cases except for **2*DCA**, exchange is either still too fast at low temperature or still too slow at elevated temperature to allow for fully disperse spectra at both temperatures. However, in all samples without exception, one of the two limits is reached, i.e. either fast exchange and four sharp signals at elevated temperature or slow exchange and two sets of signals at low temperature.
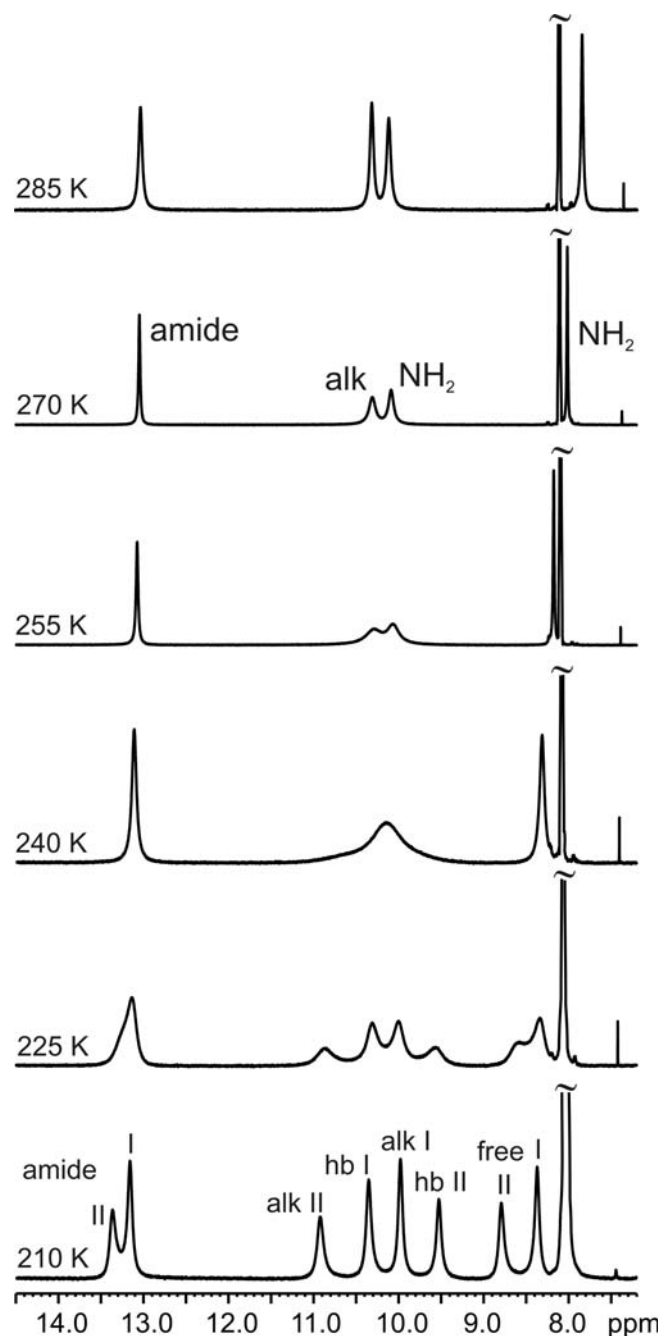
Figure 4.4: Stacked NH sections of ^{1}H spectra (600 MHz) of **2*DCA** in CD_2Cl_2 with 1.5% DMSO-d_6 at temperatures from 210 K to 285 K. Spectra were individually scaled for the sake of clarity so that no NH peaks had to be truncated. The coalescence of eight separate signals at 210 K into four signals at 285 K clearly indicates conformational exchange that is fast on the NMR timescale at elevated temperature. Assignment of NH protons is given according to the labels given in Figure 4.2.[24]

Principally, a limited assignment of the NH protons is possible by $^3J_{H,H}$ cross peaks in the COSY and with the aid of ^{1}H,^{13}C HMBC spectra. In the case of **2*DCA**, the COSY spectrum at 270 K contains one cross peak of an NH proton with the neighboring CH_2 group. This assigns NHalk unequivocally, because none of the other NH protons may couple by $^3J_{H,H}$ to

R. Kleinmaier, R. M. Gschwind, *Magn. Reson Chem.* **2010**, *submitted*.

any aliphatic CH atoms. In the COSY spectrum at 205 K, two such correlations of an NH proton are observed with two separate signals for the CH_2 group. Therefore, two resonances for NHalk are assigned to two conformations. The next possibility of assigning NH protons, the correlation of NH protons by $^2J_{H,C}$ to neighbouring carbon atoms via HMBC techniques, relies on small line widths and high signal intensity of both protons and carbons and hence was observed during this study only in few cases. However, in the case of **2*DCA**, one correlation of an NH proton with the carbonyl C is obtained and this can be used to assign NHamide. In all examples during this study where such a correlation between an acylguanidinium NH and the carbonyl carbon occurred, it was to the NH resonance with the highest chemical shift. Therefore, it is concluded that the NHamide resonance generally is the one with the highest chemical shift among the acylguanidine NH signals. Moreover, the quaternary guanidinium carbon often does not even deliver any resolved ^{13}C signal and is not helpful for the further assignment of the acylguanidinium NH protons.

At this level of assignment, the two NH_2 protons of **2*DCA** remain still unassigned. Therefore, the remaining assignment is described on the example of given on the example of **3*Boc-Asp-OBn** and will be described in the following. The assignment of **2*DCA** given in Figure 4.3 has been derived in analogy to that (for a detailed description see SI). When dedicating oneself to the problem of assigning NH protons not accessible by $^3J_{H,H}$ in COSY spectra or by $^1H,^{13}C$ HMBC spectra, NMR spectroscopy generally offers several more elaborate opportunities. The first one is isotopic labelling with ^{15}N (I = ½, natural abundance 0.37%),[25] which is present in one of the compounds of this study and thus served as reference. It is due to the high financial and experimental costs that selective ^{15}N labelling of small molecules cannot be pursued on a routine basis. The proton spectrum of **1*TFA** at 300 K in CD_2Cl_2 and DMSO-d_6 (9:1) shows four separate NH resonances, three of which are split to doublets due to $^1J_{H,N}$. This allows for an easy assignment in combination with the multiplet structure obtained for the two ^{15}N resonances, i.e. one doublet with $^1J_{H,N} = 89.0$ Hz and one triplet with $^1J_{H,N} = 92.5$ Hz. These coupling constants are retrieved in the ^1H spectrum and assign the NH_2 protons and NHamide, which has the highest chemical shift in accordance with the result of the $^1H,^{13}C$ HMBC of **1*TFA**, confirming the statement that NHamide generally has the highest chemical shift. In principle ^{15}N labelling could also contribute to the differentiation of the NH protons and to the conformational assignment of the acylguaninde moiety. The identification of individual NH_2 protons due to the different magnitudes of *cis* and *trans* $^3J_{H,N}$ scalar coupling constants across the respective partial double bonds of the planar electron-delocalized acylguanidine[26] would theoretically be a way to assign the NH_2 protons and to identify the conformations. However, even in the low temperature ^{15}N spectrum of **1*TFA** at 210 K only $^1J_{H,N}$ couplings are resolved and the line shape of the signals does not even hint at contributions of additional $^nJ_{H,N}$ couplings. Therefore, also the introduction of ^{15}N labelling does not facilitate the straightforward conformational assignment of monoalkylated acylguanidines.

Alternatively, observation of the NOE between the nuclei in question is normally an efficient way of assignment, especially for different conformations. In a complex between non-acylated Bz-Arg-OEt and bisphosphonate tweezers,[14] the NOESY spectrum could be used to confirm the proposed spatial arrangement. However, in the case of acylguanidines, the strongly elevated acidity of the acylguanidinium NHs hampers a similar conformational analysis by NOESY spectra. Despite comparable water content only completely exchange equilibrated NOESY cross peaks could be detected for the NH signals in exemplary measurements of **3*DCA** and **3*TMBA** (DCA = dichloroacetic acid; TMBA = 3,4,5-trimethoxybenzoic acid) and for the corresponding bisphosphonate complex of $[^{15}N^{\eta}_2]$-Bz-Arg(N^{η}-propionyl)-OEt.[21, 27]

In contrast, in ^{1}H,^{1}H COSY spectra carefully adjusted regarding relaxation delay, spectral resolution and number of transients (leading to experimental times of up to 24h), cross peaks between individual acylguanidinium NH protons can be detected, which allow for the remaining chemical shift assignment of the NH protons of the NH_2 group and the identification of conformations present in solution. In Figure 4.5, parts of the NH section of the COSY spectrum of **3*Boc-Asp-OBn** at 220 K in CD_2Cl_2 and DMSO-d_6 (9:1) are depicted (see SI for full NH section). Two perfectly disperse sets of four NH signals are observed and in this case, the two sets can be correlated reliably by integration (ratio 60:40).

R. Kleinmaier, R. M. Gschwind, *Magn. Reson Chem.* **2010**, *submitted*.
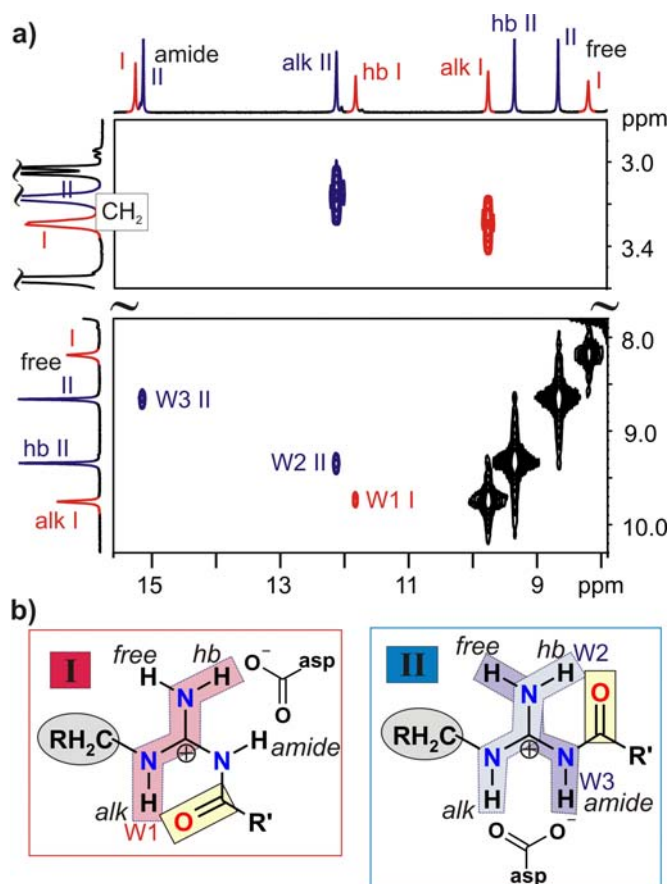
Figure 4.5: a) Sections from the ^{1}H COSY spectrum of **3*Boc-Asp-OBn** at 220 K in CD$_2$Cl$_2$ with 10% (CD$_3$)$_2$SO containing three w-couplings correlating two sets of four NH signals. The color coding reflects the assignment of the two conformations derived from this (red = conformation I, blue = conformation II). b) Structures of the two conformations following the color code and with the assignment of each individual NH proton put in italics. The w pathways are indicated in each of the conformations.

One NH signal of the major conformation shows a COSY cross peak with an aliphatic CH$_2$ group. As explained on the example of **2*DCA**, this enables the assignment of NHalk. The acylguanidinium NH resonance with the highest chemical shift generally belongs to NHamide and in the case of **3*Boc-Asp-OBn,** this again is confirmed by the correlation of this resonance with the carbonyl carbon in the ^{1}H,^{13}C HMBC. In the COSY spectrum, NHamide shows one additional small cross peak to one of the NH$_2$ protons (W3 in Figure 4.5a). NHalk shows a cross peak to the second NH$_2$ proton (W2 in Figure 4.5a). In addition, NHalk and NHamide are not correlated with each other. A comparison with the structures of acylguanidines (Figure 4.5b) shows that the small cross peaks must be $^4J_{H,H}$ long range couplings within the acylguanidine moiety.

In principle, $^4J_{H,H}$ long-range couplings of detectable magnitude occur between nuclei in a rigid planar zig-zag conformation of C-H and C-C bonds[28] and they are often referred to as w-couplings. In saturated compounds, they are quite commonly found in rigid cyclic systems, e.g. in sugars. Also in acyclic systems, they have been used for conformational studies and

been interpreted in terms of preferred conformations,[29] e.g. stabilization of a favoured conformation by a H-bond.[28] In unsaturated compounds, e.g. systems with double bonds, long-range couplings ($\geq {}^{4}J_{H,H}$) in rigid planar zig-zag conformations are known to show larger coupling constants than other conformations.[30, 31]

However, if the ${}^{4}J_{H,H}$ long-range couplings observed in the COSY of **3*Boc-Asp-OBn** occured in a cis arrangement just as well as in a trans arrangement, then a cross peak between NHamide and NHalk would have to appear no matter what their spatial arrangement, as well as a multitude of additional cross peaks between the NH protons. If e.g. the observed correlation between NHamide and one of the NH_2 protons in Figure 4.5a was due to a cis-trans pathway in conformation I (Figure 4.5b), or due to a trans-cis pathway in conformation II, then there would have to be a similar correlation between NHamide and NHalk in conformation I. However, besides the cross peaks from ${}^{4}J_{H,H}$ with all-trans pathways, in none of the COSY spectra of the 25 samples investigated here additional cross peaks assignable to a single cis orientation have been detected, not even in spectra showing cross peaks from chemical exchange (see below). Therefore, in acylguanidines the ${}^{4}J_{H,H}$ scalar couplings from all trans orientations has to be significantly stronger than from any other transfer pathway.

Byrne and Rothchild reported in 1999 the observation of a ${}^{2}J_{NH2}$ geminal coupling as well as a putative long-range ${}^{4}J_{H,H}$ w coupling between two NH protons of the acylurea moiety of the drug pheneturide arranged in a zig-zag conformation, which is stabilized by an intramolecular H-bond forming a six-membered pseudo-ring.[32] The reported six-membered ring is also formed by the acylguanidinium moiety by intramolecular H-bonding (see Figure 4.1). This corroborates the detection of ${}^{4}J_{H,H}$ w-coupling in this system exclusively in trans fashion, i.e. through a w pathway. Figure 4.2 tells us that among the three depicted conformations, only II puts two pairs of protons in planar w arrangements to allow for the couplings observed in the COSY of **3*Boc-Asp-OBn.** The w coupling of NHalk must be to the NH_2 proton in the intramolecular H-bond, the w coupling of NHamide must be to the remaining free NH_2 proton. For the remaining set of NH resonances, only one w coupling is observed for NHalk, which was equally assigned by its aliphatic cross peak. A look to Figure 4.2 yields that the second conformation must be I, because only here is a w coupling pathway for NHalk possible.

The last point that remains to be discussed is the chemical shift pattern of the two conformations which has to fit with the proposed conformations. The chemical shift dispersion of the NH signals of **3*Boc-Asp-OBn** at 220 K spans a range of more than 7 ppm, although at least NHalk and the NH_2 protons would naturally be expected to have quite similar chemical shifts. One obvious reason for the large dispersion is of course the intramolecular H-bond, which is supposed to raise the chemical shift of the proton involved. However, according to the assignment just proposed the two protons with the highest chemical shift apart from NHamide (NHhb in I and NHalk in II) are those which are just not in the intramolecular H-bond (see Figure 4.5b). This fact is brought in line with the proposed

conformations by considering the presence of a strongly H-bonded anion. These H-bonds are charge-assisted ones (i.e. classical salt bridges in the case of carboxylates), so they will raise the chemical shift of an NH proton even more than the intramolecular one.[33] The structures of the two conformations depicted in Figure 4.5a show the typical fork-like arrangement of the carboxylate towards the acylguanidinium protons. In both conformations, NHamide is affected by this interaction, while in I, NHhb is in the salt bridge and in II, NHalk is. These four are the protons with the highest chemical shifts in each conformation.

The impressive dispersion of the NH signals (i.e. base line separated with line widths between 12 and 19 Hz) found in the case of **3*Boc-Asp-OBn** is not achieved in all samples. The small line widths indicate that conformational exchange is slow on the NMR timescale under the conditions employed here. However, the approach just presented also works at conditions where the line widths are broadened and/or a subdivision into sets via integrals is no longer feasible, as is the case in the COSY of **4*Boc-Asp-OBn** depicted in Figure 4.6 with line widths between 20 Hz and 30 Hz.
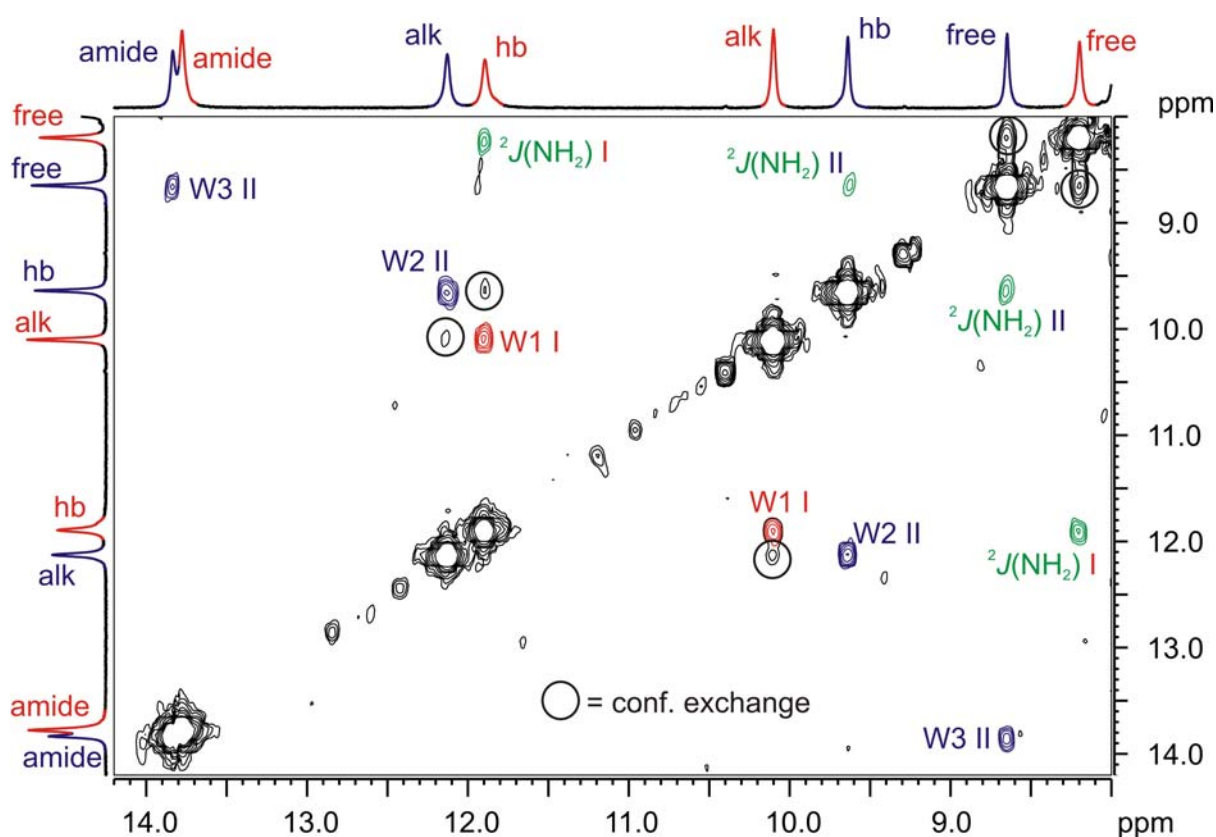
Figure 4.6: Section of COSY spectrum of **4*Boc-Asp-OBn** at 195 K containing 3 w couplings (color coded red and blue for conformations I and II, respectively), 2 $^2J(NH_2)$ couplings (green) and in addition several cross peaks arising from conformational exchange (black circles).

R. Kleinmaier, R. M. Gschwind, *Magn. Reson Chem.* **2010**, *submitted*.

The broadened lines indicate an acceleration of conformational exchange. However, the characteristic w couplings indicating conformations I and II are observed here as well. In addition, in this spectrum further peaks appear very clearly, which have been lost in T_1 noise in the case of **3*Boc-Asp-OBn**.[34] These additional peaks are firstly $^2J_{NH2}$ couplings (marked green in Figure 4.6) between the NH_2 protons that are observed for both conformations here. Geminal couplings within an NH_2 group with chemically inequivalent protons have also been reported in other sources, e.g. with values of $^2J_{NH2}$ between 1.4 Hz and 2.4 Hz in the ubiquitin molecule[35] and 3.75 Hz in thioacetamide.[36] Interestingly, in the present COSY spectrum of **4*Boc-Asp-OBn**, the $^2J_{NH2}$ couplings are quantitatively weaker than the w couplings.

Second, since conformational exchange is faster now, also cross peaks caused by this conformational exchange occur between the corresponding NH protons of each conformation. This is initially confusing, but is useful for the confirmation of the assignment on the other hand. In addition, the COSY spectrum in Figure 4.6 shows that even with an extremely good signal to noise ratio allowing for the detection of significantly smaller scalar couplings and even conformational exchange, no $^4J_{H,H}$ scalar coupling between protons in other that zig-zag arrangements are detected. This confirms once again that any cis pathway between NH protons in acylguanidines lead to significantly reduced $^4J_{H,H}$ scalar coupling constants not detectable so far.

COSY cross peaks between acylguanidinium NH protons caused by $^4J_{H,H}$ long-range couplings also were detected at 300 K as shown exemplarily in the COSY spectrum of **3*HCl** in Figure 4.7. But it is extremely important to keep in mind that these cross peaks arise from rapidly exchanging conformations. They would lead to an inexact assignment of the conformation if they were to be interpreted without further reasoning about the implications of fast exchange conditions.

In general, the detection of w couplings is strongly dependent on the line width of the NH proton signals. At reduced temperature, a fine line has to be trod between exchange broadened signals on the one hand and T_2 effects related to increased viscosity on the other. At elevated temperatures, in contrast, only a completely exchange equilibrated mixture of conformers will produce optimal line widths in all NH signals, with solvent volatility limiting the maximum feasible temperature to 300 K in the case of CD_2Cl_2. Therefore, the spectra chosen to represent each case best are derived from slightly different compounds. Figure 4.7 shows sections from the COSY spectrum of **3*HCl** at 300 K, containing two w couplings and the $^2J_{NH2}$ coupling within the NH_2 group.
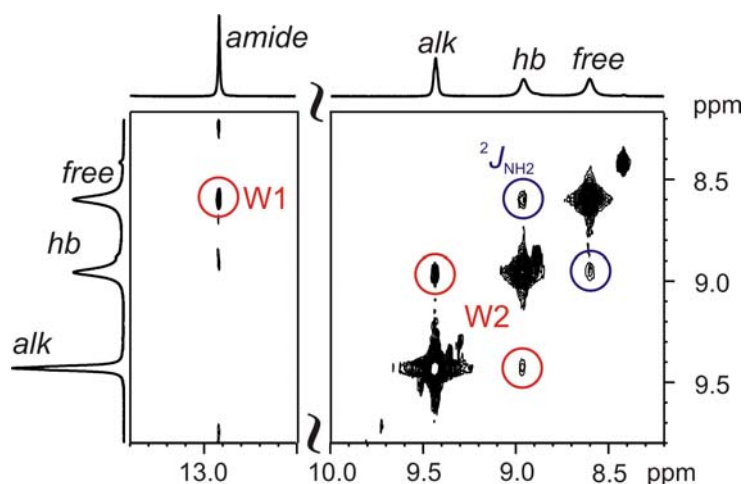
Figure 4.7: Sections of ^1H COSY spectrum of **3*HCl** at 300 K in CD_2Cl_2 with 5% DMSO-d_6. Two w couplings between two pairs of NH resonances are detected (marked W1 and W2) and additionally, the $^2J_{NH2}$ coupling of the NH_2 protons occurs in this case.

The assignment of the NHalk resonance by its COSY cross peak with the neighbouring CH_2 group as described above is of course fully correct, just as the assignment of NHamide by its high chemical shift and/or its HMBC correlation to the carbonyl C (which was observed in the case of **3*HCl**). Once again, both of these unambiguously assigned resonances show cross peaks with two different NH protons, but not with each other. This proves that the observed cross peaks are w couplings, which require a distinct spatial arrangement of the involved nuclei.

However, it should be pointed out that the application of the geometric and chemical shift criteria introduced in the conformational assignment of **2*Boc-Asp-OBn** on the 300 K COSY spectrum in Figure 4.7 would lead to the postulate that solely conformation II be present, because II contains the observed w couplings and the chemical shift of NHhb is neatly explained by the intramolecular H-bond. Nonetheless, the observed w couplings contain also a contribution from I since W2 (see Figure 4.7) between NHalk and NHhb is also possible in I (see Figure 4.5b). In Figure 4.7, W2 is qualitatively slightly more intensive than W1, which could be attributed to the fact that it is present in both conformations and W1 is not, but could just as well be dismissed as caused by relaxation phenomena or slightly different long range scalar coupling constants.

Therefore, the interpretation of w scalar couplings in terms of conformational assignment must be executed with great care and it has to be assured that the conformational assignment of protonated monoalkylated acylguanidines is performed under conditions of slow exchange where each conformation can be assigned individually. Valuable information may be lost otherwise, although the assignment is not necessarily wrong, but surely incomplete.

4.4 Conclusion

For monoalkylated acylguanidines, which are highly valued compounds in pharmaceutical applications and coordination chemistry, several NMR spectroscopic approaches for the assignment of the chemical shift and the conformations are presented. While NOESY spectra and $^3J_{NH}$ scalar couplings fail, do long range $^4J_{H,H}$ couplings between individual acylguanidinium NH resonances allow for the unequivocal chemical shift and conformational analysis of protonated monoalkylated acylguanidinium moieties, because the observation of these long range $^4J_{H,H}$ couplings is confined to an all-trans pathway for the magnetisation transfer. $^4J_{H,H}$ scalar couplings with one cis orientation are not detected and their potential ^{1}H,^{1}H COSY cross peaks are significantly lower than those caused by $^2J_{NH,NH}$ scalar couplings or chemical exchange. Thus, the required spatial arrangement for acylguanidinium NH protons correlated by all trans $^4J_{H,H}$ scalar couplings allow the chemical shift and conformational assignment, which is in accordance with the chemical shift information accounting for the influence of strong H-bond interactions with a coordinating anion. In order to achieve a concise and complete assignment of the conformations present in solution, the investigations must be performed at conditions where slow conformational exchange prevails, i.e. usually at reduced temperature. However, if the experiments are conducted under fast exchange conditions, w couplings are still detected, but they are caused by a rapidly equilibrating mixture of conformers. Therefore, the application of geometric criteria in this situation will lead to at least imperfect, if not false conclusions about the nature of the conformations present.

In summary, a successful approach for the conformational assignment of protonated monoalkylated acylguanidines has been presented that is based on geometric criteria inferred from the selective detection of w couplings in low temperature ^{1}H,^{1}H COSY spectra. It is robust enough for a broad application, once the slow conformational exchange limit can be assured. Thus, even extremely complex COSY spectra can be unambiguously interpreted, i.e. if they contain numerous cross peaks between acylguanidinium NHs caused by $^4J_{H,H}$ long-range couplings as well as $^2J_{NH2}$ and additional conformational exchange peaks.

4.5 Experimental

Substances

The syntheses of **1***TFA,[22] and of **2**, **3** and **4** as well as their salts have been published elsewhere.[23] Dichloroacetic acid (DCA) was purchased from Riedel de Haen, 3,4,5-trimethoxybenzoic acid (TMBA) and Boc-Asp-OBn were obtained from Sigma-Aldrich.

NMR solvents were purchased from Deutero and Sigma-Aldrich.

Sample Preparation

Samples were routinely prepared from the solid compounds in standard 5mm NMR tubes at concentrations from 30 mM to 50 mM. In cases where titrations with acid were performed, the acid was dissolved in the respective NMR solvent and the mixture was added stepwise until integration gave ratio 1:1. Tetramethylsilane (TMS) was added generally in order to standardize the chemical shifts.

NMR Spectroscopy

NMR spectra were recorded on a Bruker Avance 600 spectrometer equipped with standard bore 5 mm TBI [1]H-^{31}P and BBI probeheads at an operating frequency of 600.13 Hz for ^{1}H and 150.90 Hz for [13]C. The temperature was controlled with the Bruker BVT 3000 variable temperature unit. Chemical shifts are given in ppm with tetramethylsilane (TMS) as internal standard. 1D ^{1}H spectra were routinely single-scan with 32k points and spectral widths from 6000 Hz to 12000 Hz adapted to the individual compounds. 1D ^{13}C spectra were recorded with 64k points and a spectral width of 40650 Hz with the number of transients from 256 to 1k adapted to the individual sample.

In the case of **2*DCA**, 32k points were recorded with a spectral width of 12019 Hz and a 90° pulse of 8.3 µs.

COSY spectra were recorded in magnitude mode with standard Bruker cosygpqf pulse sequence. (cosygpqf avance-version (07/04/05), 2D homonuclear shift correlation, using gradient pulses for selection)

In the case of **3*HCl**, two times 4 transients and three times 2 transients were recorded and the FIDs added to a total of 14 transients for a better S/N. 256 real points were recorded in F1 and 8k complex points in F2 over spectral widths of 8402 Hz and 8389 Hz, respectively. The 90° pulse was 11.0 µs and the relaxation delay was 7.5 s. Zero filling was performed to obtain 512 real points in F1 and 16k complex points in F2, followed by SINE apodization in both dimensions and Fourier transformation.

In the case of **3*Boc-Asp-OBn**, two times 4 transients were recorded and the FIDs added to a total of 8 transients for a better S/N. 128 real points were recorded in F1 and 1k complex points in F2 over spectral widths of 10802 Hz and 10776 Hz, respectively. The 90° pulse was 11.0 µs and the relaxation delay was 6.5 s. Zero filling was performed to obtain 256 real points in F1 and 2k complex points in F2, followed by SINE apodization in both dimensions and Fourier transformation.

In the case of **4*Boc-Asp-OBn**, 4 transients were recorded with 128 real points in F1 and 1k complex points in F2 over spectral widths of 9002 Hz and 8993 Hz, respectively. The 90° pulse was 9.50 µs and the relaxation delay was 6.0 s. Zero filling was performed to obtain

256 real points in F1 and 2k complex points in F2, followed by QSINE apodization in both dimensions and Fourier transformation.

4.6 References

[1] A. R. Katritzky, B. V. Rogovoy, X. Cai, N. Kirichenko, K. V. Kovalenko, *J. Org. Chem.* **2004**, *69*, 309.

[2] F. Saczewski, Ł. Balewski, *Expert Opin. Ther. Patents* **2009**, *19*, 1417.

[3] D. C. Cole, J. R. Stock, R. Chopra, R. Cowling, J. W. Ellingboe, K. Y. Fan, B. L. Harrison, Y. Hu, S. Jacobsen, L. D. Jennings, G. Jin, P. A. Lohse, M. S. Malamas, E. S. Manas, W. J. Moore, M.-M. O'Donnell, A. M. Olland, A. J. Robichaud, K. Svenson, J. Wu, E. Wagner, J. Bard, *Bioorg. Med. Chem. Lett.* **2008**, *18*, 1063.

[4] S. Lee, T. Kim, B. H. Lee, S. Yoo, K. Lee, K. Y. Yi, *Bioorg. Med. Chem. Lett.* **2007**, *17*, 1291.

[5] M. Baumgarth, N. Beier, R. Gericke, *J. Med. Chem.* **1997**, *40*, 2017.

[6] P. Ghorai, A. Kraus, M. Keller, C. Goette, P. Igel, E. Schneider, D. Schnell, G. Bernhardt, S. Dove, M. Zabel, S. Elz, R. Seifert, A. Buschauer, *J. Med. Chem.* **2008**, *51*, 7193–7204.

[7] E. Schneider, M. Keller, A. Brennauer, B. K. Hoefelschweiger, D. Gross, O. S. Wolfbeis, G. Bernhardt, A. Buschauer, *ChemBioChem* **2007**, *8*, 1981 − 1988.

[8] A. Brennauer, S. Dove, A. Buschauer, *Structure-activity relationships of nonpeptide neuropeptide Y receptor antagonists, Vol. 162*, Springer, Berlin, Heidelberg, New York, **2004**.

[9] C. Schmuck, V. Bickert, *Org. Lett.* **2003**, *5*, 4579.

[10] C. Schmuck, W. Wienand, *J. Am. Chem. Soc.* **2003**, *125*, 452.

[11] P. Igel, E. Schneider, D. Schnell, S. Elz, R. Seifert, A. Buschauer, *J. Med. Chem.* **2009**, *52*, 2623.

[12] M. Keller, N. Pop, C. Hutzler, A. G. Beck-Sickinger, G. Bernhardt, A. Buschauer, *J. Med. Chem.* **2008**, *51*, 8168–8172.

[13] H. Kessler, D. Leibfritz, *Chem. Ber.* **1971**, *104*, 2143.

[14] R. M. Gschwind, M. Armbrüster, I. Z. Zubrzycki, *J. Am. Chem. Soc.* **2004**, *126*, 10228.

[15] W. J. Skawinski, A. Ofsievich, C. A. Venanzi, *Struct. Chem.* **2002**, *13*, 73.

[16] J. Noel, D. Germain, J. Vadnais, *Biochemistry* **2003**, *42*, 15361.

[17] E. Zeslawska, B. Oleksyn, K. Stadnicka, *Struct. Chem.* **2004**, *15*, 567.

[18] A. Pretscher, M. Brisander, A. a. Bauer-Brandl, L. K. Hansen, *Acta Crystallogr.* **2001**, *C57*, 1217.

[19] R. A. Buono, T. J. Venanzi, R. J. Zauhar, V. B. Luzhkov, C. A. Venanzi, *J. Am. Chem. Soc.* **1994**, *116*, 1502.

[20] R. L. Smith, D. W. Cochran, P. Gund, E. J. Cragoe Jr., *J. Am. Chem. Soc.* **1979**, *101*, 191.

[21] G. Federwisch, R. Kleinmaier, D. Drettwan, R. M. Gschwind, *J. Am. Chem. Soc.* **2008**, *130*, 16846–16847.

[22] R. Kleinmaier, R. M. Gschwind, *J. Label Compd. Radiopharm* **2009**, *52*, 29.

[23] R. Kleinmaier, M. Keller, P. Igel, A. Buschauer, R. M. Gschwind, *J. Am. Chem. Soc* **2010**, *submitted.*

[24] In the COSY spectrum at 210 K, two aliphatic cross peaks are detected assigning NHalk. At 270 K, only one cross peak is found for NHalk in the COSY and NHamide is assigned via ^{1}H,^{13}C HMBC. The HMBC spectrum was recorded after addition of further amounts of DMSO-d_6 to a total content of 5% in order to obtain smaller line widths at the same temperature of 270 K. For further details, see SI.

[25] S. Berger, S. Braun, H.-O. Kalinowski, *NMR-Spektroskopie von Nichtmetallen, Band 2, ^{15}N-NMR-Spektroskopie*, Georg Thieme Verlag Stuttgart New York, Stuttgart, **1992**.

[26] R. F. Dietrich, G. L. Kenyon, J. E. Douglas, P. A. Kollman, *J. Chem. Soc. Perkin. Trans. II* **1980**, 1592.

[27] Due to very low signal to noise ratios, only mixing times down to 250 ms could be used.

[28] H. Schroeder, E. Haslinger, *Magn. Reson. Chem.* **1994**, *32*, 12.

[29] S. Johns, R, R. Willing, I, D. Winkler, A, *Makromol. Chem., Rapid Commun.* **1987**, *8*, 17.

[30] S. Sternhell, *Q. Rev. Chem. Soc.* **1969**, *23*, 236

[31] H. Günther, *NMR-Spektroskopie Grundlagen, Konzepte und Anwendungen der Protonen- und Kohlenstoff-13-Kernresonanz-Spektroskopie in der Chemie*, 3 ed., Georg Thieme Verlag Stuttgart, New York, **1992**.

[32] B. Byrne, R. Rothchild, *Chirality* **1999**, *11*, 529.

[33] S. Sharif, G. S. Denisov, M. D. Toney, H.-H. Limbach, *J. Am. Chem. Soc* **2007**, *129*, 6313.

[34] Although the T$_1$ relaxation delay was even longer in the case of **3*Boc-Asp-OBn** (6.5s vs. 6.0s for **4*Boc-Asp-OBn**), the smaller line widths in **3*Boc-Asp-OBn** led to drastically increased T$_1$ noise also for the NH signals.

[35] P. Permi, *J. Biomol. NMR* **2002**, *22*, 27.

[36] M. Nee, Y. Chun, M. E. Squillacote, J. D. Roberts, *Org. Magn. Resonance* **1982**, *18*, 125.

R. Kleinmaier, R. M. Gschwind, *Magn. Reson Chem.* **2010**, *submitted.*

94

4.7 Supporting Information

Chemical Shift Assignment and Conformational Analysis of Monoalkylated Acylguanidines

Roland Kleinmaier, Ruth M. Gschwind

4.7.1 Full represention of planar conformations of monoalkylated acylguanidines
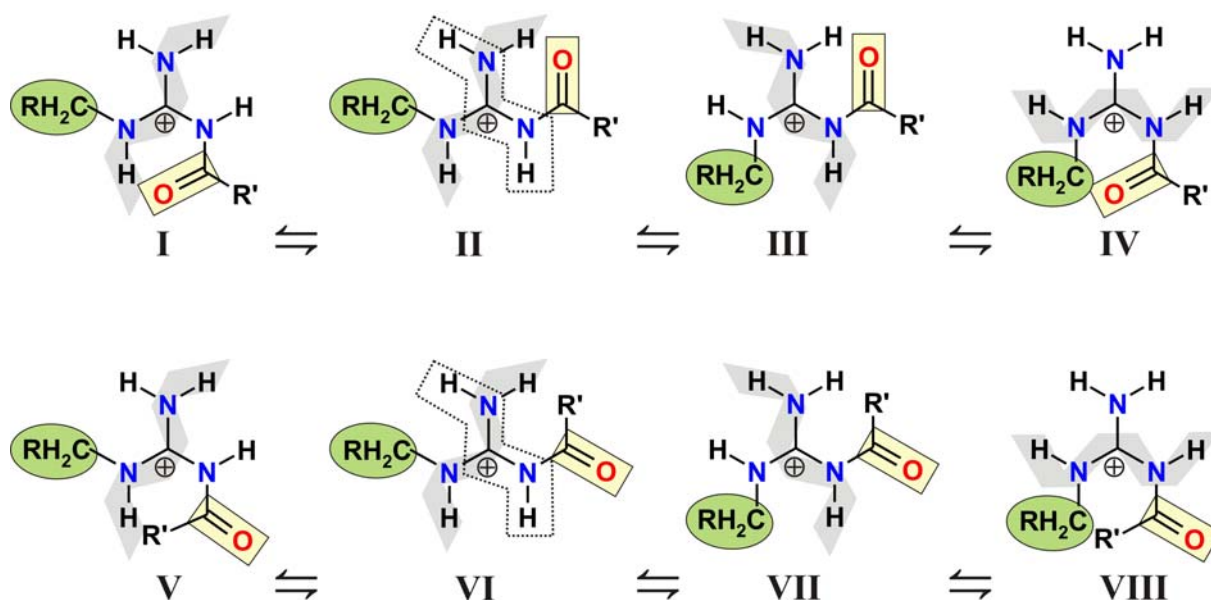
Figure S4.8: Eight planar conformations could in principle be adopted by monoalkylated acylguanidines. However, only the conformations I, II and III are stabilized by an intramolecular H-bond, while the others can be dismissed because of the lack of this H-bond and because steric hindrance occurs in all conformations from IV to VIII.

4.7.2 Additional spectra for 1*TFA
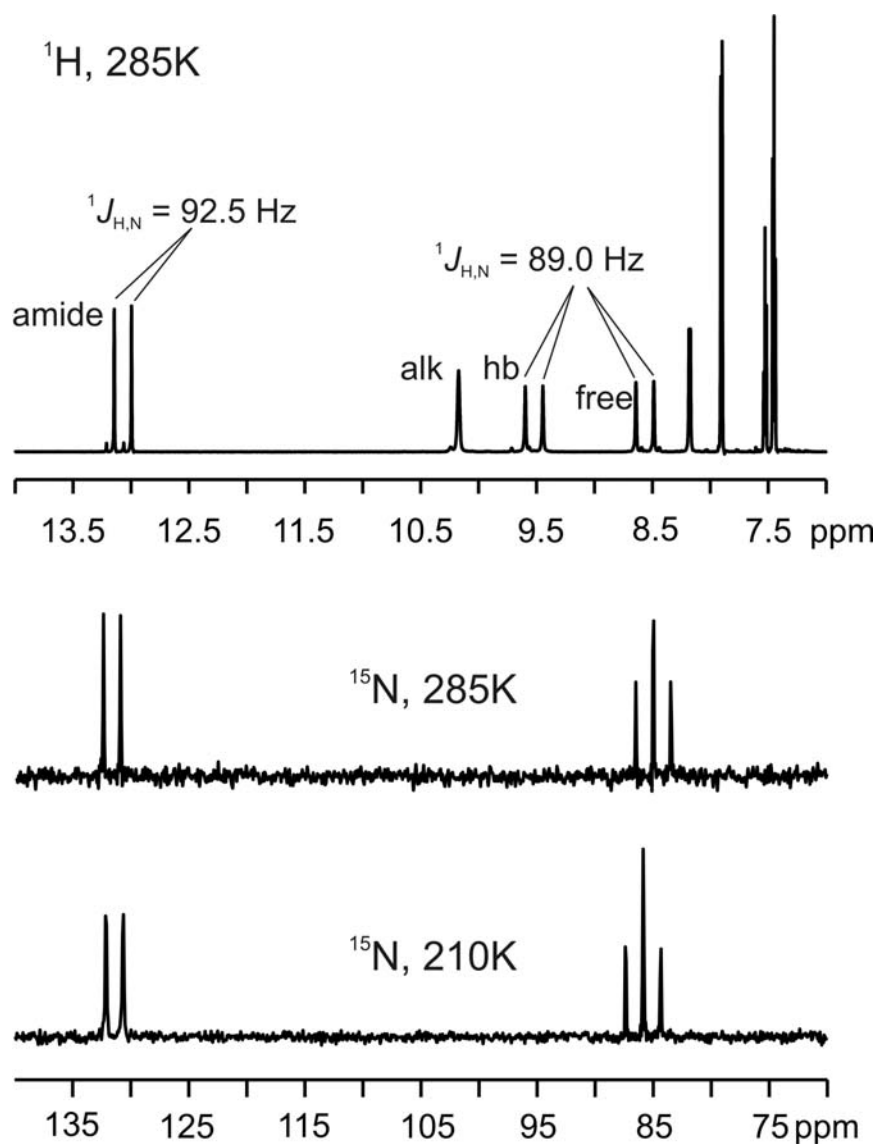
Figure S4.9: Section of ^{1}H spectrum of **1*TFA** at 285 K showing the splitting of acylguanidinium NH signals because of $^1J_{HN}$ with different values of the coupling constant for NHamide and the NH_2 protons. ^{15}N spectra of 1*TFA at 285 K and at 210 K with splitting of the resonances to a doublet due to coupling to NHamide and a triplet due to coupling to the two NH2 protons. The spectrum at 210 K, i.e. at slow exchange conditions, contains no indication of a further splitting of the resonances that would be due to any $^3J_{HN}$ of detectable magnitude.

4.7.3 Details on the assignment of 2*DCA
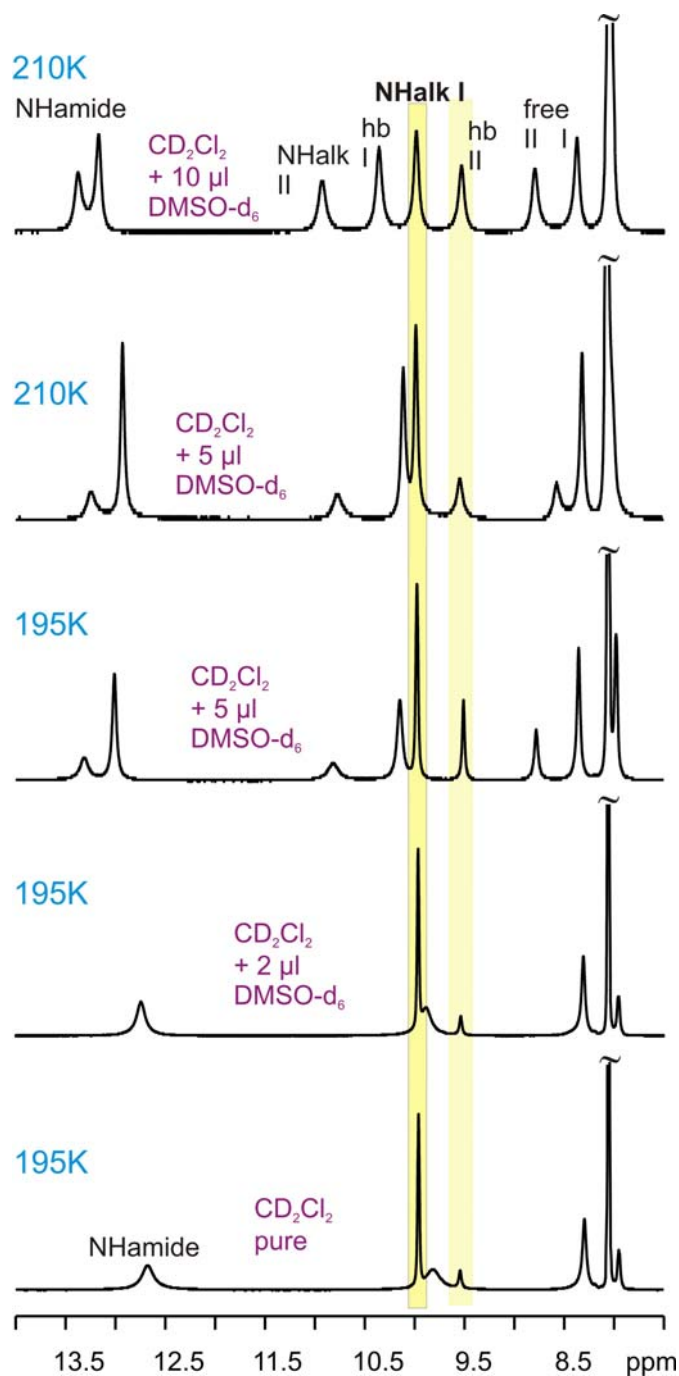
Figure S4.10: Stacked NH sections from ^{1}H spectra following the titration of **2*DCA** in CD_2Cl_2 with DMSO-d_6. The resonance for NHalk in conformation I shows an astonishing stability in its chemical shift. The spectra were scaled individually for the sake of clarity of the representation.

In Figure S4.10, stacked NH sections from ^{1}H spectra of **2*DCA** are depicted following the titration of the compound dissolved in pure CD_2Cl_2 with DMSO-d_6. At 195 K, conformational

exchange is slow on the NMR timescale, but still leads to considerable line broadening e.g. of the NHamide resonance. The addition of DMSO gradually increases the portion of the second conformation and raises the exchange rate, which is indicated by the line broadening observed in the last step when going from 5 µl DMSO to 10 µl DMSO at the same temperature of 210 K. The chemical shifts of the NH signals all undergo quite drastic changes, with the exception of two signals: The one at 9.5 ppm and the one at 10.0 ppm stay put through all the manipulations, which is marked by yellow bars for these resonances.

Especially for the resonance at 10.0 ppm, this almost complete lack of influence of the H-bond accetor DMSO and even of the type anion is a general observation throughout the vast majority of the samples of protonated monoalkylated acylguanidines. In all cases where an unequivocal assignment was performed with the help of w couplings as described in the main text, this resonance turned out to be NHalk in conformation I, which is in the intramolecular H-bond and thus not influenced by solvent molecules or anions. The second resonance which shows such high chemical shift stability here is consequently NH2hb in conformation II, which is also in the intramolecular H-bond. However, the chemical shift of this resonance is influenced significantly by the type of anion because the second NH_2 proton interacts strongly with the anion and this affects NH2hb as well.

For this reason, it is possible even for samples that do not yield a complete and unambiguous pattern of w couplings as described in the main paper for **3*Boc-Asp-OBn** and **4*Boc-Asp-OBn**, to give an assignment of the NH protons based on analogy to the assignments obtained for the latter compounds as soon as there are two clear cross peaks to the aliphatic CH_2 group for the two NHalk resonances. The NHamides are assigned by their high chemical shift and the remaining four NH_2 protons can be assigned by integration and chemical shift considerations.

Therefore, it is highly recommended to do titration experiments with DMSO at variable temperatures on samples which do not yield a satisfactory NH signal dispersion, because this may lead to sufficient information for an analogy assignment.

4.7.4 Full NH section of COSY of 3*Boc-Asp-OBn
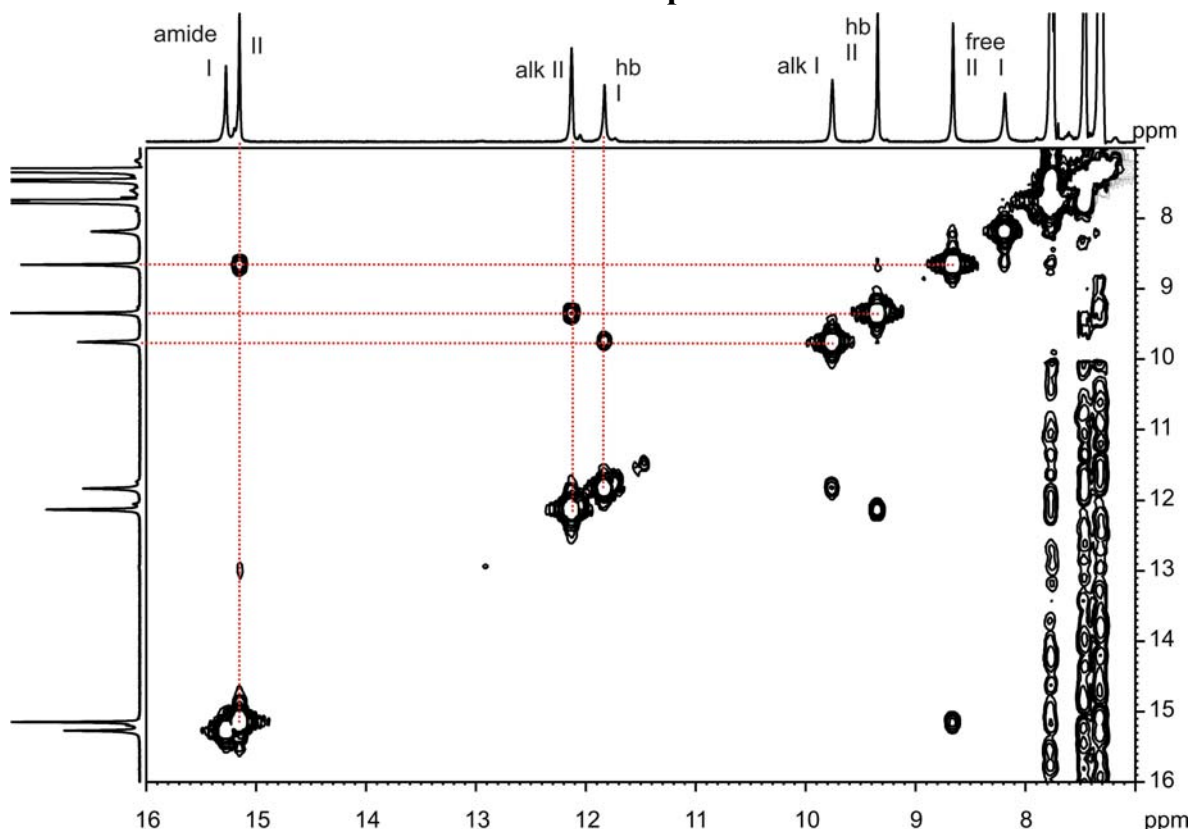
Figure S4.11: Full NH section of COSY spectrum of 3*Boc-Asp-OBn at 220 K in CD$_2$Cl$_2$ and DMSO-d6 (9:1). Three w couplings are visible. Dotted lines were inserted connecting 2D peaks with their corresponding 1D resonances for easier comprehension.

4.7.5 Complete assignment of 3*Boc-Asp-OBn with differentiation of two conformations

Table S4.1: Assignment of **3*Boc-Asp-OBn** (N-cinnamoyl-N'-butylguanidine*Boc-L-Asp-OBn) (1:1) in DCMd2 with 10% DMSOd6 at 220 K, derived via COSY, HSQC, HMBC. Referenced to TMS internal. Where two ^{13}C shifts are given, the splitting is only visible in the ^{13}C spectrum. Guanidinium NH assignment via w-coupling analysis in COSY; NHamide/NHamide' are assigned by HMBC correlation with cinnamoyl-CO as well.

Assignment	δ ^{1}H	m	δ ^{13}C	^{3}J H-H (Hz)	^{1}J ^{1}H-^{13}C (Hz)
nBu-CH$_3$	0.95	bt	14.1	-	
nBu-CH$_2$-b	1.39	bm	20.2 20.5		-
boc-CH$_3$	1.40	s	28.2		
nBu-CH$_2$-c	1.61	bm	30.0 30.4	-	
Asp-CH$_2$-β	2.62	d	39.3		

R. Kleinmaier, R. M. Gschwind, *Magn. Reson Chem.* **2010**, *submitted*.

	3.03	dd			
nBu-CH$_2$-d (split)	3.17	bm	41.3	-	
	3.29	bm	41.4		
Asp-CH-α	4.51	m	50.8		
Asp-OBn-CH$_2$ (split)	5.10	d	66.7		
	5.19	d			
Asp-NH-α	6.20	bm	-		
cinnamoyl-CH-α	6.81	d	119.0	15.84	
cinnamoyl-CH-β	7.75	d	144.9	15.84	
Aryl-Cs	7.25-7.35	m	128.0 128.2 128.7		
	7.42-7-48	m	129.2 131.2		
	7.72-7.78	m	129.2 144.9		
NH$_2$-free I	8.59	s	-	-	-
NH$_2$-free II	8.13	s	-		
NH$_2$-hb II	9.34	s	-	-	-
NH$_2$-hb I	11.85	s	-		
NHalk II	12.13	a-s	-	-	-
NHalk I	9.75	a-s	-		
NH-amide II	15.17	s	-	-	-
NH-amide II	15.29	s	-		
Quat. Carbons:					
C-boc	-		79.4		
Ph-OBn	-		136.2		
Ph-cinnamoyl	-		144.9 145.1		
boc-CONH	-		155.8		
C-guanidinium	-		154.7 155.3	-	
cinnamoyl-CONH	-		168.8 169.4		
COOBn	-		173.2		-
COO$^-$	-		178.2	-	-
	-			-	
	-			-	

R. Kleinmaier, R. M. Gschwind, *Magn. Reson Chem*. **2010**, *submitted*.

5 The NH₂ Rotational Barrier in Acylguanidines is Modelled by an N-Acyl Benzamidine – and it's Lower in the Charged State!*

Roland Kleinmaier, Ruth M. Gschwind

V

5.1 Abstract

Acylguanidines find applications in vast areas of chemistry and especially among N'-substituted N-acylguanidines, highly valued biologically active compounds are found. Still, only little is known about the driving forces for their adopting the distinct conformations that have been detected experimentally. One promising part in this puzzle is the rotational barrier of the NH$_2$ group and especially its entropic contributions. However, in the case of N'-substituted N-acylguanidines it cannot be readily investigated by dynamic NMR to yield the thermodynamic activation parameters $\Delta H^{\ddagger}$ and $\Delta S^{\ddagger}$, because rotational exchange is overlaid by conformational exchange. Therefore, the present work studies the applicability of an N-acyl benzamidine as model compound on which to investigate the NH$_2$ rotational barrier in acylguanidines. Bond distance and ^{13}C chemical shift analysis prove equivalent bonding within the N-acylamidine moiety common to both compound classes. Encouraged by this result, the $\Delta H^{\ddagger}$ and $\Delta S^{\ddagger}$ values for the rotation of the NH$_2$ group in an exemplary N-acyl benzamidine were determined by dynamic NMR in solvents with and without H-bond acceptors in charged and unprotonated state.

All these investigations show that, astonishingly, the intramolecular H-bond is weaker in the protonated state, leading to a reduced rotational barrier despite an increased double bond character of the NH$_2$-C bond. In both states, $\Delta H^{\ddagger}$ and $\Delta S^{\ddagger}$ are raised significantly by more than 25 kJ/mol and almost 100 J/(molK) upon H-bonding to solvent acceptors. Especially the entropy gain upon rotation suggests that directed H-bond interactions which restrict the NH$_2$ rotation are highly unfavourable from an entropic point of view.

5.2 Introduction

Acylguanidines are an abundant class of compounds with various applications in organic and pharmaceutical chemistry.[1-3] Especially among the subgroup of monoalkylated acylguanidines (see Figure 5.1a for a schematic representation), highly potent and selective ligands for G-protein coupled receptors have been identified.[4-6] However, they may adopt different conformations, which hampers the rational design of biologically active substances if the conformational preferences are not known.[7] Therefore, in a recent study,[8] the conformational trends of monoalkylated acylguanidines were identified. Specifically, it was suggested by selective line broadening in the NMR spectra of the NH$_2$ protons in several acylguanidines that entropic contributions from the rotation of the NH$_2$ group might be partially responsible for the experimentally observed conformational preferences. To corroborate this hypothesis, the authors faced the question for the rotational barrier of the NH$_2$ group in the amidine moiety and for the influence of solvent effects and protonation on this

rotational barrier in acylguanidines. In principle, such hindered rotations of parts of a molecule can be analyzed by dynamic NMR experiments[9-13] recording the temperature-dependent development of the line shape and the chemical shifts. The thermodynamic activation parameters $\Delta H^{\ddagger}$ and $\Delta S^{\ddagger}$ can be obtained from Eyring plots of the rate constants obtained by computational line shape analysis of NMR signals.

For this method, the prerequisite for obtaining thermodynamically reliable information on a rotational process is that its influence on the line shape of the observed signals can be clearly separated from that of other temperature dependent phenomena affecting the line shapes, intensities and chemical shifts of these signals. However, in the case of both unprotonated and protonated monoalkylated acylguanidines, the temperature dependent rotational exchange of the two NH$_2$ protons is overlaid by conformational exchange and chemical shift changes of the NH signals modulated by varying strengths of the intra- and intermolecular H-bonds, as shown exemplarily in Figure 5.1.[8]
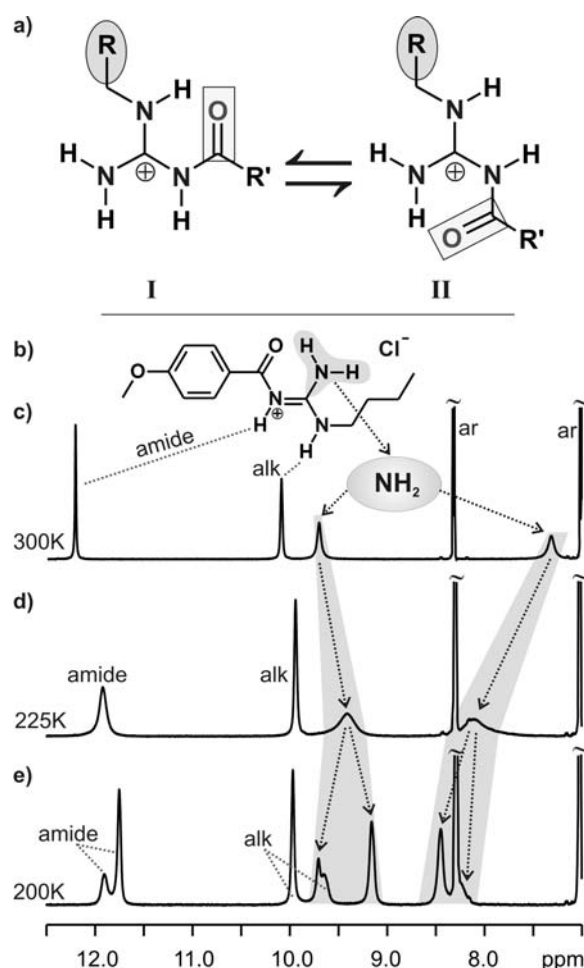
Figure 5.1: a) Conformations adopted by monoalkylated acylguanidines regarding the direction of the intramolecular H-bond.[8] N'-butyl N-p-methoxybenzoylguanidinium hydrochloride shown in b) underlies conformational exchange that can be followed by ^{1}H NMR spectra (600 MHz) of the compound in CD$_2$Cl$_2$. NH sections are depicted in c)-e), indicating that exchange is fast at c) 300 K yielding four relatively sharp NH signals, slows down at d) 225 K, leading to broadening of the NH resonances and is slow enough on the NMR timescale at e) 200 K to allow for the detection of two sets of four NH signals.

R. Kleinmaier, R. M. Gschwind, *J.Org. Chem.* **2010**, *in preparation*.

In Figure 5.1a, the two general conformations adopted by monoalkylated acylguanidines are depicted exemplarily for the protonated state. ^{1}H NMR NH sections of N'-butyl N-p-methoxybenzoylguanidinium hydrochloride depicted in Figure 5.1b are displayed in Figure 5.1c)-e). At 300 K, four sharp NH resonances are detected indicating conformational exchange being fast on the NMR time scale (Figure 5.1c). When the temperature is lowered, the signals broaden (Figure 5.1d) until two sets of four signals are detected once conformational exchange is slow enough on the NMR timescale (Figure 5.1e). In addition, the considerable change of the chemical shift dispersion of the NH protons indicates temperature dependent changes in the intermolecular interactions with the anion. The spectra presented in Figure 1 show that in acylguanidines, contributions of at least conformational exchange together with intermolecular interactions contribute to the signal line width of the two NH$_2$ protons besides the rotation of the NH$_2$ group.

Therefore, an equivalent model compound was selected to circumvent at least the effects of conformational exchange and nevertheless to investigate the rotational barrier of the NH$_2$ group. Such a compound needs a rotatable NH$_2$ group capable of forming an intermolecular H-bond in the same way as the acylguanidines, but must adopt only one conformation. In addition, the molecular scaffold must provide an equivalent bonding situation. These requirements are met well by the closely related compound class of the N-acyl benzamidines (Figure 5.2). In contrast to the acylguanidines, these lack the third nitrogen and thus will persist generally in the conformation depicted in Figure 5.2 because this is the only one stabilized by an intramolecular H-bond.
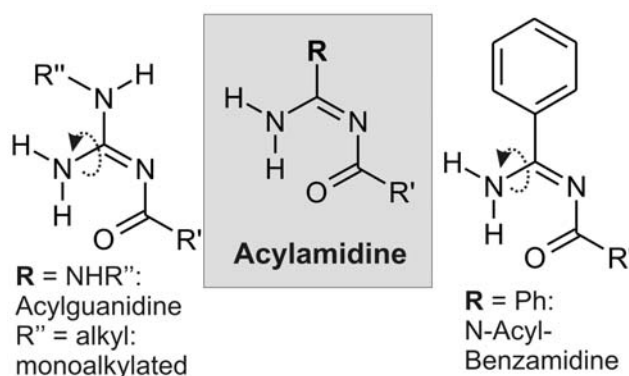
Figure 5.2: Both acylguanidine (left) and N-acyl benzamidine (right) are derived from the same principal amidine scaffold (middle), but in the case of the N-acyl benzamidine, only one conformation is stabilized by an intramolecular H-bond. The rotation of the NH$_2$ group is indicated by dashed arrows.

The bonding situation in principle is expected to be quite similar regarding the hybridization of the atoms because the underlying amidine scaffold carrying an acyl residue stays unchanged. Only the third substituent is varied from a nitrogen atom, which is planar and pseudo-sp^2 hybridized due to electron delocalization over the guanidine, to an sp^2 hybridized

aromatic carbon. Verification of this similarity of the bonding situation is expected to be possible by an analysis of bond lengths from crystal structures of acylguanidines and N-acyl benzamidines.

Therefore, in this study, the rotational barrier of the NH$_2$ group in N-acyl benzamidines is investigated and the influence of solvent effects and protonation on this rotation is presented as a possible explanation for the observed conformational preferences in the biologically important class of N'substituted N-acylguanidines. The applicability of the N-acyl benzamidine **1** (see Figure 5.3) as model compound to investigate the rotation of the NH$_2$ group is confirmed by a comparison of bond lengths derived from crystal structures as well as by the comparison of ^{1}H and ^{13}C chemical shifts of acylguanidines and **1** both in the unprotonated and the protonated state. In addition, these crystal structures allow for an analysis of the bonding situation in these compounds, while the change of the ^{1}H chemical shift of the NH$_2$ protons with different solvents and upon protonation offers a clue to the solvent interactions of the two NH$_2$ protons and the strength of the intramolecular H-bond. Furthermore, also the ^{13}C chemical shifts of the carbons in the acylamidine scaffold are sensitive to the effect protonation and yielded insights into electronic changes in the acylamidine upon protonation.

In order to elucidate the influence of protonation on the thermodynamic activation parameters $\Delta H^{\ddagger}$ and $\Delta S^{\ddagger}$ of the NH$_2$ rotation, experimental values of $\Delta H^{\ddagger}$ and $\Delta S^{\ddagger}$ were obtained by dynamic NMR spectroscopy on samples of **1** and its tetrafluoroborate salt **1-HBF$_4$** at temperatures between 195 K and 370 K and. In order to investigate the influence of H-bonding to acceptors provided by solvent molecules, CD$_2$Cl$_2$ was compared to CD$_2$Cl$_2$/DMSO-d_6, DMSO-d_6 and CD$_3$CN as solvents.

5.3 Results and Discussion

5.3.1 Compound pool

In addition to **1,** further compounds were selected for this study (see Figure 5.3) focusing on the comparability of structural features between N-acyl benzamidines and acylguanidines. Secondly, the availability of crystal structures of the selected compounds was considered essential in order to prove the structural equivalence. Therefore, **1** was chosen because the p-methoxybenzoic acid moiety as acyl substituent is present also in the acylguanidine **2a**, which was subject of a conformational study of monoalkylated acylguanidines.[8] In addition, crystal structures of the protonated **2a-HCl** (also incorporating the p-methoxybenzoyl substituent) and of the unprotonated acylguanidine **2c**[8](closely related to **2a**) are available as well as a crystal structure of the unprotonated N-acyl benzamidine **1b** in literature,[14] which structurally differs only slightly from **1** in that its benzoyl moiety is substituted with a

hexadecyloxy residue instead of a methoxy group. Also for the acylguanidines **3**[4] and **4**,[15] crystal structures are available from literature, which are therefore also included in the discussion. Finally, **1-HClO$_4$** yielded the to our knowledge first crystal structure of a protonated N-acyl benzamidine, which was obtained as part of this work, and therefore completes the pool of compounds. **2b** was included in the analysis of ^{1}H and ^{13}C chemical shifts.
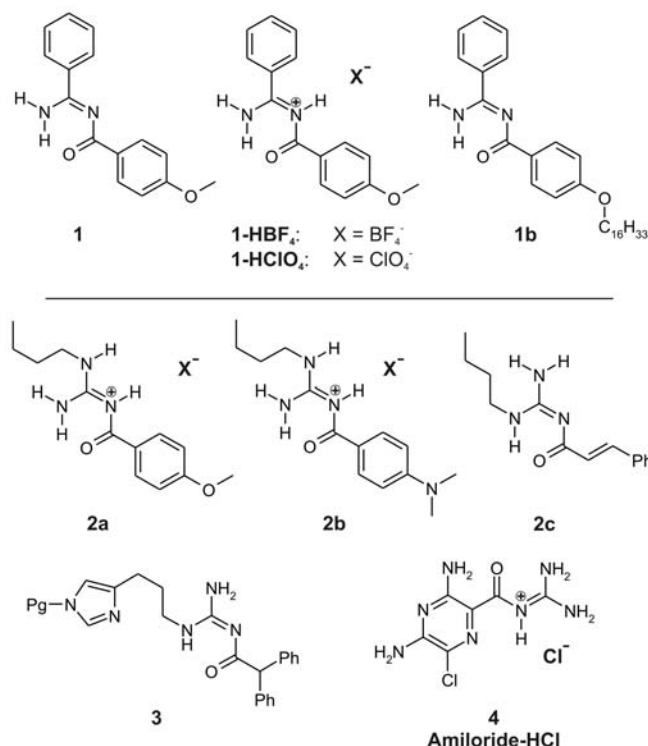
Figure 5.3: The pool of compounds discussed in this study comprises the N-acyl benzamidine **1** and its protonated forms **1-HBF$_4$** and **1-HClO$_4$**, the closely related **1b** as well as the N-butyl-N'-acylguanidines **2a-c** and finally the structurally more deviating acylguanidines **3** and **4**.

Details on the preparation of **1** and the protonated derivatives of **1-HClO$_4$**, **1-HBF$_4$** as well as on the production of the X-ray crystal structure of **1-HClO$_4$** are given in the SI part, while synthetic details on the compounds **1b**,[14] **2a-c**,[8] **3**,[4] and **4**[15] have been published elsewhere.

5.3.2 Dynamic NMR spectra of benzamidines

The hindered rotation of the NH$_2$ group generally observed in temperature dependent NMR spectra of **1** and **1-HBF$_4$** is exemplarily shown on spectra of **1** in DMSO-*d$_6$*. Two well separated ^{1}H signals are detected for the NH$_2$ group at 300 K (see Figure 5.4) followed by

coalescence of the signals at 332.5 K. This simple signal pattern allowed for line shape analysis of the NH$_2$ groups of **1** in all cases investigated, although under varying experimental conditions it was often not possible to obtain spectra above the coalescence point.
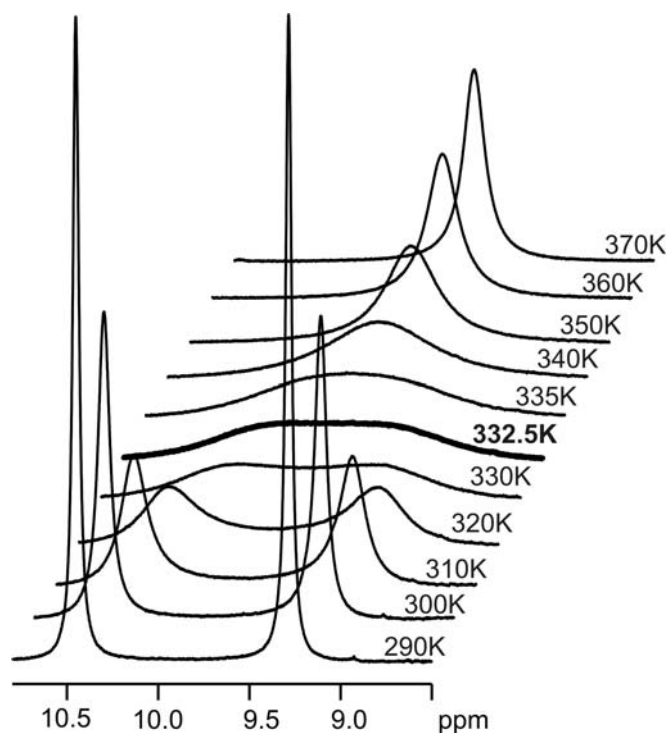
Figure 5.4: Stack of NH$_2$ sections of ^{1}H spectra (600 MHz) of **1** in DMSO-d_6 showing the line shape development of the two NH$_2$ resonances (fully separated at 290 K). Signal broadening with increased temperature can be followed through the coalescence point (thick line) at 332.5 K to one single resonance at 370 K.

The spectra depicted in Figure 5.4 demonstrate that the rotation of the NH$_2$ group in **1** is hindered in contrast to the usually observed situation, where fast rotation of the NH$_2$ group on the NMR timescale prevents the detection of separate signals, so that one (usually broad) resonance with an integral of two is obtained e.g. for the α-NH$_2$ group in amino acids and also for the NH$_2$ groups of unsubstituted guanidine.[16] In addition, it demonstrates that N-acyl benzamidines provide a newly identified model for the investigation of the rotational barrier of NH$_2$ groups in such intramolecular H-bonds and of the influence of the solvent and protonation on this rotation.

R. Kleinmaier, R. M. Gschwind, *J.Org. Chem.* **2010**, *in preparation*.

5.3.3 X-ray crystal structure analysis

First, the equivalence of the bonding situation in N-acyl benzamidines and acylguanidines was checked in order to validate the benzamidine as closely similar model for monoalkylated acylguanidines concerning the rotation of the NH$_2$ group. For this purpose, bond lengths derived from crystal structures of substances from both compound classes in the protonated and unprotonated state were compared. In addition to a check of equivalent bonding, the analysis of the bond lengths offers a highly valuable clue to the double bond character of the bonds in the amidine scaffold as well as to the expected strength of the intramolecular H-bond. The effect of protonation, i.e. the introduction of a positive charge, on both of these parameters can be investigated because crystal structures of both protonated and unprotonated compounds from both classes are now available. The crystal structure of **1-HClO$_4$** (shown in Figure 5.5) was accomplished as part of this work and is to the authors' knowledge the first crystal structure of a protonated N-acyl benzamidine, which can thus be compared to the crystal structure of the unprotonated N-acyl benzamidine **1b**. Figure 5.5 shows that the conformation of the acyl substituent in **1-HClO$_4$** is such that the NH$_2$ group can form an intramolecular H-bond to the carbonyl oxygen.
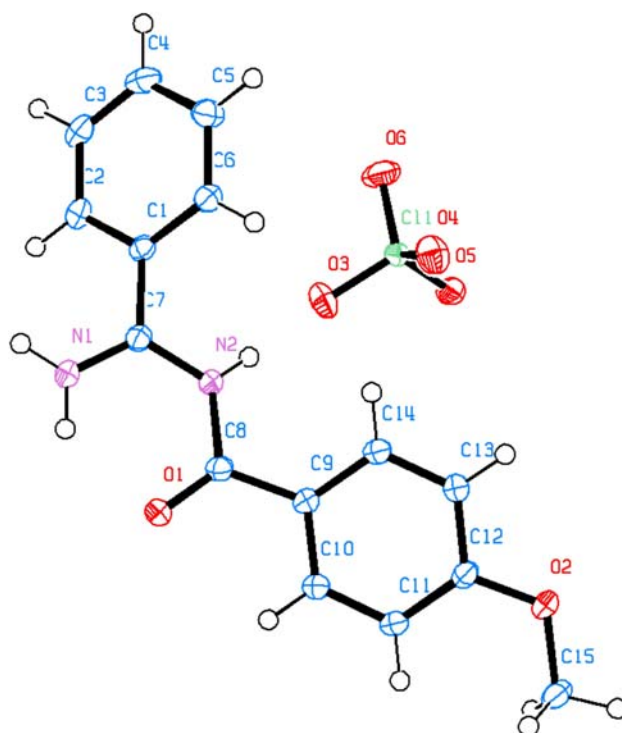
Figure 5.5: Ortep plot of crystal structure of **1-HClO$_4$**. The NH$_2$ group forms an intramolecular H-bond to the carbonyl oxygen.

R. Kleinmaier, R. M. Gschwind, *J.Org. Chem.* **2010**, *in preparation*.

In the following table (Table 5.1), two crystal structures of the unprotonated N-acyl benzamidine 1b and the salt 1-HClO$_4$, two from unprotonated acylguanidines (2c and 3) and two from protonated ones (2a-HCl and 4) are presented. Figure 5.6a gives the assignment of the atomic distances used in Table 5.1 and in Figure 5.6b, the effect of protonation on the bond lengths is represented schematically for the two benzamidines 1b and 1-HClO$_4$. The atomic distances in Å put besides the bonds in Figure 5.6b indicate the change in the bond lengths occurring upon protonation. However, the trends shown exemplarily on the comparison of 1b and 1-HClO$_4$ are also present in the acylguanidines.
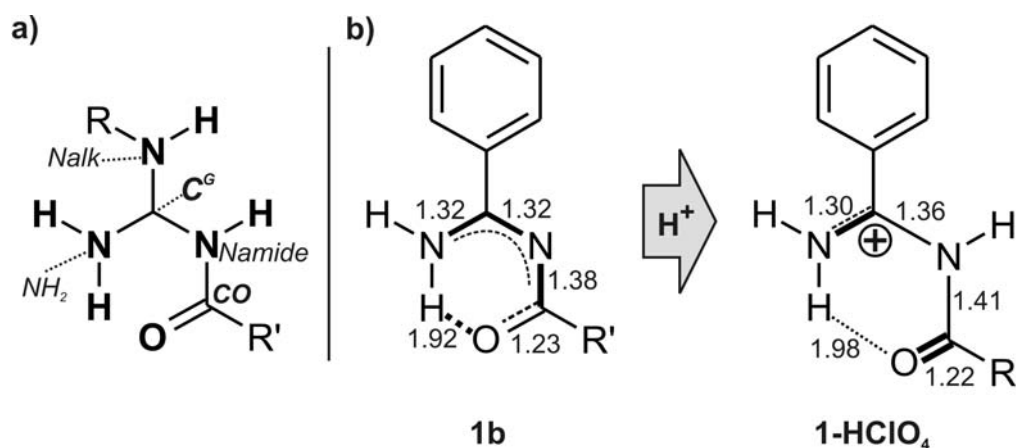
Figure 5.6: a) Nomenclature applied for the description of bond distances. b) Schematic representation of the effect that protonation has on the bond lengths on the example of the benzamidines **1b** (unprotonated) and **1-HClO$_4$** (protonated).

Table 5.1: Interatomic distances from X-ray crystal structures of the benzamidine **1b** in the free base form and of the salt **1-HClO$_4$**, of two unprotonated acylguanidines (**2c** and **3**) and of two protonated ones (**2a-HCl** and **4**).

	Distance in Å					
	Nalk-C^G	**NH$_2$-C^G**	**Namide-C^G**	**Namide-CO**	**CO-O**	**CO-HN-** *HB*
Species						
Benzamidines						
1b	-	**1.323**(2) *HB*	**1.317**(2)	**1.384**(2)	**1.231**(2)	**1.918**
1-HClO$_4$	-	**1.300**(2)	**1.357**(2)	**1.406**(2)	**1.221**(2)	**1.98**
Unprotonated Acylguanidines						
2c	**1.334**(2) *HB*	**1.329**(2)	**1.360**(2)	**1.344**(2)	**1.260**(2)	**1.89**(2)
3	**1.335**(2) *HB*	**1.326**(2)	**1.366**(2)	**1.351**(2)	**1.249**(2)	**1.89**(2)
Protonated Acylguanidines						
2b-HCl	**1.321**(2)	**1.312**(2) *HB*	**1.375**(2)	**1.384**(2)	**1.223**(2)	**2.02**(2)
4 (Amiloride-HCl) (2 different molecules in cell)	-	**1.313**(2) / **1.316**(3) *HB* **1.311**(2) / **1.298**(3)	**1.364**(2) / **1.365**(2)	**1.394**(2) / **1.388**(2)	**1.226**(2) / **1.233**(2)	**2.08**(3) / **1.95**(3)[17]

5.3.4 Comparison of bond lengths between N-acylbenzamidines and acylguanidines

A direct comparison of the interatomic distances is of course only feasible comparing first 1b with the unprotonated acylguanidines 2c and 3 and then 1-HClO$_4$ with the protonated acylguanidines 2b-HCl and 4. Regarding structural similarity with a view to the rotation of the NH$_2$ group, the most important bonds are the NH$_2$-C^G bond and the intramolecular CO-HN H-bond. In Table 5.1, it is seen that for both bond distances in protonated and unprotonated state, the values are very similar comparing the acyl benzamidines with the acylguanidines, respectively, and differ by only 0.01 Å in most cases. The C-O bond length is by 0.03 Å longer in the uncharged acylguanidines and again almost equal within the error range in the protonated state. There are two bond distances which show a larger deviation comparing benzamidine with acylguanidine: Namide-C^G is longer in 1b than in 2c and 3 by about 0.04 Å, while in the protonated state, it seems to be equal within the error range. Secondly, Namide-CO is longer by about 0.02-0.03 Å in both states in the benzamidine. For the latter two distances, the deviations are supposed to be due to the absence of the third

R. Kleinmaier, R. M. Gschwind, *J.Org. Chem.* **2010**, *in preparation*.

nitrogen in the benzamidine, which changes the electron delocalization and the Namide-C distances seem to be affected most as they mediate the conjugation to the acyl unit. However, the deviations are mostly marginal (below 2.5% except for Namide-C^G), while the two bonds which are especially important for the rotational barrier of the NH$_2$ group, i.e. NH$_2$-C^G and CO-HN, are almost equal.

5.3.4.1   Effect of protonation on the bond distances

Principally, the rotation of the NH$_2$ group in an acylamidine (see Figure 5.2) around the C-N bond is expected to be subject to two major influences: First, the partial double bond character of the C-N bond hinders the rotation because of the π-contribution to the binding. The larger the π-contribution, the higher is the rotational barrier.

The experimental separation of these influences is not trivial. However, the bond lengths obtained from X-ray crystal structures are reasonable indicators of the amount of delocalization over the acylamidine moiety, i.e. of the double bond character of the individual bonds.

In Figure 5.6, the general effect of protonation, which is observed in both acylguanidines and benzamidines, is represented schematically on the example of 1b and 1-HClO$_4$. Upon protonation, a significant increase (see also Table 5.1) in the distances of Namide-C^G, Namide-CO and of the intramolecular H-bond is observed generally for both the benzamidine and the acylguanidines. This elongation of the bonds may be explained by a repulsive effect of the positive charge against the positively polarized carbonyl carbon. It also means a decrease of the double bond character in these bonds. On the other hand, C-O and NH$_2$-C^G become slightly shorter (by about 0.02 Å) upon introduction of the positive charge.

Astonishingly, this means that the double bond character in these bonds increases upon protonation. Expectation would have held that upon protonation, the double bond would be delocalized and the bond distances within the amidine moiety would rather assimilate. The opposite is the case, both for the acylguanidines and for the acyl benzamidines. As a consequence, the intramolecular H-bond is longer by 5% in the protonated state, i.e. it is weaker although the H-bond donor quality of the NH$_2$ group is supposed to become a lot better when the nitrogen shares the positive charge, because the NH acidity is increased.[18]

The overall result of the bond length analysis is that the application of an N-acyl benzamidine as model compound to study the rotation of the NH$_2$ group is feasible. The relevant bonds show very similar distances comparing the benzamidine with the acylguanidine, both in charged and uncharged state. Protonation has the same effect in both cases: The acyl residue is pushed away, possibly because of electrostatic repulsion. The delocalization of the double bond is actually reduced.

R. Kleinmaier, R. M. Gschwind, *J.Org. Chem.* **2010**, *in preparation.*

Regarding the rotation of the NH_2 group, this has two opposing consequences. First, the intramolecular H-bond is longer and thus weaker in the protonated state, which should reduce the rotational barrier. On the other hand, the NH_2-C^G bond has more double bond character in the protonated state, which should increase the rotational barrier.

Next, direct comparisons of ^1H and ^{13}C chemical shifts between acylguanidines and the benzamidine **1** are made for both unprotonated and protonated state. This shall further corroborate the equivalence of **1** as a model for the rotation of the NH_2 group.

5.3.4.2   NMR investigations of chemical Shifts

Secondly, H-bonding of the NH_2 protons will greatly reduce the free rotation of the NH_2 group. This second point can be subdivided into the effect of intramolecular vs. intermolecular H-bonds. The intramolecular H-bond between one NH_2 proton and the carbonyl oxygen in a six-membered ring-like arrangement is commonly observed in acylated amidines, e.g. acylguanidines, acylureas and acylbenzamidines. Rotation of the NH_2 group around the C-N bond is supposed to be drastically retarded by this H-bond which manifests itself in the splitting of the ^1H NMR signal of the NH_2 protons.[14,19-21] Intermolecular H-bonds, on the other hand, may be formed between two acylamidine molecules as well as to solvent molecules.

Concerning the H-bonds, one would expect a relatively small effect of the type of solvent as long as aprotic solvents without any strong H-bond acceptors or donors are employed. In contrast, H-bond accepting solvents compete with the carbonyl oxygen and are supposed to weaken the intramolecular H-bond. A differentiation of this effect from the impact such a solvent has on the intermolecular H-bonding phenomena may be possible by the analysis of the NMR chemical shifts of the NH_2 protons involved and of the carbonyl carbon.

The ^1H and ^{13}C chemical shifts of **1** and **1-HBF$_4$** in different solvents were investigated. HBF_4 was chosen because its anion is known to be non-coordinating due to its electron-delocalized character.

First, in order to investigate the solvent dependence of the ^1H chemical shifts of the NH_2 protons of **1,** their values in $CDCl_3$, CD_2Cl_2, CD_3CN, DMSO-d_6 and a mixture of CD_2Cl_2 with 5% DMSO-d_6 are compared in Table 5.2.

The ^1H chemical shift of the NH_2 proton in the intramolecular H-bond is supposed to be a good indicator of the strength of this H-bond because H-bonding increases the chemical shift of NH protons. In **1**, the shift of this resonance proves quite stable throughout all the solvents in Table 5.2 (δ 10.42-10.67; $\Delta \delta$ < 0.3 ppm at 300 K).

Table 5.2: [1]H chemical shifts of the NH_2 protons of **1** in different solvents at 300 K. The proton in the intramolecular H-bond shows a quite stable shift, while the second (solvent exposed) one shows a strong solvent dependence.

Solvent	δ NH_2 ppm (intramol HB)	δ NH2 ppm (solvent exposed)
$CDCl_3$	10.55	6.91
DCM-d_2	10.67	6.66
DCM-d_2 +5% DMSO-d_6	10.62	7.72
CD_3CN	10.50	7.54
DMSO-d_6	10.42	9.24

In contrast, the chemical shift of the solvent exposed NH_2 proton increases from δ 6.66 to 9.24 ppm (Δ δ > 2.7 ppm), indicating significant interactions with solvents providing H-bond acceptors. In addition, the temperature dependence of the chemical shifts of the NH_2 protons is much larger in the case of the solvent exposed proton (Δ δ > 1.7 ppm vs. 0.3 ppm in DCM+5% DMSO over the range of 195 K to 300 K), also indicating solvent H-bonds.

The chemical shift of the proton in the intramolecular H-bond is only slightly influenced by the solvent. The reduced chemical shift in the presence of solvents with H-bond acceptor properties, i.e. CD_3CN and DMSO-d_6, which is actually a strong competitive acceptor, seems to be correlated to the increased chemical shift of the second NH_2 proton. The additional H-bonds to this solvent exposed NH proton and maybe even to the NH proton in the intramolecular H-bond seem to weaken the intramolecular H-bond as well. This may lead to the observed chemical shift. The observation of stable chemical shifts of the NH_2 proton in the intramolecular H-bond in contrast to a strong solvent dependence of the shift of the solvent exposed one is closely reproduced in the study of the acylguanidines **2a** and **2b** (for details see SI).

Next, the ^{1}H chemical shifts of the NH_2 protons of **1-HBF₄** were investigated. Here, pure CD_2Cl_2 could not be used as solvent because of the decent solubility of the compound. Therefore, mixtures of CD_2Cl_2 with four different contents of DMSO-d_6 (approx. 5%, 10%, 15% and 20%) were compared with samples in pure CD_3CN and pure DMSO-d_6. All samples containing DMSO up to pure DMSO show stable chemical shifts of all three NH protons (Δ δ less than 0.2 ppm at 300 K through the whole series, see Table 5.3 and for spectra see SI).

Table 5.3: [1]H chemical shifts are presented of NH protons in **1-HClO$_4$** in four different mixtures of CD_2Cl_2 with DMSO-d_6, in pure DMSO-d_6 and in CD_3CN.

Solvent	δ NH$_2$ ppm (intramol HB)	δ NH2 ppm (solvent exposed)	δ NH amidic ppm
CD$_2$Cl$_2$ + x% DMSO-d_6			
a) 5%	12.40	11.45	11.17
b) 10%	12.48	11.59	11.20
c) 15%	12.48	11.63	11.21
d) 20%	12.43	11.53	11.20
DMSO-d_6	12.39	11.43	11.17
CD$_3$CN	9.88 (unres.)		10.97

In contrast, changing the solvent to CD_3CN invokes a shift of the NH_2 resonances (unresolved at 300 K) to lower ppm values by about 2 ppm, which is supposedly because of the weaker H-bond acceptor properties of CD_3CN. This again proves H-bond interactions of the NH_2 protons with the solvent and in this case, the two protons are more or less equally affected by them, which may also point to a reduced strength of the intramolecular H-bond. Furthermore, reduced electrostatic interactions with the anion may add to the reduced shift in CD_3CN since it is able to solvate the anion better than DMSO, because it is also a weak H-bond donor, in contrast to DMSO.[22,23] However, the chemical shift of the amidic proton is reduced by only 0.2 ppm in Table 5.3. Comparing these findings with results obtained for samples of the protonated acylguanidine **2a-DCA** and **2a-Boc-Asp-OBn** (for details on this carboxylate anion see SI), it can be stated that the chemical shift of the NH proton in the intramolecular H-bond is almost uninfluenced by the amount of DMSO present (for details see SI), just as is the case for **1-HBF$_4$**.

Finally, the ^{1}H chemical shifts of the NH_2 protons of **1** were compared with those of **1-HBF$_4$**.

Both resonances are shifted to higher ppm values by about 2 ppm (compare Table 5.2 and Table 5.3) by the deshielding effect of the positive charge. This accords with the expectation that protonation of the amidine should render the protons more acidic. However, the chemical shifts of the NH_2 protons are much more similar to one another in **1-HBF$_4$**, which points to a weaker differentiation due to a weaker intramolecular H-bond. Thus, the result of the bond length analysis that the intramolecular H-bond is weaker in the charged state of the acylamidine is corroborated by the ^{1}H chemical shift analysis.

In order to investigate the change in electron density at the carbonyl (CO) and amidine (C[G]) carbons upon protonation, the ^{13}C chemical shifts of the C[G] and CO carbons of compounds **1** and **1-HBF$_4$**, **2a** and **2a-HCl**, **2b** and **2b-TFA**, and **2c** and **2c-HCl** were

measured (see Table 5.4). Since solvent and temperature effects on the ^{13}C chemical shift of these carbons were found to be negligible compared to the difference between free base and salts, sample conditions are listed in detail only in the SI in addition to further ^{13}C data of supplementary compounds confirming the trend derived from Table 5.4.

Table 5.4: ^{13}C chemical shifts of carbonyl (CO) and amidine (C^G) carbons in uncharged and charged states. In the case of **2c**, two conformations delivered two sets of signals.

Compound	δ ^{13}C (ppm) free base		δ ^{13}C (ppm) protonated	
	CO	C^G	CO	C^G
1/ 1-HBF$_4$	179.2	165.0	170.7	167.9
2a/ 2a-HCl	176.7	161.8	168.6	155.1
2b/ 2b-TFA	177.4	161.7	169.4	155.7
2c/ 2c-HCl	176.0/ 176.7	161.9/ 161.4	168.2	155.3

Table 5.4 shows that the ^{13}C chemical shifts of all the carbonyl (CO) carbons are lowered by more than 7 ppm in the protonated state. This means that surprisingly the electron density at the carbonyl C increases, i.e. that the carbonyl C is less positively polarized upon protonation. This is in agreement with the reduced C-O bond length in the protonated state derived from the crystal structures (Table 5.1). Both results indicate a stronger double bond character in the C-O bond and a less polarized C-O bond, leading to reduced H-bond acceptor properties of the carbonyl oxygen in the protonated state.

This nicely matches the increased NH-OC distance in the crystal structures of the protonated acylamidines indicating weakened intramolecular H-bonds in the protonated state.

The central amidine carbon has a slightly increased chemical shift in **1-HBF$_4$** compared to **1** (see Table 5.4), whereas in the case of the acylguanidines, its chemical shift is uniformly lowered from about 161 ppm to about 155 ppm. It seems to be affected most by the structural differences between the N-acyl benzamidine and the acylguanidine, i.e. the presence of a third nitrogen bound to it. This nitrogen can participate in electron pair delocalization to compensate the charge, which thus is shown to be distributed over the acylguanidinium moiety rather than being localized at the central carbon or the amidic nitrogen, which is the actual site of protonation. Therefore, the electron density at the C^G carbon even increases upon protonation and the nucleus gets shielded. However, looking again at Table 5.1, the NHalk-C^G and NH$_2$-C^G bonds become shorter upon protonation, while Namide-C^G is slightly elongated, but Namide-CO is stretched significantly (by 0.04Å). Therefore, it is again found that the considerable delocalization of the charge is unsymmetric and rather than being

R. Kleinmaier, R. M. Gschwind, *J.Org. Chem.* **2010**, *in preparation*.

conjugated to the acyl moiety, it drives the two molecule parts away from each other. These considerations actually fit to the increased chemical shift in the case of the benzamidine: Because there is one nitrogen less for delocalization and the phenyl ring obviously adds little to it, the nucleus is deshielded compared to the uncharged state. Interestingly, despite the more localized charge, the electrostatic repulsion of the benzamidine moiety against the carbonyl carbon does not lead to a significantly greater increase in the sum of the Namide-C^G and Namide-CO distances (see Table 5.1) than in the acylguanidines.

In summary, the results of the ^{13}C chemical shift analysis are very similar for the acyl benzamidine and the acylguanidines and they again support the findings from the crystal structure analysis.

5.3.4.3 Thermodynamic analysis of 1

Additionally, it may be proposed that breaking the intramolecular H-bond during rotation will be mainly enthalpy-governed[24] (because a bond has to be broken, since H-bonds have partly covalent character) while any intermolecular H-bonds to the solvent need not necessarily be disrupted since the small solvent molecules are extremely mobile and flexible. Therefore, these intermolecular interactions will have a largely entropic contribution. A survey of the thermodynamic activation parameters $\Delta H^{\ddagger}$ and $\Delta S^{\ddagger}$ for the NH$_2$ rotation process can thus give insights into changes of the dominant interactions when conditions such as solvent or protonation state are varied.

Next, the thermodynamic activation parameters $\Delta H^{\ddagger}$ and $\Delta S^{\ddagger}$ for the rotation of the NH$_2$ group were determined by dynamic NMR studies. In order to elucidate the influence of protonation and of H-bonding to the solvent, **1** and **1-HBF$_4$** were investigated at temperatures between 195 K and 370 K in CD$_2$Cl$_2$, CD$_3$CN, DMSO-*d$_6$* and mixtures of CD$_2$Cl$_2$ with DMSO-*d$_6$*. Solvents are not supposed to influence the general bonding situation, so the contribution of the double bond parts in the C^G-NH$_2$ bond will be the same throughout the solvents. As mentioned in the discussion of the ^{13}C chemical shifts of the benzamidines and acylguanidines (see above) no significant effect of the solvent on the ^{13}C chemical shifts of the relevant carbons CO and C^G was detected. Therefore, any change in $\Delta H^{\ddagger}$ and $\Delta S^{\ddagger}$ with the solvent will comprise indication of the solvent's influence on the strength of intra- or intermolecular H-bond interactions. In general, solvent permittivity is not expected to greatly influence the strength of an intramolecular H-bond,[25] so the main effect is supposed to be produced by competitive H-bonding.

Temperature dependent rate constants for the NH$_2$ rotation were obtained by line shape analysis using SpinWorks (see SI for details). The resulting Eyring plots are shown in Figure 5.8. $\Delta H^{\ddagger}$ and $\Delta S^{\ddagger}$ are calculated according to the Eyring equation:[9]

R. Kleinmaier, R. M. Gschwind, *J.Org. Chem.* **2010**, *in preparation*.

$$k = \frac{k_B T}{h} \exp\frac{\Delta S^{\#}}{R} \exp\frac{-\Delta H^{\#}}{RT}$$, where k is the rate constant, k_B the Boltzmann constant, h Planck's constant, R the gas constant and T is the absolute temperature. A plot of $ln(k/T)$ against $1/T$ yields $-\Delta H^{\ddagger}/R$ as slope and $\Delta S^{\ddagger}/R + ln\ (k_B/H)$ as y-intercept.

From these plots the thermodynamic activation parameters $\Delta H^{\ddagger}$ and $\Delta S^{\ddagger}$ are derived, which are presented in Table 5.5.

R. Kleinmaier, R. M. Gschwind, *J.Org. Chem.* **2010**, *in preparation*.

5. The NH$_2$ Rotational Barrier in Acylguanidines is Modelled by an N-Acyl Benzamidine – and it's Lower in the Charged State!
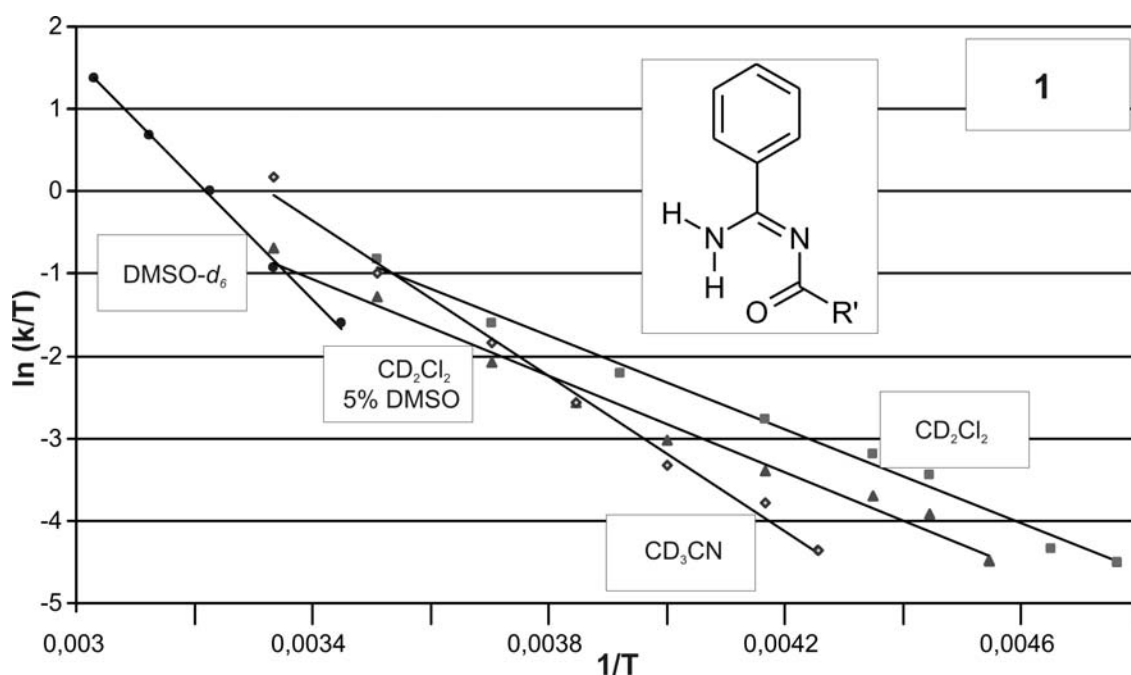
Figure 5.7: Eyring plots of **1** in CD$_2$Cl$_2$, CD$_3$CN, DMSO-d_6 and a mixtures of CD$_2$Cl$_2$ with 5%DMSO-d_6. Rate constants k were obtained from dynamic NMR experiments. The structure of **1** is inset.
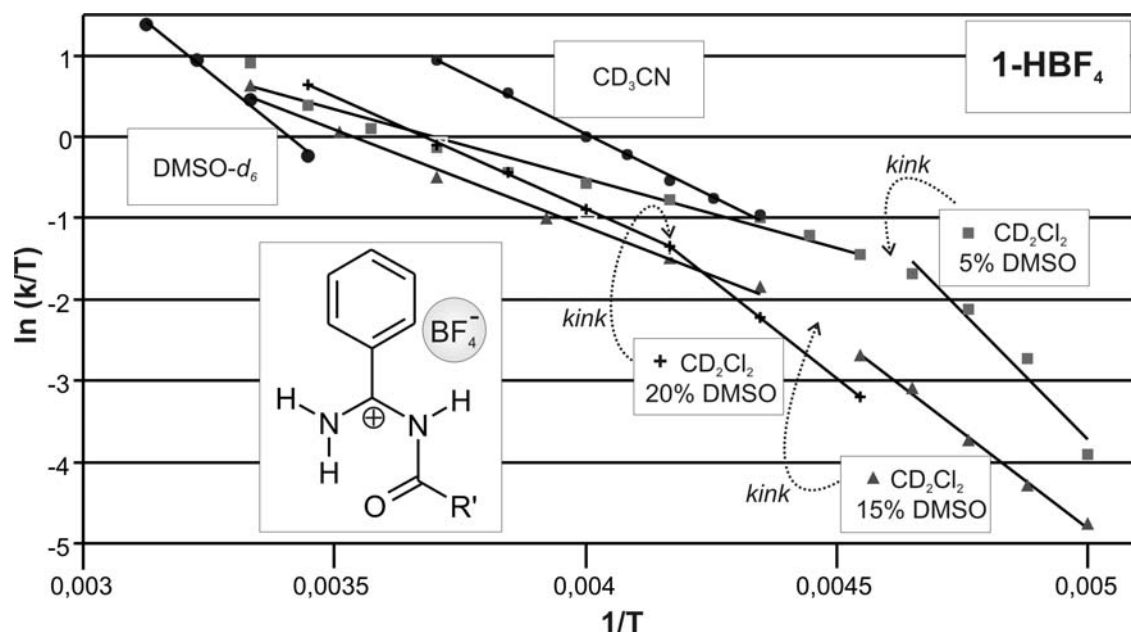
Figure 5.8: Eyring plots for **1-HBF$_4$** in CD$_2$Cl$_2$, CD$_3$CN, DMSO-d_6 and mixtures of CD$_2$Cl$_2$ with DMSO-d_6. In the solvent mixtures, kinks in the graph are obtained, which are indicated by dotted arrows. Therefore, the two parts of the graph were fitted separately in these cases. Rate constants k were obtained from dynamic NMR experiments. The structure of **1-HBF$_4$** is inset.

R. Kleinmaier, R. M. Gschwind, *J.Org. Chem.* **2010**, *in preparation*.

Table 5.5: Thermodynamic activation parameters obtained from Eyring plots. In the case of the HBF$_4$ salt, the graph showed a kink around 220 K and the two linear parts A and B were fitted separately. Extrapolation delivered in each case the y-intercept needed for $\Delta S^{\ddagger}$ in addition to the slope yielding $\Delta H^{\ddagger}$.

Entry	$\Delta H^{\ddagger}$	$\Delta S^{\ddagger}$
	kJmol^{-1}	Jmol^{-1}K^{-1}
free base		
CD$_2$Cl$_2$ pure	23.7	-122
CD$_2$Cl$_2$ +5% DMSO-d_6	24.4	-124
CD$_3$CN	39.2	-67
DMSO-d_6	60.3	-3
HBF$_4$-salt		
CD$_2$Cl$_2$ +5% DMSO-d_6; **A, 200K-215K**	52.3	33
CD$_2$Cl$_2$ +15% DMSO-d_6; **A, 200K-220K**	39.2	-41
CD$_2$Cl$_2$ +20% DMSO-d_6; **A, 220K-240K**	40.5	-40
CD$_2$Cl$_2$ +5% DMSO-d_6; **B, 220-300K**	14.1	-145
CD$_2$Cl$_2$ +15% DMSO-d_6; **B, 225-300K**	19.9	-127
CD$_2$Cl$_2$ +20% DMSO-d_6; **B, 240-290K**	23.0	-113
CD$_3$CN	25.4	-95
DMSO-d_6	41.2	-57

A positive value of $\Delta H^{\ddagger}$ is interpreted as unfavourable for the activation. The higher $\Delta H^{\ddagger}$, the less favourable is the rotation of the NH$_2$ group in terms of enthalpy. A positive value for $\Delta S^{\ddagger}$ is interpreted as a sign for an entropy gain in the transition state, i.e. the transition state has additional degrees of freedom. The higher $\Delta S^{\ddagger}$, the more entropically favoured is the NH$_2$ rotation.

Free base.

In CD$_2$Cl$_2$, i.e. a solvent without H-bond acceptor properties, $\Delta H^{\ddagger}$ is the lowest (23.7 kJ/mol) combined with a highly negative $\Delta S^{\ddagger}$ value (-122 J/(molK)). Interestingly, the addition of the relatively small amount of 5% DMSO-d_6 to the CD$_2$Cl$_2$ solution changes neither the enthalpy nor the entropy of activation of the NH$_2$ rotation significantly. In contrast, in pure CD$_3$CN and DMSO-d_6, gradually increased values of $\Delta H^{\ddagger}$ and $\Delta S^{\ddagger}$ are obtained, up to 60.3 kJ/mol and -3 J/(molK) in DMSO-d_6.

R. Kleinmaier, R. M. Gschwind, *J.Org. Chem.* **2010**, *in preparation*.

By expectation, the intramolecular H-bond should be weakened by competition from the strong H-bond acceptor DMSO upon its addition to the pure CD$_2$Cl$_2$ solution. As mentioned in the discussion of the ^{1}H chemical shifts, there definitely is an interaction of the second NH$_2$ proton with DMSO and so a possible explanation for the seeming indifference of $\Delta H^\ddagger$ and $\Delta S^\ddagger$ against the addition of 5% DMSO is that even if DMSO weakens the intramolecular H-bond, it also forms new H-bonds to the second proton and the two effects are outbalanced regarding both enthalpy (breaking of H-bonds) and entropy (e.g. disruption of a possibly H-bonded solvent shell).

Similarly, the large value of $\Delta H^\ddagger$ in pure CD$_3$CN and DMSO, i.e. the competitive H-bond forming solvents, cannot mean that the intramolecular H-bond is strongest here. Rather, the formation of additional H-bonds between accepting solvent molecules and the proton in the intramolecular H-bond can be documented by its reduced ^{1}H chemical shift compared to the other solvents. Obviously, this effect is weaker for CD$_3$CN than for pure DMSO, where it is so pronounced that $\Delta H^\ddagger$ is raised drastically and $\Delta S^\ddagger$ almost becomes positive. This corresponds well to the Kamlet-Taft H-bond basicities (β) of the two solvents (β(CH$_3$CN) = 0.40, β(DMSO) = 0.76; large values assign strong H-bond acceptors).[22,23]

In order to exclude the possibility that the differences observed between the solvents are caused by aggregation phenomena, the tendencies of self-aggregation were studied by DOSY (diffusion ordered spectroscopy) measurements of the samples used for the dynamic NMR investigations at various temperatures from 220 K to 300 K. Molecular mass estimation referenced to internal TMS[26] (tetramethylsilane) delivered experimental values for the macroscopic degree of aggregation, which comprises both contributions from self-aggregation and solvent interactions. These experiments did not yield any indication of significant self-aggregation and even at low temperature only slightly increased values were obtained (for details see SI).

HBF$_4$ salt.

The graphs depicted in Figure 5.8 show a kink for all three CD$_2$Cl$_2$/DMSO mixtures (i.e. content of DMSO = 5%, 15% and 20%). Thus, as has been reported in literature,[27] the two arms of the curve can be fitted separately to obtain two linear parts. For this reason, for each of the DMSO contents two pairs of values (**A** and **B**) are given in Table 5.5.

The values denoted **A** are derived from the lower temperature part and those denoted **B** belong to the part of the curve recorded at increasing temperatures (compare Figure 5.8). DOSY experiments of the sample with 20% DMSO showed a drastic increase in the viscosity of the sample below 240 K (details see SI), i.e. at the temperature where the kink occurred. Therefore, the increased values of the $\Delta H^\ddagger$ and $\Delta S^\ddagger$ values likely are due to this increased viscosity. Interestingly, with decreasing amounts of DMSO, the temperature of the viscosity change is reduced, but the increase in the $\Delta H^\ddagger$ and $\Delta S^\ddagger$ is biggest in the sample with 5%

DMSO. However, a proper evaluation of the values derived from the **A** parts of the graphs in Figure 5.8 seems not possible considering the fact that the actual mechanism of the viscosity change and its implications are not known so far. For this reason, only the **B** values are discussed in the following with regard to the rotation of the NH$_2$ group. It should be pointed out that despite the observed increase in viscosity, the Eyring analysis of the **A** parts of the curve delivered plots with good to excellent linearity (R^2: 0.95-0.99).

In the **B** parts, a gradual increase in $\Delta H^{\ddagger}$ upon increase of the DMSO content is observed (see Table 5.5) and in CD$_3$CN the value of $\Delta H^{\ddagger}$ is even larger than in the CD$_2$Cl$_2$/ 20% DMSO mixture, while it is again highest in pure DMSO (41.2 kJ/mol), as found already in the study of the free base **1**. The $\Delta S^{\ddagger}$ values undergo the same development, i.e. they become ever more positive with increasing amounts of DMSO and the value in CD$_3$CN lies between the CD$_2$Cl$_2$/ 20% DMSO mixture and pure DMSO (-57 J/(molK), see Table 5.5).

However, both $\Delta H^{\ddagger}$ and $\Delta S^{\ddagger}$ are not as large in the salt **1-HBF$_4$** as in the free base **1** when comparing the corresponding solvents directly. This fact may be attributed to the changed electronics in the protonated amidinium moiety. The positive charge is supposed to make the NH$_2$ group a better H-bond donor, but it decreases the acceptor quality of the carbonyl oxygen because it inductively withdraws electron density from it. It seems that the latter is the stronger impact and that the reduced electron density is not compensated by the additional H-bond now formed by the amide NH to DMSO. The intramolecular H-bond in the salt is about 0.1 Å longer, i.e. much weaker, and so $\Delta H^{\ddagger}$ is 20 kJ/mol smaller in **1-HBF$_4$** than in **1** comparing the samples in pure DMSO, although the stronger double bond character of the NH$_2$-C^G in the salt points in the opposite direction.

5.4 Conclusion

In summary, it has been shown that N-p-methoxybenzoyl-benzamidine **1** is a suitable model compound for the investigation of the rotational barrier of the NH$_2$ group in acylguanidines. Bond length analysis of several crystal structures showed a highly similar bonding situation in the amidine moiety and so did a comparison of the ^{13}C chemical shifts of the relevant carbon atoms. Solvent influences on the ^{1}H chemical shifts of the NH$_2$ protons due to H-bonding to solvent acceptors are equivalent in acylguanidines and **1**.

The rotational barrier of the NH$_2$ group of **1** has been shown to be influenced strongly by the formation of an intramolecular H-bond to the carbonyl oxygen. This situation makes the rotational barrier sensitive to microsolvation by H-bond acceptors of the solvent in terms of enthalpy and entropy.

Eyring plots of data derived from dynamic NMR delivered the thermodynamic activation parameters $\Delta H^{\ddagger}$ and $\Delta S^{\ddagger}$. Both **1** and its HBF$_4$ salt yield the highest enthalpy of

activation and the least negative entropy of activation in pure DMSO, which is attributed to the strongly increased formation of additional H-bonds to the solvent.

In a direct comparison of the individual solvents, the enthalpy of activation of the rotation is smaller in the protonated state, although the H-bond should be stronger when the donor nitrogen is charged. However, the crystal structures showed that the H-bond is stretched and thus weakened in the charged state because the acyl moiety is separated from the guanidine part as the positive polarization of the carbonyl carbon evades the positive charge. Therefore the acyl moiety participates much less in the delocalization. This is confirmed by several crystal structures of N-acyl benzamidines and acylguanidines. In addition to the increased H-bond distance, they indicate an increased double bond character of the C^G-NH$_2$ bond that actually raises the rotational barrier.

In a nutshell, the rotational barrier is lower in the protonated state, despite the increased double bond character that should raise it. At the same time, the intramolecular H-bond is weaker. The weakening of the intramolecular H-bond by far outweighs the effect of the increased double bond parts in the NH$_2$-C^G bond. This shows clearly the significant contribution of the intramolecular H-bond to the rotational barrier of the NH$_2$ group in N-acylated amidines.

Finally, the high gain in entropy upon rotation of the NH$_2$ group in N-acylamidine indicates the heavy loss in entropy when this rotation is restricted. The strong increase of especially $\Delta S^\ddagger$ upon H-bonding to solvent molecules suggests that in complexes or aggregates, H-bonding interactions allowing for rotation of the NH$_2$ group retaining these interactions will be greatly entropically favoured over such interactions that restrict the NH$_2$ rotation and need to be dissolved for the NH$_2$ group to rotate. Therefore, a distinct conformation of an acylguanidine may be preferred because it allows for the rotation of the NH$_2$ group without breakage of H-bonds, while another one does not.

5.5 References

(1)   Berlinck, R. G. S.; Burtoloso, A. C. B.; Kossuga, M. H. *Nat. Prod. Rep.* **2008**, *25*, 919–954.

(2)   Katritzky, A. R.; Rogovoy, B. V.; Cai, X.; Kirichenko, N.; Kovalenko, K. V. *J. Org. Chem.* **2004**, *69*, 309-313.

(3)   Saczewski, F.; Balewski, Ł. *Expert Opin. Ther. Patents* **2009**, *19*, 1417-1448.

(4)   Ghorai, P.; Kraus, A.; Keller, M.; Goette, C.; Igel, P.; Schneider, E.; Schnell, D.; Bernhardt, G.; Dove, S.; Zabel, M.; Elz, S.; Seifert, R.; Buschauer, A. *J. Med. Chem.* **2008**, *51*, 7193–7204.

(5)   Igel, P.; Schneider, E.; Schnell, D.; Elz, S.; Seifert, R.; Buschauer, A. *J. Med. Chem.* **2009**, *52*, 2623-2627.

R. Kleinmaier, R. M. Gschwind, *J.Org. Chem.* **2010**, *in preparation*.

(6)   Keller, M.; Pop, N.; Hutzler, C.; Beck-Sickinger, A. G.; Bernhardt, G.; Buschauer, A. *J. Med. Chem.* **2008**, *51*, 8168–8172.

(7)   Kubinyi, H. *Pharm. Acta Helv.* **1995**, *69*, 259-269.

(8)   Kleinmaier, R.; Keller, M.; Igel, P.; Buschauer, A.; Gschwind, R. M. *J. Am. Chem. Soc* **2010**, *submitted*.

(9)   Kincaid, J., F. ; Eyring, H.; Stearn, A., E. *Chem. Rev.* **1941**, *28*, 301.

(10)   Basso, E. A.; Oliveirab, P. R.; Wiectzycoskia, F.; Pontesa, R. M.; Fiorina, B. C. *J. Mol. Struct. (Theochem)* **2005**, *753*, 139-146.

(11)   Pontes, R. M.; Basso, E. A.; dos Santos, F. P. *J. Org. Chem.* **2007**, *72*, 1901-1911.

(12)   Aydeniz, Y.; Oğuz, F.; Yaman, A.; Konuklar, A. S.; Doğan, I.; Aviyente, V.; Klein, R. A. *Org. Biomol. Chem.* **2004**, *2*, 2426-2436.

(13)   Kawabata, T.; Jiang, C.; Hayashi, K.; Tsubaki, K.; Yoshimura, T.; Majumdar, S.; Sasamori, T.; Tokitoh, N. *J. Am. Chem. Soc.* **2009**, *131*, 54-55.

(14)   Prigge, J. Doctoral, Westfaelische Wilhelms-Universitaet Muenster, 2004.

(15)   Pretscher, A.; Brisander, M.; Bauer-Brandl, A. a.; Hansen, L. K. *Acta Crystallogr.* **2001**, *C57*, 1217-1219.

(16)   Kessler, H.; Leibfritz, D. *Chem. Ber.* **1971**, *104*, 2143-2157.

(17)   The shortening of the H-bond distance for the second molecule of **4** in the unit cell (2.08(3) Å vs. 1.95(3) Å) may be due to additional H-bond interactions of the second guanidino NH_2 group in this molecule, which influence the atomic distances. These interactions are documented in the X-ray structure and unique for the second molecule in the cell.

(18)   Steiner, T. *Angew. Chem.* **2002**, *114*, 50-80.

(19)   Byrne, B.; Rothchild, R. *Chirality* **1999**, *11*, 529-535.

(20)   Federwisch, G.; Kleinmaier, R.; Drettwan, D.; Gschwind, R. M. *J. Am. Chem. Soc.* **2008**, *130*, 16846–16847.

(21)   Schmuck, C.; Bickert, V. *Org. Lett.* **2003**, *5*, 4579-4581.

(22)   Marcus, Y. *Chem. Soc. Rev.* **1993**, *22*, 409-16.

(23)   Reichardt, C. *Solvents and Solvent Effects in Organic Chemistry. 2nd Ed.*; Wiley-VCH: Weinheim, 1988.

(24)   Winzor, D. J.; Jackson, C. M. *J. Mol. Recognit.* **2006**, *19*, 389–407.

(25)   Beeson, C.; Pham, N.; Shipps Jr., G.; Dix, T. A. *J. Am. Chem. Soc* **1993**, *115*, 6803-6812.

(26)   Crutchfield, C. A.; Harris, D. J. *J. Magn. Res.* **2007**, *185* 179–182.

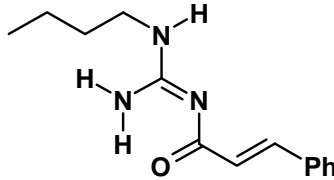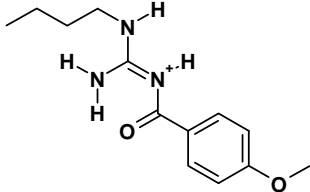(27)   Truhlar, D. G.; Kohen, A. *PNAS* **2001**, *98*, 848-851.
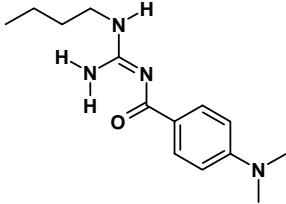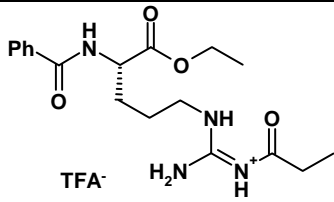
5.6   Supporting Information

The Rotational Barrier in Acylguanidines is Modelled by an Acyl Benzamidine – and it's Lower in the Charged State!

Roland Kleinmaier, Ruth M. Gschwind

5.6.1 ^{13}C chemical shifts of C^G and CO: Protonated vs. unprotonated acylguanidines

Table S5.6: Overview of ^{13}C chemical shifts of C^G and CO carbons from TMS (two values for one carbon indicate two distinct conformations).

Sample	$\delta\ ^{13}C$ CO	$\delta\ ^{13}C$ C^G		
2c				
free base, 240K CD_2Cl_2 / DMSO-d_6 1:1	176.0 / 176.7	161.9 / 161.4		
HCl salt, 285 K CD_2Cl_2 + 7% DMSO-d_6	168.2	155.3		
Boc-Asp-OBn salt, 225K CD_2Cl_2 + 10% DMSO-d_6	168.8 / 169.4	154.7 / 155.3		
2a				
free base, 225K, CD_2Cl_2	176.67	161.78		
HCl salt, 300K, $CDCl_3$	168.6	155.1		
DCA salt, 270K CD_2Cl_2 + 8% DMSO-d_6	169.9	155.4		
2b				
free base, 220K, CD_2Cl_2	177.36	161.74		
TFA salt, 300K, CD_2Cl_2 + 10% DMSO-d_6	169.4	155.7		
Boc-Asp-OBn salt, 220K CD_2Cl_2 + 2% DMSO-d_6	170.54	n.a.		
'N^G-acyl-Arginine'[1]				
Bz-Arg(N^η-propionyl)-OEt, TFA salt, 300K CD_2Cl_2 + 10% DMSO-d_6	177.9	154.6		

R. Kleinmaier, R. M. Gschwind, *J.Org. Chem*. **2010**, *in preparation*.

5.6.2 DOSY measurements for the investigation of self-aggregation

1. Free base **1**

Table 5.7: Macroscopic degrees of aggregation for the samples of **1** in the given solvents obtained by DOSY spectroscopy and molecular mass estimation according to Crutchfield et al.[2]

	Degree of aggregation at temperature			
	220K	**250K**	**270K**	**300K**
Solvent				
DCM	1.1	1.0	0.8	0.9
DCM/ 5%DMSO	1.4	1.2	1.1	1.0
CD$_3$CN	-	1.2	1.1	0.9
DMSO	-	-	-	1.2

2. **1-HBF$_4$**

Table 5.8: Macroscopic degrees of aggregation for the samples of **1-HBF$_4$** in the given solvents obtained by DOSY spectroscopy and molecular mass estimation according to Crutchfield et al.[2]

	Degree of aggregation at temperature in K			
	230	**250**	**270**	**300**
Solvent				
DCM/DMSO	-	-	1.7	1.6
CD$_3$CN	1.8	1.8	1.6	1.3

In the case of **1-HBF$_4$,** a strong increase of the viscosity of the solvent mixture prevented the determination of proper diffusion coefficients below 250 K. This viscosity increase was detected by the diffusion coefficients for the internal standard TMS dropping drastically.

5.6.3 Stable chemical shift of acylguanidine NH resonances in intramolecular H-bonds

In the following, stacked spectra of several acylguanidines are depicted following titration experiments conducted in order to check the solvent dependence of the NH chemical shifts.

In monoalkylated acylguanidines, conformational equilibria are at work which cannot be described here in detail. Details on the chemical and conformational assignment[3] of the NH protons as well as on the conformational equilibria[4] have been published by the authors.

R. Kleinmaier, R. M. Gschwind, *J.Org. Chem.* **2010**, *in preparation*.

One part of the figures is in each case an overview of the two observed conformations which also give the assignment used in the spectra.

Figure S5.9: Stack of NH sections from ^{1}H spectra of **2a** at 225 K upon titration of the solution in pure CD$_2$Cl$_2$ with DMSO-d_6. The blue dashed lines mark the two resonances in the intramolecular H-bond in each of the two conformations depicted above the spectra, which also give the NH assignment as used in the spectra. Their chemical shifts are stable against the addition of DMSO, while the other NH resonances are undergoing quite large chemical shift changes as indicated by red dashed lines.

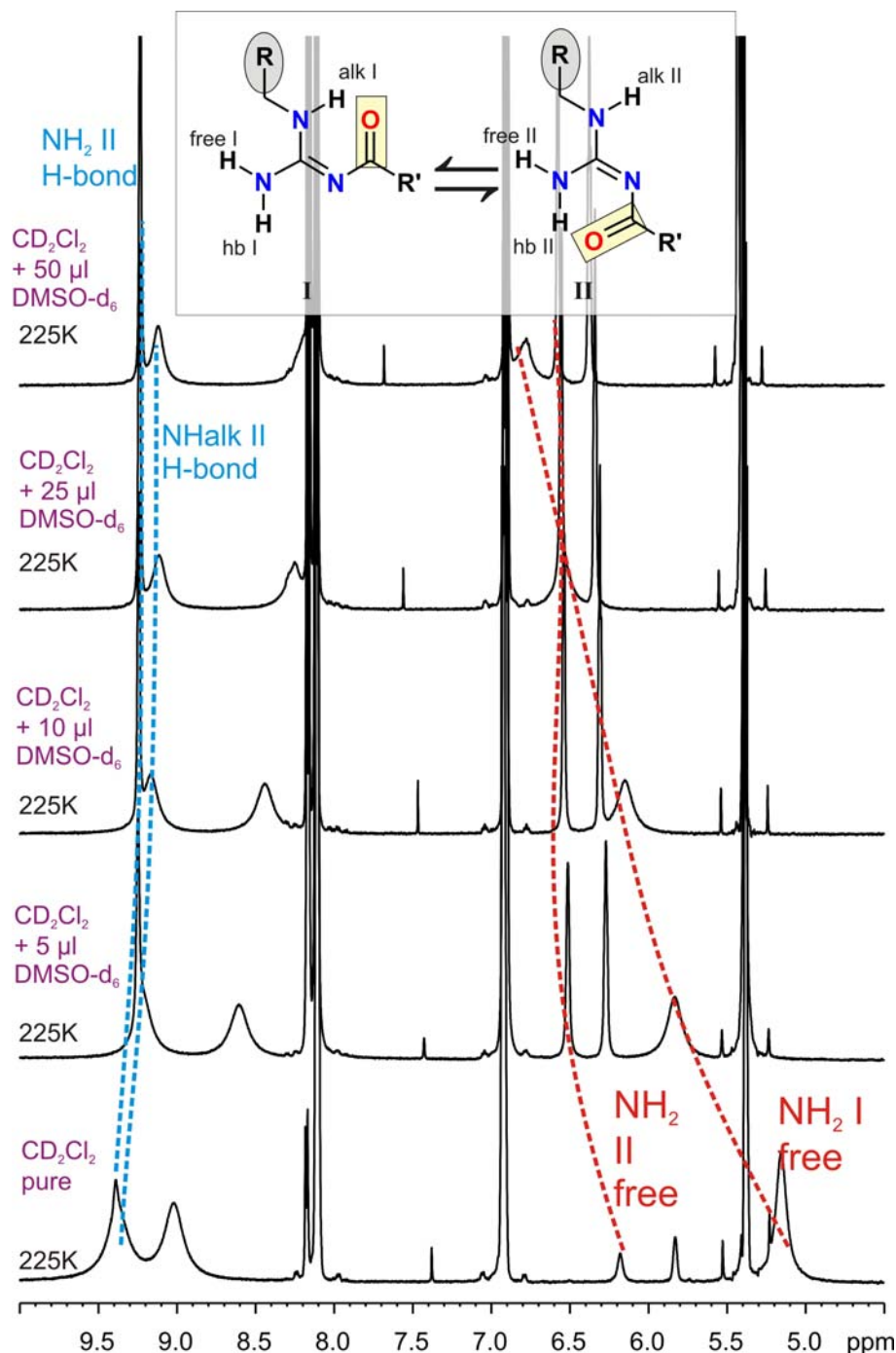R. Kleinmaier, R. M. Gschwind, *J.Org. Chem.* **2010**, *in preparation*.

Figure S5.10: Stack of NH sections from ^{1}H spectra of **2b** at 210 K upon titration of the solution in pure CD_2Cl_2 with DMSO-d_6. The blue dashed lines mark the two resonances in the intramolecular H-bond in each of the two conformations depicted above the spectra, which also give the NH assignment as used in the spectra. Their chemical shifts are stable against the addition of DMSO, while the other NH resonances are undergoing quite large chemical shift changes as indicated by red dashed lines.

R. Kleinmaier, R. M. Gschwind, *J.Org. Chem.* **2010**, *in preparation*.
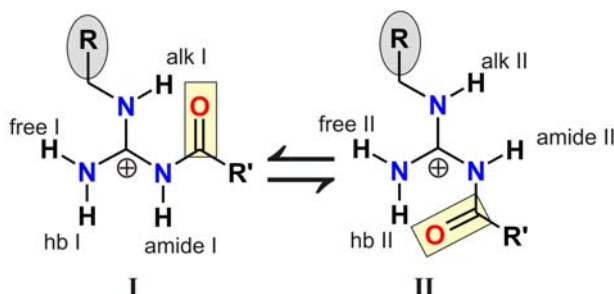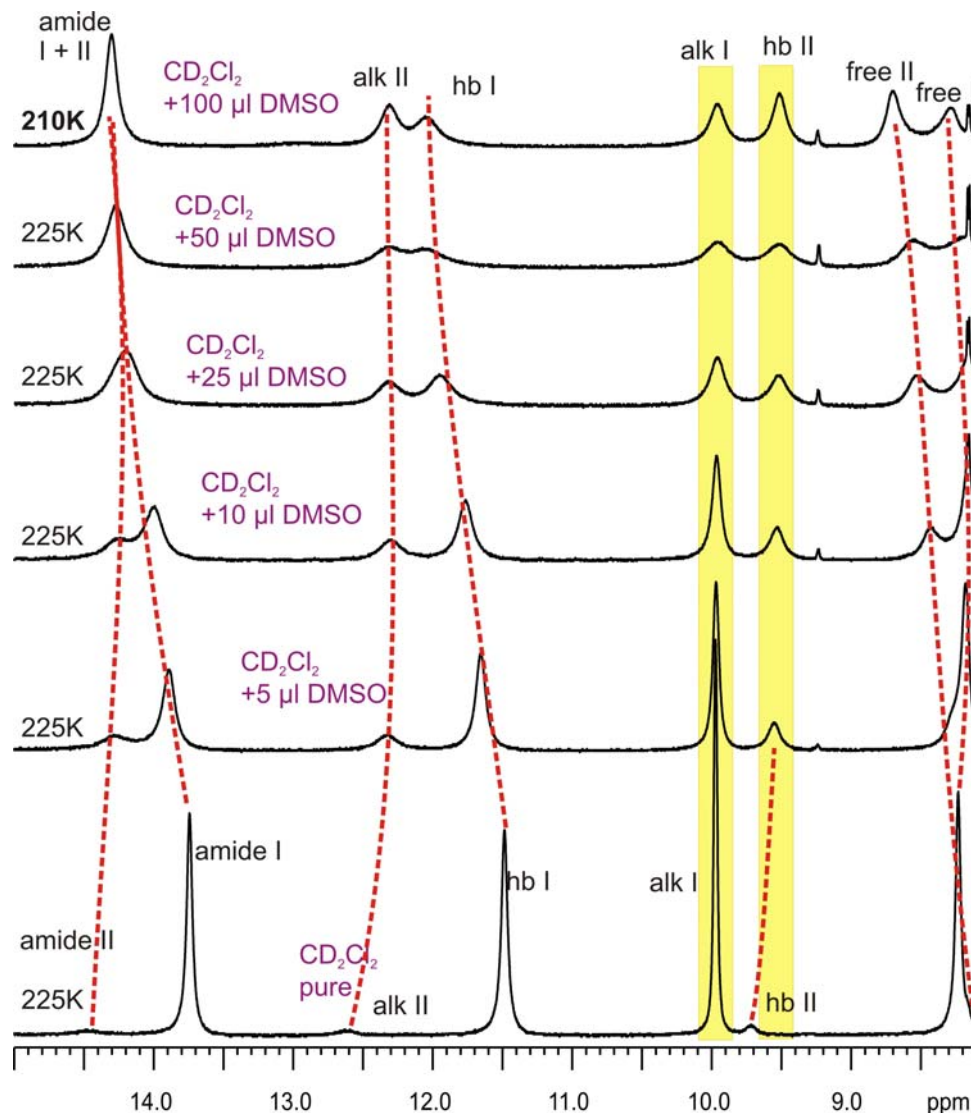
Figure S5.11: Stack of NH sections from ^{1}H spectra of **2a- Boc-Asp-OBn** upon titration of the solution in pure CD$_2$Cl$_2$ with DMSO-d_6. The yellow bars mark the two resonances in the intramolecular H-bond in each of the two conformations depicted below the spectra, which also give the NH assignment as used in the spectra. Their chemical shifts are stable against the addition of DMSO, while all other NH resonances are undergoing quite large chemical shift changes as indicated by red dashed lines.
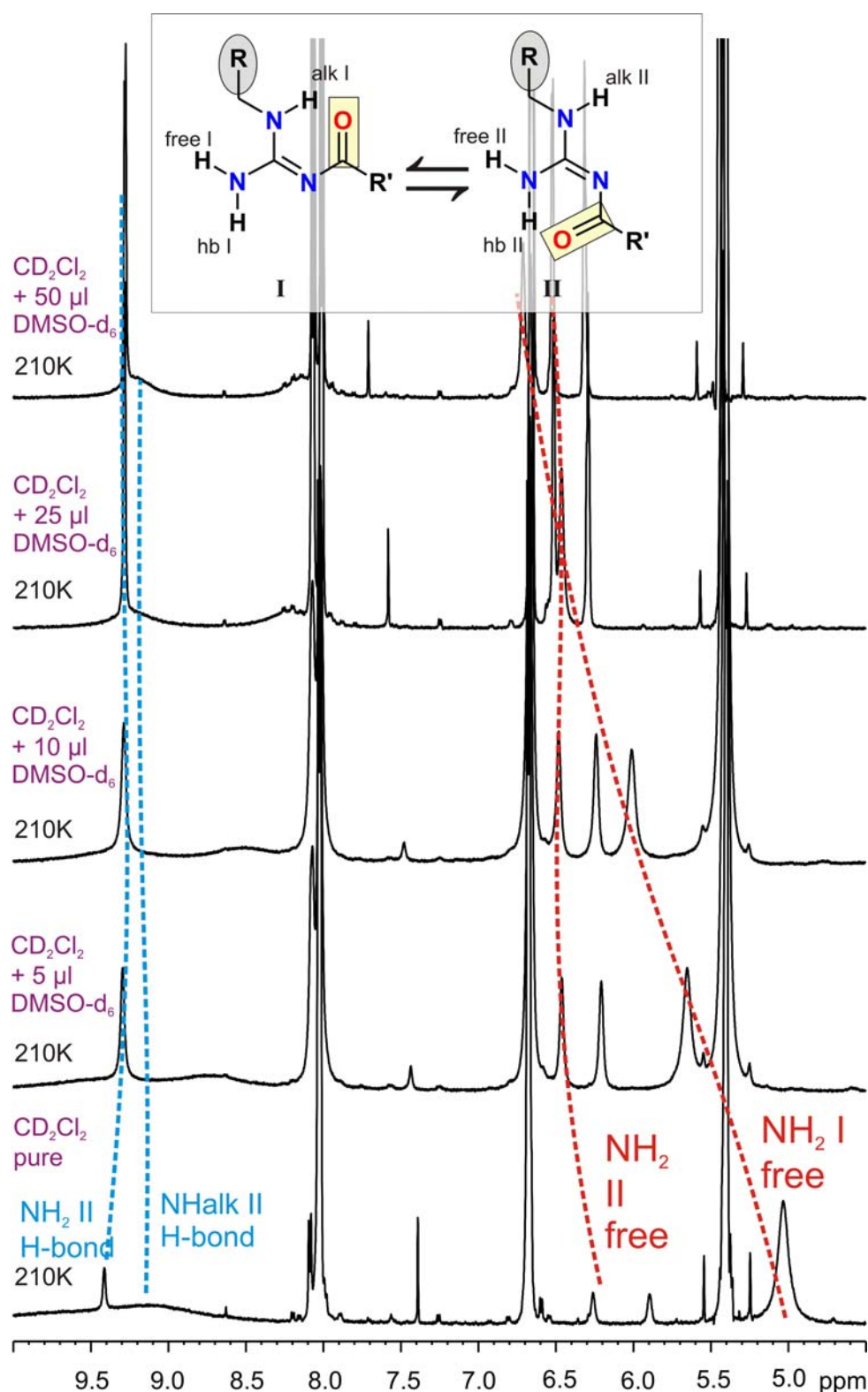
R. Kleinmaier, R. M. Gschwind, *J.Org. Chem.* **2010**, *in preparation*.
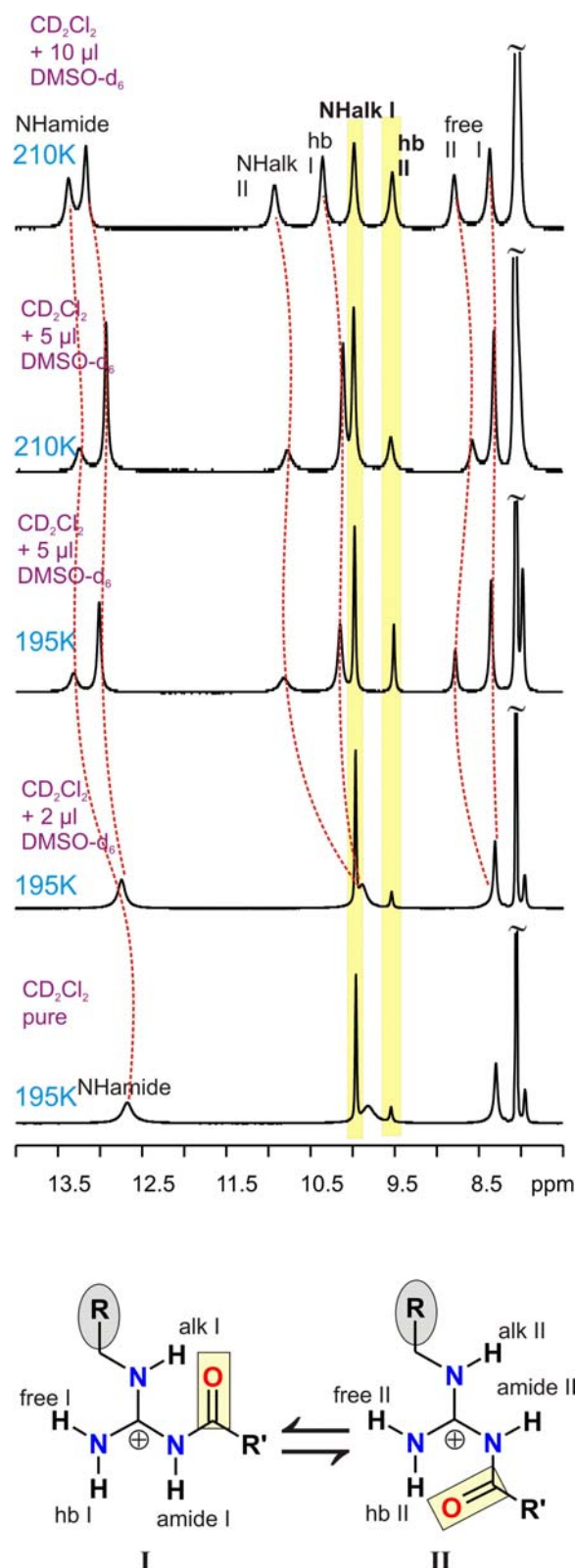
Figure S5.12: Stack of NH sections from ^{1}H spectra of **2a-DCA** upon titration of the solution in pure CD$_2$Cl$_2$ with DMSO-d_6. The yellow bars mark the two resonances in the intramolecular H-bond in each of the two conformations depicted below the spectra, which also give the NH assignment as used in the spectra. Their chemical shifts are stable against the addition of DMSO, while all other NH resonances are undergoing quite large chemical shift changes as indicated by red dashed lines.

R. Kleinmaier, R. M. Gschwind, *J.Org. Chem.* **2010**, *in preparation*.

5.6.4 Chemical shift stability observed for 1-HBF$_4$ in different solvents
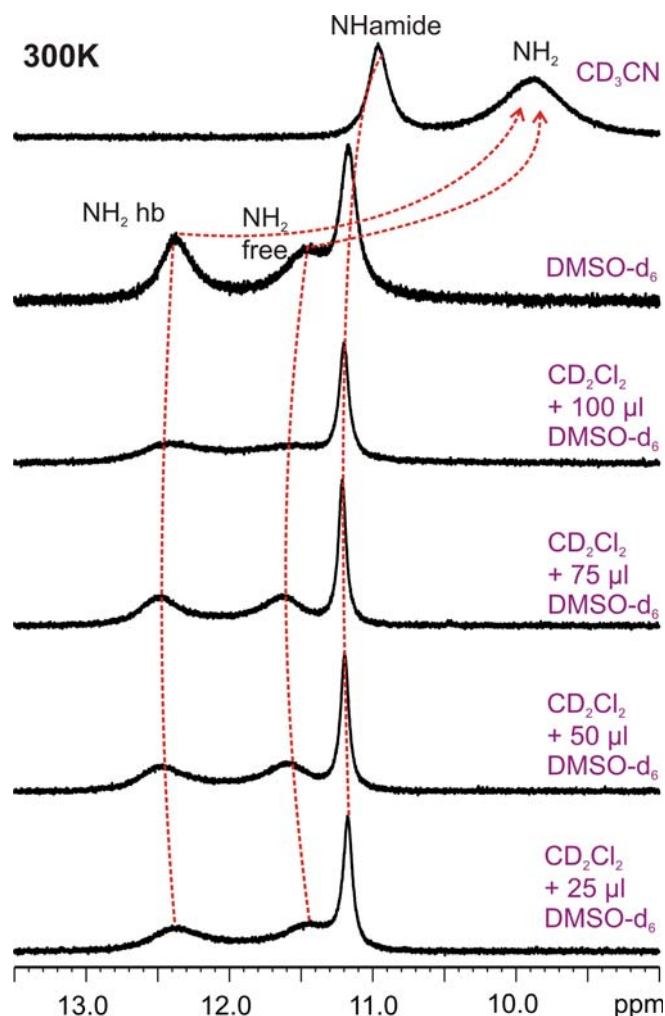
Figure S5.13: NH sections from ^{1}H spectra of **1-HBF$_4$** at 300 K in solvents as given. Through all samples where DMSO is present, the chemical shifts of all NH resonances are quite stable, while in CD$_3$CN, the chemical shift of all resonances is reduced.

5.6.5 Details on the execution of the Eyring analysis

Rate constants k were fitted to the experimental spectra using the DNMR toolset of the SpinWorks program (version 2.5.5., 1999-2006, Kirk Marat) with mutual exchange of two chemical configurations, permutation vector 2: 2,1,0,0,0.

In some of the experimental spectra, different line widths were observed for the two NH$_2$ protons. In these cases, generally the peak with the smaller line width was used for the simulation. The values used for the parameter "effective T2", i.e. the T$_2$* time of the nucleus,

as well as the $^2J_{NH2}$ coupling constant (if used) are given below. T_2* times were usually derived from the smallest line width found for the NH protons in low temperature spectra (by $T_2* = 1/(\pi*\Delta v^{1/2})$), and where this was not possible, i.e. in pure DMSO-d_6, those from the mixtures of DMSO-d_6 with CD_2Cl_2 were used as an approximation. Where a value is given, $^2J_{NH2}$ was detected from signal splitting in ^1H spectra at low temperature.

Standard sample volume 0.7 ml

free base

Sample CD_2Cl_2, m (**1**) = 7.5 mg, T2* = 0.064s, $^2J_{NH2}$ = 4.7 Hz

Sample CD_2Cl_2 + 25 μl DMSO-d_6, m (**1**) = 6.2 mg, T2* = 0.063s, $^2J_{NH2}$ = 3.8Hz

Sample CD_3CN, m (**1**) = 8.0 mg, T2* = 0.029s, $^2J_{NH2}$ = 0

Sample DMSO-d_6, m (**1**) = 9.0 mg T2* = 0.063s, $^2J_{NH2}$ = 3.8Hz

HBF$_4$ salt

Sample CD_2Cl_2 + 25 μl DMSO-d_6, m (**1-HBF$_4$**) = 4.7 mg, T2* = 0.039s

Sample CD_2Cl_2 + 75 μl DMSO-d_6, m (**1-HBF$_4$**) = 4.7 mg, T2* = 0.054s

Sample CD_2Cl_2 + 100 μl DMSO-d_6, m (**1-HBF$_4$**) = 4.7mg, T2* = 0.038s

Sample CD_3CN, m (**1-HBF$_4$**) = 7.0 mg, T2* = 0.029s

Sample DMSO-d_6, m (**1-HBF$_4$**) = 6.7 mg, T2* = 0.039s

5.6.6 Preparative Details

Synthesis of 1

Benzamidinium-HCl (1.00 g, 6.4 mmmol) was dissolved in acetone (30 ml) at 0° C and 2M aq. NaOH (8.0 ml) was added. A solution of 4-methoxybenzoyl chloride (1.09 g, 6.4 mmol)) in acetone (20 ml) was added with a dropping funnel. The mixture was stirred for 0.5 h and allowed to come to room temperature. The acetone was removed in vacuo and the oily residue was extracted with ethylacetate. The organic phase was washed once with sat. aq. $NaHCO_3$ and dried over Na_2SO_4 and the solvent evaporated in vacuo. Subsequent column chromatography (pentanes/ethylacetate 1:2, R_F= 0.6) over silica gel yielded **1** in 90% yield.

NMR data see below, HR-Mass: EI-MS calc. [M+] 254.1055, found 254.1050.

R. Kleinmaier, R. M. Gschwind, *J.Org. Chem.* **2010**, *in preparation*.

1-HBF$_4$

1 (0.05 g, 1.8 mmol) was dissolved in diethyl ether (3 ml) and HBF$_4$-Et$_2$O (0.03 g, 1.8 mmol) was added. The colorless precipitate was sucked off and dried in vacuo. This yielded **1-HBF$_4$** purely and quantitatively.

1-HCl

1 (0.10 g, 3.6 mmol) was dissolved in diethyl ether (10 ml) and 1M aq. HCl (2 ml) was added. The colorless precipitate was sucked off and dried in vacuo. This yielded **1-HCl** purely and quantitatively.
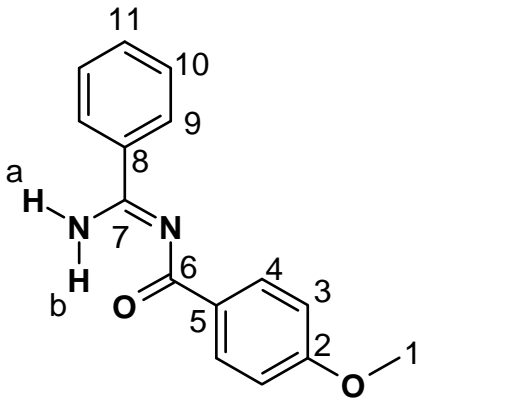
1-HClO$_4$

1 (0.10 g, 3.6 mmol) was dissolved in diethyl ether (5 ml) and 30% aq. HClO$_4$ (0.5 ml) was added. The colorless precipitate was sucked off and dried in vacuo. Recrystallization from acetonitrile yielded colorless needles of **1-HClO$_4$** that were suitable for single crystal x-ray diffraction.

5.6.7   Spectral Part

Assignment of 1 in toluene-d_8 at 300 K, 600 MHz
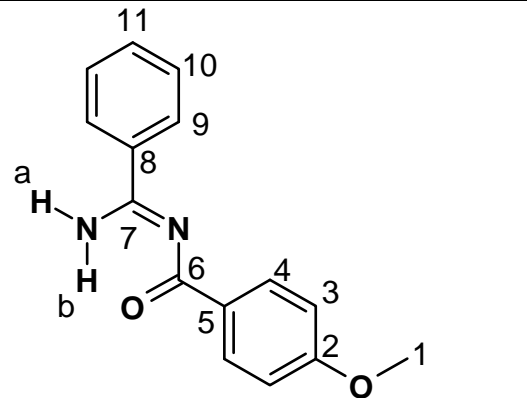
Table S5.9: Assignment of **1** in toluene-d_8 at 300 K, 600 MHz

Position	δ ^{1}H	δ ^{13}C
1	3.10	53.8
2	-	162.2
3	6.60	112.6
4	8.5	131.5
5	-	130.8
6 (CO)	-	**179.2**
7 (C^G)	-	**165.0**
8	-	135.0
9	7.48	126.7
10	6.89	127.6
11	6.96	127.3
NHa	5.29	
NHb	10.55	

R. Kleinmaier, R. M. Gschwind, *J.Org. Chem.* **2010**, *in preparation*.

NMR chemical shifts of **1** in DMSO-d_6 (300 MHz, 300 K): δ ^{1}H 3.825 (s, 3H, -OMe), 7.013 (d, 2H, ar), 7.50-7.66 (m, 3H, ar), 8.188 (d, 2H, ar), 8.237 (d, 2H, ar), 9.239 (s, 1H, NH), 10.418 (s, 1H, NH); δ ^{13}C 55.31, 113.36, 127.89, 128.47, 130.53, 131.14, 132.07, 134.73, 162.22, **165.61, 178.05**.
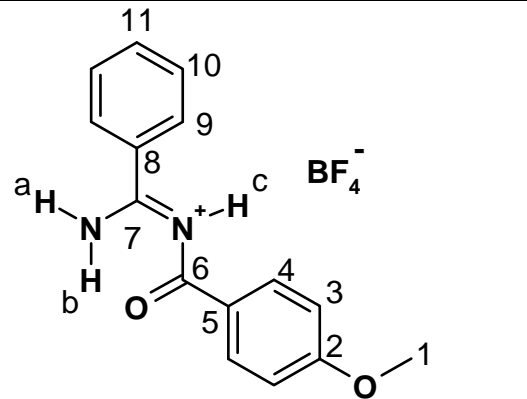
Assignment of 1 in CD$_3$CN at 300K, 600MHz

Table S5.10: Assignment of **1** in CD$_3$CN at 300K, 600MHz

Position	δ ^{1}H	δ ^{13}C	
1	3.86	56.2	
2	-		
3	6.98	114.3	
4	8.29	132.5	
5	-		
6 (CO)	-	**180.2**	
7 (C^G)	-	**167.4**	
8	-		
9	8.11	128.8	
10	7.54	129.7	
11	7.62	133.2	
NHa	7.54		
NHb	10.50		

Assignment of 1-HBF$_4$ in CD$_2$Cl$_2$ / 5% DMSO-d_6 at 275 K, 600 MHz

Table S5.11: Assignment of **1-HBF$_4$** in CD$_2$Cl$_2$ / 5% DMSO-d_6 at 275 K, 600 MHz

Position	δ ^{1}H	δ ^{13}C	
1	3.92	56.2	
2	-	165.4	
3	7.05	114.4	
4	8.15	132.4	
5	-	123.2	
6 (CO)	-	**170.7**	
7 (C^G)	-	**167.9**	
8	-	128.1	
9	7.91	135.4	
10	7.68	129.6	
11	7.84	129.9	

R. Kleinmaier, R. M. Gschwind, *J.Org. Chem.* **2010**, *in preparation*.

NHa	11.64		
NHb	12.63		
NHc	11.21		

Comparison of chemical shifts in 1 (toluene) and 1-HBF$_4$ (CD$_2$Cl$_2$ / 5% DMSO-d_6):

Table S5.12: Comparison of chemical shifts in **1** and **1-HBF$_4$**.

	δ ^{1}H fb	δ ^{1}H prot.	δ ^{13}C fb	δ ^{13}C prot.
1	3.10	3.92	53.8	56.2
2	-	-	162.2	165.4
3	6.60	7.05	112.6	114.4
4	8.5	8.15	131.5	132.4
5	-	-	130.8	123.2
6 (CO)	-	-	179.2	170.7
7 (C^G)	-	-	165.0	167.9
8	-	-	135.0	128.1
9	7.48	7.91	126.7	135.4
10	6.89	7.68	127.6	129.6
11	6.96	7.84	127.3	129.9
NHa	5.29	11.64		
NHb	10.55	12.63		
NHc		11.21		

5.6.8   References

(1)   Kleinmaier, R.; Gschwind, R. M. *J. Label Compd. Radiopharm* **2009**, *52*, 29-32.

(2)   Crutchfield, C. A.; Harris, D. J. *J. Magn. Res.* **2007**, *185* 179–182.

(3)   Kleinmaier, R.; Gschwind, R. M. *Magn. Reson. Chem.* **2010**, submitted.

(4)   Kleinmaier, R.; Keller, M.; Igel, P.; Buschauer, A.; Gschwind, R. M. *J. Am. Chem. Soc* **2010**, submitted.

R. Kleinmaier, R. M. Gschwind, *J.Org. Chem.* **2010**, *in preparation*.

134

6 Selective [$^{15}N^{\eta}_2$] labelling of an N^G-propionylated arginine derivative*

Roland Kleinmaier, Ruth M. Gschwind

VI

7 Summary

VII

Acylguanidines are an abundant class of compounds with various applications in organic and pharmaceutical chemistry. In recent years, highly potent and selective ligands for G protein coupled receptors containing an N'-alkylated N-acylguanidine moiety have been identified as well as inhibitors of enzymes related to diseases like Alzheimer's and Parkinson's. Their suggested recognition pattern upon interaction with carboxylate anions in proteins is very similar to the strong charge-assisted hydrogen bonds (salt bridges) commonly observed e.g. between arginine side chains and aspartate/glutamate residues. Despite the undoubted importance of the acylguanidines, the actual mode of binding of the acylguanidine moiety to a biological target, i.e. the conformation that is bound by the target, often remains a matter of speculation and cannot be reliably predicted in many cases. However, an intimate knowledge of general and/or individual conformational preferences of this compound class is highly desirable: Progress in the predictability of the preferred conformation of a monoalkylated

acylguanidine compound and of its hydrogen bond (H-bond) network would greatly support the rational design of biologically active substances incorporating this structural motif.

Therefore, the objective of this work was on the one hand the disclosure of a ready access to the identification of the conformations of monoalkylated acylguanidines. Secondly, making use of such an analytical approach, the investigation of conformational equilibria of structurally diverse monoalkylated acylguanidines under various influences such as complexation by a model receptor and H-bonding to anions and solvent molecules should add to the comprehension of the driving forces behind the observed conformational preferences of monoalkylated acylguanidines.

Intending to take advantage of a diverse pool of compounds, guanidinylation reagents based on both 1H-pyrazole and thiourea were used in this work for the preparation of monoalkylated acylguanidines. Especially, selective isotopic labelling of an acylated arginine derivative with the ^{15}N isotope was accomplished starting from the commercially available starting material [^{15}N$_2$] thiourea.

In the course of this work, a straightforward approach to the unambiguous chemical shift and conformational assignment of monoalkylated acylguanidines by NMR spectroscopy was developed utilizing the detection of long-range scalar couplings (w couplings) between individual NH protons. The observation of these couplings in homonuclear 2D (COSY) spectra was shown to be restricted to all-trans pathways. This rigid geometric criterium can be exploited to assign chemical shifts and conformations of monoalkylated acylguanidines unequivocally.

With this reliable assignment technique in hands, the conformational preferences of structurally diverse monoalkylated acylguanidines, including two biologically active GPCR ligands, were investigated by NMR spectroscopy in various organic solvents at temperatures between 195 K and 300 K and by the analysis of several X-ray crystal structures. The utmost emphasis should be placed on the fact that throughout the whole of this study, exclusively two out of the eight principally possible conformations of monoalkylated acylguanidines were detected both in solution by NMR and in the solid state; two of these crystal structures were obtained as part of this work from substances also investigated by NMR, thereby achieving direct comparability of the individual results.

It was shown that strong and selective H-bond interactions with anions lead to the preference of one conformation, while the disruption of these selective H-bonds reduces that preference or even inverts it towards a second conformation. Such disruptive forces may be exerted by the formation of more complex H-bond networks to a competitive solvent providing H-bond acceptors, e.g. DMSO, or to a high-affinity model receptor such as bisphosphonate tweezers.

The binding of two side chain acylated arginine derivatives to bisphosphonate tweezers was studied by 1D, 2D and 3D NMR spectroscopic techniques. For the first time, $^{3h}J_{N,P}$ scalar couplings across H-bonds were detected in addition to $^{2h}J_{H,P}$ in a complex between two small molecules. This was made possible using the ^{15}N labelled acylarginine derivative mentioned above. It was found that the combined evaluation of the intensity of these trans-hydrogen couplings allowed for the geometric analysis of the H-bond network formed upon binding and offered a valuable clue about the spatial arrangement of the molecules in the complex.

Experimental evidence for the rotation of the NH_2 group of acylguanidines even at low temperature occurred during the conformational studies. Therefore, the hypothesis that entropic contributions from this rotation may lead to the preference of one conformation of monoalkylated acylguanidines over another was checked and corroborated in the last part of this work by combined crystal structure and dynamic NMR studies.

In summary, in this work, several synthetic routes to acylguanidines were examined and applied. Especially, a selectively ^{15}N labelled acylarginine derivative was produced. The conformations of monoalkylated acylguanidines were analyzed by a specifically developed, but generally applicable NMR spectroscopic approach. Spatial information about monoalkylated acylguanidines was obtained by modern multi-dimensional NMR techniques. Monoalkylated acylguanidines adopt two out of eight principally possible conformations, as was shown by the exclusive and uniform detection of these two conformations in the solid state and in solution. Intermolecular interactions are decisive for the position of the equilibrium between these two conformations as shown with the help of different solvents and counterions. The cornerstone for further studies on the energetic reasons for the conformational preferences of monoalkylated acylguanidines that were observed in this study has been laid and it is hoped that future investigations will shed an even brighter light on this intriguing question.

8 Outlook

VIII

As usual in experimental work, many promising paths were trodden in this work, some of which did not lead to the desired results; some ended in the middle of nowhere. But then there were also some approaches that gave results every bit as promising as the initial perspectives. Yet as a matter of time and focus and due to the need to prioritize, they could not be transformed to scientific outcome within the scope of the present thesis.

In this outlook chapter, a short vista of some potential projects shall be given.

8.1 Tweezers

One point that surely can be mentioned here is the ongoing research into the obviously "privileged structure" of the bisphosphonate tweezers model receptor (see Figure 8.1 below and **T1** in chapter 3, Bis-[tetrabutylammonium-p-(methoxyoxyphosphorylmethyl)]-sulfone). It has been shown in the work of G. Federwisch[1] that many other bisphosphonate tweezers incorporating the same principal binding motif do not yield complexes which are suitable for NMR spectroscopic investigations to the extent observed for **T1**. This was attributed to the presence of the sulfonyl group allowing for a greater molecular flexibility in contrast to quite rigid phenyl or diphenyl scaffolds.

In the current work, the complexation of the biologically active BIBP 3226[2] derivative N^G-pentanoyl BIBP 3226 (**3** in chapter 3, UR-MK50) was investigated and it was shown that the most stable conformation of the bound guest within the tweezers yielding sharp NMR signals corresponds to the conformation found in the study presented in chapter 2. However, an additional conformation was visible, though with a lesser portion and yielding broad signals. This second conformation might very well be caused not by a change in the acylguanidine, but much rather in the northern part of the molecule: Additional strong H-bond interactions with protons in this part were detected via NMR. Therefore, the increase in the number of possible interaction sites comparing the two investigated guests also raises the number of conformations possible without changing the conformation of the acylguanidine. Most important, since the binding of the acylguanidine moiety is not symmetric (visible in the splitting of the symmetric tweezers' ^{31}P resonances) and since there is a second stereo center in the α position of the amino acid scaffold, two diastereomeric complexes (by supramolecular asymmetry, see Figure 8.1) might be formed simply by one single 180° rotation of the acylguanidine moiety around the N^ε-C^ζ bond. In addition there are a large number of other possible conformations considering that any combination of the three H-bond donors in the northern part of the guest might bind to the tweezers.
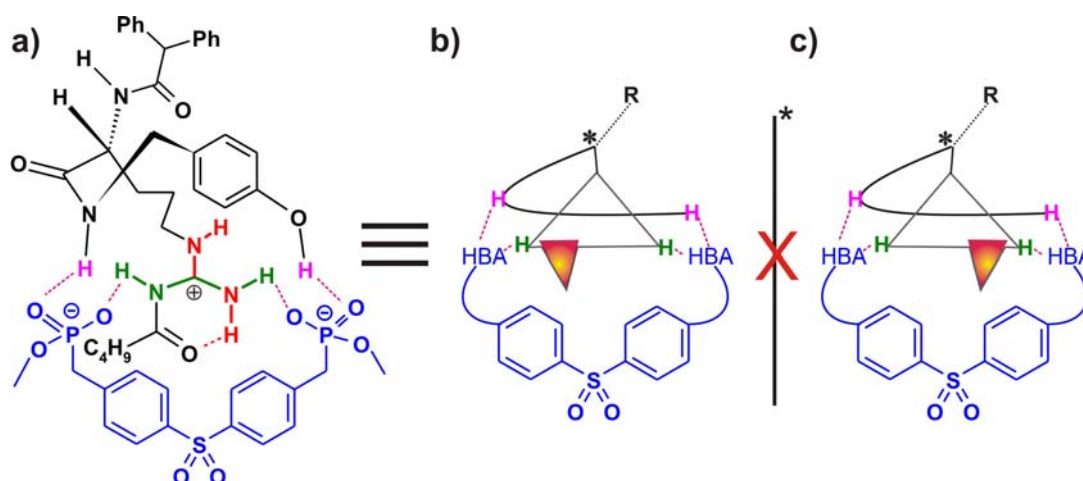
Figure 8.1: a) Schematic representation of the complex between N^G-pentanoyl BIBP 3226 and the bisphosphonate tweezers **T1**. In the simplified depictions of this complex in b) and c), the H-bond accepting phosphonate groups are denoted "HBA", while the large grey triangle represents the planar H-bond donating acylguanidinium moiety and the arched line is meant to describe the bent northern part of the molecule. In b), the complex in a) is reproduced while in c) the putative diastereomer of b) is depicted, which is formed after rotation of the acylguanidinium moiety while the interactions of the northern part of the guest are retained, i.e. b) and c) are not mirror images.

Therefore, the most straightforward way to investigate the hypothesis that the additional conformations are due to the large number of possible interactions and also maybe confirm the formation of supramolecular asymmetry would be to remove the stereo center and offer H-bond donors in a geometric arrangement as detected in the complex, but in a symmetrical fashion. Such a guest might have the structure depicted in Figure 8.2.
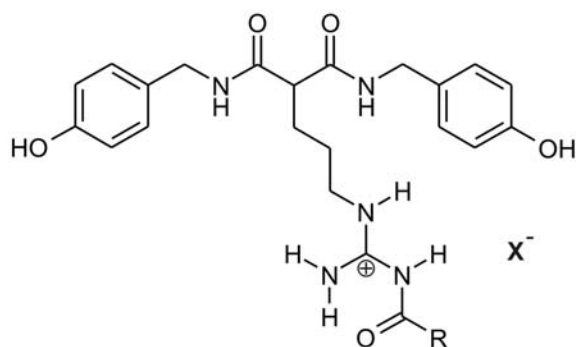
Figure 8.2: Potential guest for **T1** with symmetric substitution on the former C^α. R = alkyl, aryl.

Since the magnetization transfer between the phenolic OH and the OP group was by far the strongest one (see Figure S3.23), this site should definitely be kept. Replacement of the diphenylacetic amide function by exactly the same substituent that is already present would remove the stereocenter and yield a molecule which should still be able to bind the tweezers.

With this molecule, the contributions of different H-bond interactions of the tweezers with the northern part of N^G-pentanoyl BIBP 3226 to the observed further conformation(s) could be tapped.

In addition to these notions, ongoing efforts within this topic are concerned with further development of the tweezers and in a second approach, fluorescence labelling of the guest molecules is hoped to enable the reliable determination of binding constants by fluorescence titration methods.

8.2 Rotational barrier of the NH$_2$ group in acylamidines

In chapter 5, the determination of experimental values of the thermodynamic activation parameters $\Delta H^{\ddagger}$ and $\Delta S^{\ddagger}$ of the rotation of the NH$_2$ group in N-p-methoxybenzoyl benzamidine was discussed. The $\Delta H^{\ddagger}$ and $\Delta S^{\ddagger}$ values were found to be strongly dependent of the strength of the intramolecular H-bond. However, absolute values of the contribution of this H-bond to the rotational barrier in terms of $\Delta H^{\ddagger}$ and $\Delta S^{\ddagger}$ were not presented. Such a value could be derived from the comparison with a molecule which is structurally equivalent regarding the bonding situation in the amidine, but is rigidized in a conformation that prevents the carbonyl oxygen of the acyl residue from forming the intramolecular H-bond. Exemplary compounds fulfilling this requirement are depicted in Figure 8.3.
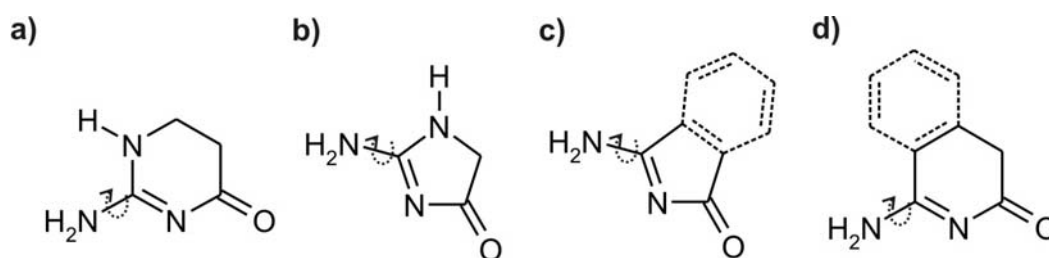

Figure 8.3: Structural formulas of possible candidates for the investigation of the rotation of the NH$_2$ group without it being influenced by an intramolecular H-bond. Dashed lines in c) and d) indicate the corresponding benzamidines.

With the help of these molecules, first the difference in the rotational barrier between acylguanidines (see Figure 8.3a) and b) and N-acylated alkyl- and benzamidines (Figure 8.3c) and d), and c) and d) with dashed lines, respectively) could be investigated and secondly, they would yield sort of a zero value for the rotational barrier without influences from an intramolecular H-bond. However, these compounds are by their looks very likely to dimerize in solution via intermolecular H-bonds, so this has to be checked and maybe prevented by the addition of microsolvators like DMSO.

8.3 Isotopic labelling

As has been presented in chapter 6, the preparation of isotope labelled compounds relies heavily on high yields from first to last step and only most unwillingly would synthetic chemists accept an unreliable reaction to be part of their strategy towards a compound when milligram quantities of starting material may cost hundreds of euros. Therefore, the production of such compounds remains a challenge, however rewarding the outcome may be (e.g. the first detection of $^{3h}J_{N,P}$ between small molecules, see chapter 1). Nevertheless, the current work is also a statement in favour of taking on the risk of losses and tedious optimization procedures because the products may deliver insights which would never be accessible with an unlabelled compound. With regard to future investigations of acylguanidines, it is clear that any studies with our beloved bisphosphonate tweezers will greatly profit from isotopic labels and especially concerning the observed strong interactions with the northern part of acylarginines, a complete labelling of all nitrogens in the molecule with ^{15}N would mean drastically deconvoluted spectra due to the possibility to perform isotope filtering (e.g. $^{1}H,^{15}N$ HSQC) and simple assignment by the readout of $^{1}J_{H,N}$ in 1D proton spectra. Extending the geometric information obtained from the combined detection of $^{3h}J_{N,P}$ and $^{2h}J_{H,P}$ onto such a fully labelled system might enhance the understanding of the spatial arrangement of acylguanidines in receptors in general.

Overall it is hoped that this and the ongoing work in the group will contribute some teaspoons of knowledge on the way towards a more rational design of biologically active compounds.

8.4 References

(1)   Federwisch, G. *NMR-spektroskopische Untersuchungen von Wasserstoffbrueckennetzwerken in Argininkomplexen und Rotaxanen*; Verlag Dr. Hut: Munich, 2009.
(2)   Rudolf, K.; Eberlein, W.; Engel, W.; Wieland, H. A.; Willim, K. D.; Entzeroth, M.; Wienen, W.; Beck-Sickinger, A. G.; Doods, H. N. *Eur. J. Pharmacol.* **1994**, *271*, R11-R13.

9 Zusammenfassung

IX

Acylguanidine stellen eine vielfältig vertretene Verbindungsklasse dar, die breite Verwendung in der organischen und pharmazeutischen Chemie findet. In den vergangenen Jahren wurden zahlreiche biologisch aktive Substanzen entwickelt, die die Substruktur des monoalkylierten Acylguanidins enthalten, darunter hochpotente und selektive Liganden zur Bindung an G-Protein-gekoppelte Rezeptoren, sowie auch Inhibitoren von Enzymen, die bei Krankheiten wie Alzheimer und Parkinson eine Rolle spielen. Ihr vorgeschlagenes Strukturmotiv zur Erkennung von Carboxylat-Anionen in Proteinen ähnelt in hohem Maße den starken ladungs-untersützten Wasserstoffbrücken (Salzbrücken), die man üblicherweise zwischen Seitenketten des Arginins und den Carboxylaten von Aspartat und Glutamat beobachtet. Trotz dieser zweifellos großen Bedeutung bleibt der tatsächliche Bindungsmodus ans biologische Zielmolekül, d.h. die Konformation des Acylguanidins, die vom Rezeptor gebunden wird, oft der Spekulation überlassen und es ist selten möglich, diese Konformation verlässlich vorherzusagen. Allerdings wäre die genaue Kenntnis der grundlegenden oder auch speziellen Konformationspräferenzen dieser Verbindungen höchst erstrebenswert. Fortschritte bei der Vorhersage der bevorzugten Konformation eines monoalkylierten Acylguanidins wären sehr hilfreich für die rationelle Entwicklung von biologisch aktiven Substanzen, die dieses Strukturmotiv beinhalten.

Zielsetzung dieser Arbeit war es daher einerseits, einen leicht gangbaren Weg zur Konformationsbestimmung von monoalkylierten Acylguanidinen aufzutun. Zweitens sollte mit dieser Analysemethode das Konformationsgleichgewicht strukturell unterschiedlich angelegter Acylguanidine untersucht werden. Verschiedene Einflüsse auf dieses Gleichgewicht, wie die Komplexierung durch ein artifizielles Rezeptormolekül sowie die Bildung von Wasserstoffbrücken zu Anionen und Lösungsmittelmolekülen, sollten berücksichtigt werden, um das Verständnis der Triebkraft hinter der beobachteten Bevorzugung bestimmter Konformationen zu verbessern.

Um Zugriff auf einen möglichst vielfältigen Verbindungsschatz zu erlangen, umschlossen die in dieser Arbeit genutzten Synthesewege für monoalkylierte Acylguanidine Guanidinylierungs-Mittel auf Basis von 1H-Pyrazol und auch von Thioharnstoff. Insbesondere gelang die Herstellung eines selektiv mit ^{15}N isotopenmarkierten Argininderivats ausgehend vom käuflich erhältlichen Edukt [^{15}N$_2$]-Thioharnstoff.

Im Verlauf dieser Arbeit wurde eine einfache und direkte Möglichkeit entwickelt, um mit Hilfe der NMR-Spektroskopie eine eindeutige Zuordnung sowohl der chemischen Verschiebungen als auch der Konformationen monoalkylierter Acylguanidine zu treffen. Dabei wurde die Detektion skalarer Weitbereichs-Kopplungen zwischen einzelnen NH-Protonen ausgenutzt. Es konnte gezeigt werden, dass diese nur über einen all-trans-Weg der skalaren Kopplung in detektierbarer Intensität übertragen werden können. Diese Tatsache liefert ein striktes geometrisches Kriterium an Hand dessen die Konformationen von monoalkylierten Acylguanidinen eindeutig bestimmt werden können.

Diese zuverlässige Zuordnungsmethode ermöglichte die Untersuchung der Konformationspräferenzen monoalkylierte Acylguanidine durch NMR-Spektroskopie in verschiedenen organischen Lösungsmitteln bei Temperaturen zwischen 195 K und 300 K. Größte Bedeutung kommt nun der Tatsache zu, dass über den Verlauf der gesamten Studie ausschließlich zwei der acht grundsätzlich möglichen Konformeren der monoalkylierten Acylguanidine beobachtet wurden. Dies gilt sowohl für die Röntgenkristallstrukturen, also den festen Zustand, als auch für die Untersuchung von Lösungen durch NMR. Hierzu ist anzumerken, dass zwei der untersuchten Kristallstrukturen im Rahmen dieser Arbeit von Verbindungen erhalten wurden, die auch in Lösung durch NMR untersucht wurden, was die Relevanz dieser Ergebnisse auf Grund der direkten Vergleichbarkeit (in Lösung/fest) nur noch unterstreichen kann.

Es wurde gezeigt, dass starke, selektive Wechselwirkungen über H-Brücken mit Anionen zur Bevorzugung einer bestimmten Konformation führen, während das Aufbrechen dieser selektiven Wechselwirkungen die Bevorzugung auflöst und sogar invertieren kann in Richtung einer zweiten Konformation. Zu einem solchen Brechen der selektiven

Wechselwirkungen kommt es durch die kompetitive Ausbildung komplexer Netzwerke von Wasserstoffbrücken, entweder zu Akzeptoren, die durch Lösungsmittelmoleküle gestellt werden, oder zu einem hochaffinen Rezeptor wie z.B. einer Bisphosphonat-Zange.

Die Komplexierung zweier an der Guanidin-Funktion der Seitenkette acylierter Argininderivate durch eine Bisphosphonat-Zange wurde mit Hilfe von 1D-, 2D- und 3D-Methoden der NMR-Spektroskopie untersucht. Zum ersten Mal konnten hier skalare $^{3h}J_{N,P}$-Kopplungen über Wasserstoffbrücken in einem Komplex zwischen zwei kleinen Molekülen detektiert werden, zusätzlich zu den bereits bekannten und hier reproduzierten $^{2h}J_{H,P}$-Kopplungen. Die Kombination verschiedener Kriterien in der Auswertung der Intensität dieser beiden Kopplungen lieferte Anhaltspunkte über die räumliche Anordnung der Moleküle im Komplex.

Experimentelle Hinweise auf eine auch bei tiefer Temperatur noch signifikante Rotation der NH_2-Gruppe warf die Frage nach einem entropischen Beitrag dieser Rotation zur Bevorzugung einzelner Konformationen auf. Daher wurde die Rotationsbarriere dieser NH2-Gruppe an Hand einer sorgfältig geprüften Modellverbindung durch dynamische NMR-Spektroskopie untersucht. Die Kombination von Ergebnissen der Auswertung von Kristallstrukturen mit den thermodynamischen Aktivierungsparametern $\Delta H^{\ddagger}$ und $\Delta S^{\ddagger}$ der NH_2-Rotation zeigte, dass die Rotationsbarriere dieses Vorgangs im protonierten Zustand geringer ist, da die intramolekulare Wasserstoffbrücke mit der Protonierung des Moleküls schwächer wird, was der gängigen Erwartung völlig widerspricht. Sowohl $\Delta H^{\ddagger}$ als auch $\Delta S^{\ddagger}$ werden durch Bildung von Wasserstoffbrücken zwischen NH-Protonen und Akzeptoren des Lösungsmittels deutlich erhöht. Dies legt nahe, dass unter Beibehaltung des grundlegenden Wasserstoffbrückennetzwerkes eine Konformation entropisch stark benachteiligt sein könnte, wenn sie die Rotation der NH_2-Gruppe behindert, verglichen mit einer anderen Konformation, die eine relativ freie Drehbarkeit dieser Gruppe gestattet.

Somit untermauert dieser letzte Teil der Arbeit die Hypothese, dass entropische Beiträge für die Bevorzugung einer bestimmten Konformation des monoalkylierten Acylguanidins ausreichen können.

Abschließend lässt sich also sagen, dass in im Rahmen dieser Arbeit verschiedene Synthesewege für Acylguanidine geprüft und angewendete wurden. So gelang insbesondere die Herstellung eines selektiv ^{15}N-markierten Argininderivats. mit dieser Arbeit die Konformationen monoalkylierter Acylguanidine mit Hilfe einer hierfür entwickelten, aber für diese Verbindungsklasse allgemein anwendbaren Methodik untersucht wurden. Es konnten geometrische Informationen über monoalkylierte Acylguanidine abgeleitet werden durch die Anwendung moderner multi-dimensionaler NMR-Methoden. Es wurden genau zwei der acht möglichen Konformere nachgewiesen und zwar einheitlich sowohl in Lösung als auch in Kristallstrukturen. Intermolekulare Wechselwirkungen über H-Brücken erwiesen sich als

entscheidend für die Lage des Gleichgewichtes zwischen diesen Konformationen. Der Grundstein für die weitere Untersuchung der energetischen Grundlagen der Konformationspräferenzen monoalkylierter Acylguanidine, die in dieser Studie beobachtet wurden, konnte gelegt werden und man darf hoffen, dass in Zukunft weitere Arbeiten dieses spannende Gebiet noch tiefer durchdringen werden.

10 Appendix

157

10.1   Curriculum vitae

Roland Kleinmaier, *30.12.1980, Bad Reichenhall, Germany

Eduaction

Dissertation (PhD)

03/07 – 05/10	PhD Student with Prof. Dr. Ruth M. Gschwind, Institut für Organische Chemie, Universität Regensburg, Field of Research: „Structural Investigations of Acylguanidines".
09/07 – 05/10	Active member of the Graduate College of the Deutsche Forschungs-gemeinschaft GRK 760 „Medicinal Chemistry: Molecular Recognition - Ligand-Receptor Interactions"

Studies of Chemistry

01/07	Graduation as Dipl. Chem. Univ. (University Diploma in Chemistry)
05/06 – 01/07	Diploma Thesis (Organic Chemistry): Title: „Synthesis and NMR Investigations of Arginine Derivatives"
10/01 – 01/07	Chemistry Studies (Diploma, Specialization in Medicinal Chemistry) at the University of Regensburg

09/91 – 06/00	A-levels (Abitur), Karlsgymnasium Bad Reichenhall

Teaching

from 05/06	Teaching assistance at the Institute of Organic Chemistry (University of Regensburg): -Student laboratory courses -Conceptual design and supervision of master and bachelor theses, also with Erasmus-Students (european exchange program)

Languages

German (native)
English (fluent spoken and written)
French (advanced knowledge, international certificate UNIcert II),
Spanish (advanced knowledge, international certificate UNIcert I)
Russian (basic knowledge)
Latin (Latinum), Ancient Greek (Graecum)

10.2   Scientific Life

10.2.1 Publications

(1)   G. Federwisch, R. Kleinmaier, D. Drettwan and R. M. Gschwind, *J. Am. Chem. Soc.*, *130*, 16846–16847, **2008**: "The H-Bond Network of Acylguanidine Complexes: Combined Intermolecular $^{2h}J_{H,P}$ and $^{3h}J_{N,P}$ Scalar Couplings Provide an Insight into the Geometric Arrangement".

(2)   R. Kleinmaier and R. M. Gschwind, *J. Label Compd. Radiopharm*, *52*, 29-32, **2009**: "Selective [$^{15}N^{\eta}_2$] labelling of an N^{η}-propionylated arginine derivative".

(3)   R. Kleinmaier, M. Keller, P. Igel, A. Buschauer, R.M. Gschwind, *J. Am. Chem. Soc.*, **2010**, submitted: "Conformations, Conformational Preferences and Conformational Exchange of N'-Substituted N-Acylguanidines – Intermolecular Interactions Hold the Key"

(4)   R. Kleinmaier, R.M. Gschwind, *Magn. Reson. Chem.*, **2010**, submitted: "Chemical Shift Assignment and Conformational Analysis of Monoalkylated Acylguanidines".

(5)   R. Kleinmaier, R.M. Gschwind, *J. Org. Chem.*, **2010**, in preparation: "The NH_2 Rotational Barrier in N-acylguanidines is Modelled by an N-Acyl Benzamidine – and it's Lower in the Charged State!"

10.2.2 Presentations

(1)   10. Weihnachtskolloquium des Instituts für Organische Chemie, **17.12.08**, Regensburg, Title: *„Bond, H-Bond: A Quantum of NMR"*

(2)   Symposium „Molekulare und pathophysiologische Analyse des Histamin-H_4-Rezeptors", **20.02.09**, Regensburg, Title: *„NMR-Analyse von H_4R-Liganden"*

10.2.3 Stipends and Prizes

(1)   Travel Stipend of the organising commitee, SMASH NMR conference **2009**.

(2)   Poster-Prize: "Best Poster" for the contribution: "*H-Bond Network Elucidation of Guanidines via NMR*", endowed with one year's subscription of the Journal Magnetic Resonance in Chemistry.

10.2.4 Conferences and Posters

(1)   3rd Summer School "Medicinal Chemistry" (GRK 760), Regensburg, **2006**
Poster: <u>R. Kleinmaier</u>, G. Federwisch, R.M. Gschwind, "*NMR detection of NH-OP hydrogen bond networks in artificial arginine receptors*".

(2)   Tag der Naturwissenschaften, Regensburg, **2006**
Poster: <u>R. Kleinmaier</u>, G. Federwisch, R.M. Gschwind, "*NMR investigations of hydrogen bonds, controlling dynamic and structural properties on a molecular level.*"

(3)   GRK-Retreat (GRK 760 & GRK 677), Nürnberg, **2007**
Poster: <u>R. Kleinmaier</u>, G. Federwisch, R.M. Gschwind, "*NMR investigations of hydrogen bonds, controlling dynamic and structural properties on a molecular level*".

(4)   Symposium Future Perspectives of Biomolecular NMR, München, **2008**

(5)   Frontiers in Medicinal Chemistry (GDCh and DPhG), Regensburg, **2008**
Poster: <u>R. Kleinmaier</u>, G. Federwisch, R.M. Gschwind, "*Understanding Hydrogen Bond Networks – One Power of NMR Spectroscopy*".

(6)   GDCh Discussion Group Meeting NMR, Regensburg, **2008**
Poster: <u>R. Kleinmaier</u>, G. Federwisch, D. Drettwan, R. M. Gschwind, "*Geometry of Arginine H-bond networks – Preorganization of Acylguanidines*".

(7)   4th Summer School "Medicinal Chemistry" (GRK 760), Regensburg, **2008**
<u>R. Kleinmaier</u>, G. Federwisch, R.M. Gschwind, Poster: *The N^G-pentanoyl-BIBP sidechain conformation: H-Bond network elucidation via NMR*.

(8)   16th European Symposium on Organic Chemistry, Prag, Tschechische Republik, **2009**
Poster: <u>R. Kleinmaier</u>, G. Federwisch, D. Drettwan, R.M. Gschwind, "*H-Bond Network Elucidation of Guanidines via NMR*".

(9) SMASH conference, Chamonix, Frankreich, **2009**
Poster: <u>R. Kleinmaier</u>, G. Federwisch, D. Drettwan, R.M. Gschwind, *"H-Bond Network Elucidation of Guanidines via NMR"*.

(10) International COST Meeting (BM0806) "BioMedChem on Histamine H_4 Receptor", Frankfurt, **2009**

(11) NMR Bruker User Meeting, Ettlingen, **2009**